THE UNIVERSITY OF SUSSEX

# Analytical and Numerical Approaches to Inflationary Cosmology

Proty Jiun-Huei Wu
Supervised by Dr. Andrew R. Liddle

Submitted for the degree of M. Sc. in Astronomy

31 July, 1996

CONTENTS

LIST OF FIGURES

LIST OF TABLES

THE UNIVERSITY OF SUSSEX

**Analytical and**

**Numerical Approaches**

**to**

**Inflationary Cosmology**

Submitted for the degree of M. Sc. in Astronomy

31 July, 1996

Proty Jiun-Huei Wu

Supervised by Dr. Andrew R. Liddle

## ABSTRACT

One of the outstanding problems in cosmology today is undoubtedly to develop an understanding of the early universe. With the conundrums of the standard Big Bang model, we first conceptually introduce Inflationary Cosmology for solving these problems. We review the mechanism of inflation and techniques to investigate it, with particular emphasis on the viability of slow-roll approximation, the application of perturbation theory in the regime of Inflationary Cosmology, and the power of numerical simulation for probing various problems. By using these techniques, the overall features of inflation and the behaviour of several inflationary models are investigated. This includes power-law inflation, intermediate inflation, polynomial chaotic inflation, and especially hybrid inflation whose slow-roll solution is presented. The slow-roll approximation used is classified into two variants: the potential-slow-roll approximation (PSRA) and the Hubble-slow-roll approximation (HSRA). With the help of numerical simulations, we verify that the former is good enough to cope with the investigation of almost all inflationary models, although the latter is more precise. We also demonstrate that the distinctions amongst various inflationary models can be represented by the degree of the tilt from scale-invariant spectrum of density perturbation and by the portion of gravitational waves they predict. With recourse to the four-year COBE normalization obtained this year, we find the constraints on the parameters of each model and the general solution of parameters involved in hybrid inflation. We then conclude with a brief summary table of the features of various inflationary models mentioned above, and the prospect of distinguishing these models by further observations with higher accuracy in the future.

## ACKNOWLEDGMENTS

It is a pleasure to thank my supervisor Dr. Andrew R. Liddle for those uncountably stimulating and penetrating discussions which have helped to clarify some points of information and arguments presented, for his revising my English in this thesis, and for invaluable advice and encouragement in both academic work and daily life. I would also like to express my warm thanks to my parents for providing me with financial support, and to my two beautiful sisters for their concern during my study here. Many special thanks to my girl friend of seven years, Miss Yi-Tsun Lin, for her spiritual support of weekly international calls and daily E-mails.

I wish to thank all the friendly faculty in Sussex Astronomy Centre, especially to the MSc course convenor Dr. R. C. Smith for all his help and constructive criticism; to my lecturers Prof. R. J. Tayler, Dr. P. Roche (with lovely baby), Dr. P. A. Thomas, Dr. M. Hendry and Dr. D. Wands for their careful teaching; to Dr. J. Gribbin for his two intriguing books; and to the star man Stu and the PhD student Ian who eagerly instructed me how to use the computing facilities. I would also like to thank all my classmates for giving me an enjoyable time in Sussex. They are Andrew Barber, Tino Canosa, Robert Hynes, Dominic Clancy, Steve Ord, Gabriel Pratt, Chris O'Toole, Chris Mahy and Saleh Al-Shidhant.

I am very grateful to Ali and Kathy for teaching me English and being my good friends and advisors during my stay in Sussex; to my Taiwanese friends Wen-Kung Chang, Yon-Yuan Yang, Guo-Shuan Tsun, Yu-Wei Shu, Pai-Chi Hau, Zen-Duo Yiau for their distant support and considerable help throughout; and finally to Dr. G. Smith from Oxford for his strongly recommending Sussex Astronomy Centre to me. Without him, I would not have found such a fantastic place.

## DECLARATION

I have read and understood the definition of 'Plagiarism' as set out in the General Assessment Handbook for Masters and Postgraduate Diploma Candidates under item 9. This dissertation is my own work, except where explicitly stated.

Signature: Date:

........................................................................... ....................................

Proty Jiun-Huei Wu

CHAPTER 1

# INTRODUCTION

Cosmology is a subject studying what the universe looks like and why it evolves to its present situation as a whole. An outstanding problem today is to develop a more precise understanding of the early universe as increasingly powerful experiments have presented great leaps in our knowledge of it through the last decade. The historical development in this respect can be roughly divided into two stages. The first stage is the well known competition between the Steady-State theory and the Hot Big Bang model. Even Einstein was once susceptible to the appeal of the perfect cosmological principle that is the cornerstone of the Steady-State theory. However, the vital discovery of the Cosmic Microwave Background Radiation (CMBR) in 1965 [83] effectively sounded the death knell for the Steady-State theory and made the standard Big Bang model survive until the present. The past decades have witnessed the remarkable success of this standard model in providing a reliable and tested account of the history of the universe from at least as early as the time of nucleosynthesis until today [52]. Nevertheless, there are still several conundrums associated with this model, although most of them seem more metaphysical than physical. Therefore, the second stage of the historical development was triggered by **Inflationary Cosmology** that was introduced by Guth in 1981 [40] to cope with these problems.

The most important conundrums with the Big Bang model are:

1. The flatness problem—why is the universe so close to spatial flatness? The density parameter $\Omega$ today has the order of around unity which is the value for a spatially flat universe. Its estimated value is around 0.01 upwards from studies of galaxies and between 0.010 and 0.017[1] from nucleosynthesis [28, 27]. However, in the standard Big Bang model its value should have been diluted to almost zero or collapsed to infinity within the first few seconds since the creation, unless the universe is originally

[1] This range refers only to the baryonic matter.

precisely flat.

2. The horizon problem—why is the temperature of the CMB sky observed to be so homogeneous and isotropic? Since the speed of light has a limit, the CMB sky, which corresponds to the surface of last scattering, should not have had enough time to have established thermal equilibrium throughout the entire universe unless the initial state of Big Bang is homogeneous. Thus the CMB sky should be composed of many independent regions with their own temperatures due to the existence of horizons. Obviously this is not the case from the CMBR observations. Even if we adopt an initially homogeneous state for Big Bang, we also have doubt the naturalness of having this.

3. The monopole problem—where are the monopoles today? In the regime of the Grand Unified Theory (GUT), a great amount of magnetic monopoles must be formed whenever the symmetry of the fundamental interactions[2] is broken. Because monopoles are very massive stable particles, even if only a small amount is formed they should have dominated the matter source in the present universe. On the contrary, none have yet been observed today.

4. The entropy problem—why is the entropy in our present horizon so large? The observed entropy (number of photons) today is around $10^{88}$! Since the entropy contained in a comoving horizon in an adiabatically expanding universe should be a constant, we have to wonder how to get such a huge amount of entropy within our limited horizon.

All of these problems, one after another, have been either completely resolved or considerably relaxed since the Inflationary Cosmology was proposed. As we shall see in Chapter 2, the main role of inflation is to set up an initial condition for the standard Big Bang model, even if inflation just lasts for only a small fraction of a second.

Although the purpose of inflation is the same, there exist many different inflationary models which possess their own features. The most well known ones are De Sitter expansion, power-law inflation, intermediate inflation, chaotic inflation, hybrid inflation, etc. In Chapter 2, we shall review analytical techniques for investigating inflationary models and then apply these techniques to various models appearing in the literature.

[2] Electromagnetism, the weak interaction and the strong interaction.

The most popular technique at present is the **slow-roll approximation**. It includes two different variants—the potential-slow-roll approximation and the Hubble-slow-roll approximation, which treat the potential and the Hubble parameter as fundamental quantities respectively. The distinction between them is based not only on the difference of their fundamental quantities, but also on the accuracy with which they perform. The latter is much more precise than the former, although the former is well suited to most models since only the potential form is specified in a general case.

To set up the initial condition of the standard model, solving its conundrums, is the original motivation to have inflation, but not its only role in modern cosmology. After the DMR experiment on the COsmic Background Explorer (COBE) satellite in 1992 detected anisotropies [17, 94, 106], inflation was employed to explore the **anisotropies** in more detail. It includes the study of the spectrum of density perturbation with the possibility to have non-negligible gravitational waves contributing to the full spectrum. This progress enabled detailed quantitative tests of inflationary models for the first time and these tests were further promoted when the recent four-year COBE normalization was obtained [**?**]. In Chapter 3, we shall first review the perturbation theory and relevant techniques in the inflationary regime, and then employ them to investigate various models with recourse to the recent COBE normalization.

Among various inflationary models, **hybrid inflation** is favoured recently due to the motivation of model building in the context of particle physics. It is different from other models in several important ways. This includes the much lower energy scale at the end of inflation, different behavior of the spectrum of density perturbation, etc. Therefore, we shall investigate this model independently in Chapter 4 by employing all the analytical techniques developed in Chapter 2 and 3.

In addition to the analytical techniques, the new developments in computing facilities have provided us a more precise way to investigate inflationary models. In Chapter 5, we shall make use of **numerical simulations** to explore various inflationary models in more detail. This includes the detailed investigation of the behaviour of each model and a more accurate estimation of the values of their parameters constrained by COBE normalization. Let us start with the introduction and analysis of Inflationary Cosmology.

CHAPTER 2

# INFLATIONARY COSMOLOGY

## 2.1 The Mechanism

Cosmology is the study of an entire smoothed-out Universe. It is usual to only consider universes that satisfy the cosmological principle[1] allowing the replacement of local irregularities with an average matter tensor.[2] The metric for a complete universe that embodies the cosmological principle is the **RW (Robertson-Walker)** metric

$$ds^2 = -dt^2 + a^2(t)\left(\frac{dr^2}{1-kr^2} + r^2(d\theta^2 + \sin^2\theta d\phi^2)\right) \tag{2.1}$$

Here $a(t)$ is the **scale factor**; the time-coordinate $t$ is the **cosmic time**; $k = -1, 0$ or $+1$ is the spatial **curvature** for an open, flat or closed cosmology respectively [78].

For an Einstein's equation following (2.1), the reduced non-trivial field equations can be rewritten to give the **Friedmann equation**

$$\left(\frac{\dot{a}}{a}\right)^2 + \frac{k}{a^2} = \frac{8\pi}{3m_{\rm Pl}^2}\rho \tag{2.2}$$

and the **fluid equation**

$$\dot{\rho} + 3\left(\frac{\dot{a}}{a}\right)(\rho + p) = 0 \tag{2.3}$$

where overdots indicate derivatives with respect to cosmic time $t$ and $m_{\rm Pl}$ is the Planck mass ($m_{\rm Pl} \equiv 1/\sqrt{G} = 1.02 \times 10^{19}$ GeV, where G is Newton's constant, and $\hbar \equiv c \equiv 1$ is used.) (2.2) and (2.3) are the equations determining the dynamics of the scale factor. By differentiating (2.2) and using (2.3), we can obtain the **evolution equation**

$$\frac{\ddot{a}}{a} = -\frac{4\pi}{3m_{\rm Pl}^2}(\rho + 3p) \tag{2.4}$$

By the strong energy condition, $\rho + 3p > 0$, from (2.4) we know $\ddot{a}$ must be negative. Therefore, as we know the universe is expanding (the Hubble expansion, i.e. $\dot{a} > 0$),

[1] The universe on average was homogeneous and isotropic.

[2] This tensor is taken to be the same at all places but not necessarily to be the same at all times.

we can conclude that in the past $a$ must have once equalled zero. This is known as the standard **Big Bang** model [23]. However, for **Inflationary Cosmology**, the fundamental definition is just simply assuming that the Universe has once undergone an era of an *accelerated* expansion

$$\ddot{a} > 0 \tag{2.5}$$

which allowed the strong energy condition to be violated [14, 56, 45]. This is the **generic condition** in which inflation happens. It shows an epoch in which the scale factor increased dramatically. In subsection 2.4.2 we shall see that, to its extreme case, the increase in the scale factor is exponential. A characteristic physical quantity to measure the "amount" of inflation is the so-called **number of $e$-foldings** specified by

$$N(t_{\mathrm{i}}, t_{\mathrm{f}}) \equiv \ln\left(\frac{a(t_{\mathrm{f}})}{a(t_{\mathrm{i}})}\right) = \int_{t_{\mathrm{i}}}^{t_{\mathrm{f}}} H dt \tag{2.6}$$

where the subscripts $i$ and $j$ indicate the beginning and end of inflation respectively, and $H = \dot{a}/a$ is the Hubble parameter. Here $t_{\mathrm{f}}$ is determined by the violation of equation (2.5).

### 2.1.1 Inflationary dynamics

During this stage, inflation is so effective at diluting the density of other matter, the effective of curvature, etc. that the only energy density concerned here is donated by a real scalar field, $\phi$, which is self-interacting but also coupled with other "ordinary" relativistic matter (radiation). This scalar field is generally referred to as **inflaton**. It can be thought of as a new type of particle which is spinless but has yet to be observed. Now, assuming $\phi$ is homogeneous and isotropic so that $\phi \equiv \phi(t)$, and likewise the space-time metric which is therefore (2.1), the energy density and pressure satisfying the Lagrangian mechanism are given respectively by

$$\rho_\phi = \frac{1}{2}\dot{\phi}^2 + V(\phi) \tag{2.7}$$

$$p_\phi = \frac{1}{2}\dot{\phi}^2 - V(\phi) \tag{2.8}$$

which supplant the equation of state $p = (\gamma - 1)\rho$ for a barotropic fluid. Note the potential energy here is not diminished by the expansion as it is simply a function of $\phi$. Equations (2.2) and (2.3) can be rewritten to yield

$$H^2 + \frac{k}{a^2} = \frac{8\pi}{3m_{\mathrm{Pl}}^2}\left(\frac{1}{2}\dot{\phi}^2 + V(\phi)\right) \tag{2.9}$$

and

$$\ddot{\phi} + 3H\dot{\phi} = -V' \tag{2.10}$$

respectively, where $' \equiv d/d\phi$ denotes the derivative with respect to $\phi$. Here (2.10) describes the motion of the field. This is an analogue to the equation of motion in classical dynamics, where $\phi$ is the coordinate of a particle moving in a potential $V(\phi)$, subject to frictional damping by the Hubble expansion. Notice that substituting (2.7) and (2.8) into (2.4) and using (2.5) yields an alternative *generic condition* allowing inflation:

$$V(\phi) > 2\left(\frac{\dot{\phi}^2}{2}\right) \tag{2.11}$$

This implies that, during inflation, the energy density $\rho_\phi$ is dominated by the potential energy $V(\phi)$ with a portion of at least two thirds.

To link this inflationary regime to the conventional Big Bang evolution, we need an appropriate scenario for inflation. In literature, different authors have had different versions to illustrate this from time to time [40, 43, 46, 67, 5, 64, 41, 52]. Here is a version quoting most of the conceptually important features of inflation.

### 2.1.2 A scenario

In the standard inflationary scenario, the process of inflation is introduced as a GUT symmetry-breaking phase transition. In the early Universe, as the temperature falls down to a critical temperature, $T_c$, below the GUT scale, around $10^{14}$GeV, the scalar field potential $V(\phi)$ develops a second minimum other than the symmetric point at $\phi = 0$. Finally $V(\phi)$ develops the form shown in Figure 2.1.[3] It possesses two vacuum states: the **false vacuum** (at $\phi = 0$),which is the original minimum of the era above GUT scale storing the energy of the Universe, $\rho_{\text{vac}} = V(0) \equiv M^4 \geq (10^{14}\text{GeV})^4$; and the **true vacuum**, which is now the global minimum for $\phi$ to evolve towards. The "false" here means metastable and, therefore, temporary; the "vacuum" means the state of the lowest possible energy density.

When $\phi$ evolves away from the false vacuum, as it is no longer the global minimum, it will, if necessary, negotiates any barrier[4] and then it enters the inflationary epoch governed by equation (2.10). At this stage, the potential $V(\phi)$ possesses two crucial features:

[3] The form provided here is just for the convenience of illustrating some generic features of inflation; it is not necessarily the form taken in all realistic models.

[4] See further discussion in subsection 2.4.1.

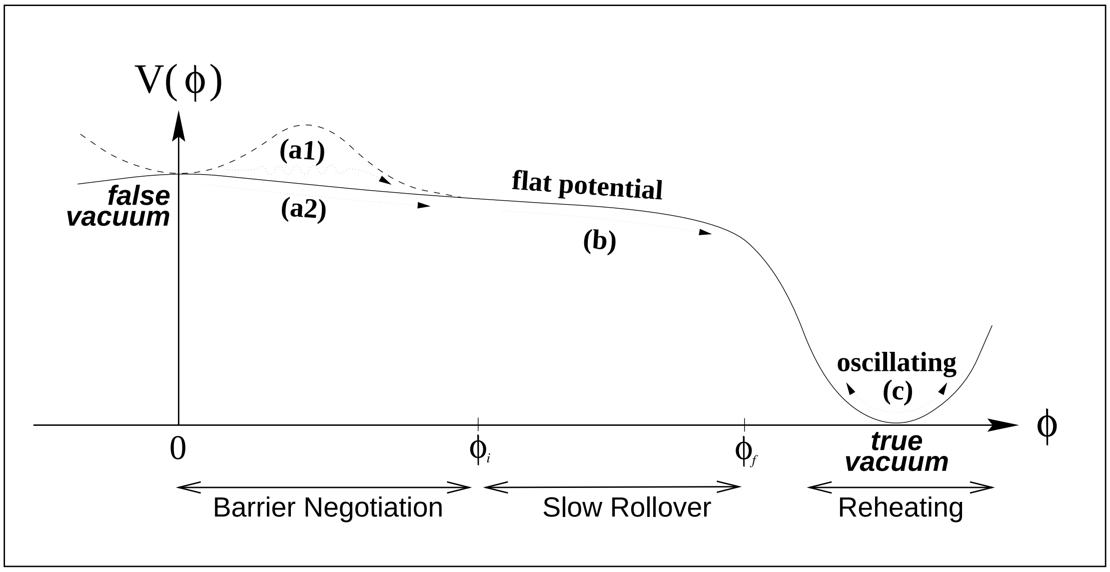


Figure 2.1: A form of the potential energy function $V(\phi)$ leading to inflation. The stages for $\phi$ evolving from the false vacuum to the true vacuum include: (a) barrier negotiation (if any); (b) slow rollover; and (c) reheating.

1. It must be sufficiently "flat" so that $\phi$ can remain here long enough (rolling slowly here) to generate sufficient inflation to solve the problems with the standard Big Bang model. The importance of this flatness during inflation will be illustrated in more detail in subsections 2.3.1 and 2.4.2; the concept of *cosmologically sufficient inflation* will be made more explicit in section 2.2.

2. Since $\phi$ is rolling slowly on that flat potential (i.e. $\dot{\phi}$ is small), the "frictional damping" to the system governed by (2.10) must be small and the "kinetic term" in (2.7) must be small as well. In other words, the total energy of the dynamic system $\dot{\phi}^2/2 + V(\phi) \equiv \rho_\phi$ is almost conserved and dominated by the potential energy $V(\phi)$. (This is confirmed by (2.11).)

This period is referred to as "**slow rollover**".

When $\phi$ rolls down the potential, the violation of (2.5) will terminate inflation and $\phi$ will finally reach the true vacuum and then oscillate around it. As $\phi$ is coupled to other fields, a damping term $\Gamma_\phi\dot{\phi}$ for the "decay" of $\phi$ on a time scale $\Gamma_\phi^{-1}$ should be put into the left-hand side of equation (2.10) [6, 1, 31]. During inflation, $3H \gg \Gamma_\phi$ so that the decay mode is negligible. However, during the oscillating phase, once $t \simeq \Gamma_\phi^{-1}$, the decay mode becomes significant, and therefore converts the scalar field into ordinary relativistic matter.

This is called the **reheating** process and can be regarded as a phase transition converting the energy stored in the false vacuum, $\rho_{\rm vac} \equiv M^4$, into ordinary matter. When the matter has thermalised, resulting in a temperature $T_{\rm reh}$ which has almost the same order as the beginning of GUT symmetry breaking, the scenario rejoins the standard cosmological model, the Hot Big Bang evolution. Actually, the whole issue of the reheating process is still rather uncertain and its details are controversial in the relevant literature [43, 46]. Nevertheless, the concept of the oscillating phase is appreciated.

## 2.2 Solving The Problems With The Big Bang Model

Armed with our concept of inflation, we can solve the intrinsic problems with the Big Bang model very easily step by step:

### 2.2.1 Solving the flatness problem

The condition to have inflation, equation (2.5), is equivalent to the following expression

$$\dot{a} = aH = \left(\frac{H^{-1}}{a}\right)^{-1} \quad \text{increasing} \tag{2.12}$$

To solve the flatness problem, we rewrite equation (2.2) as

$$|\Omega - 1| = \frac{|k|}{a^2 H^2} \tag{2.13}$$

where $\Omega = \rho/\rho_{\rm c}$ is the **density parameter** and $\rho_{\rm c} = 3m_{\rm Pl}^2 H^2/8\pi$ is the **critical density** making the Universe flat in equation (2.2). Obviously, by (2.12), the right-hand side of (2.13) was decreased rapidly during inflation. This means that $\Omega$ can be driven as close to unity as we want provided *cosmologically sufficient inflation* occurs. As a result, we have set up a perfect initial condition for the standard Big Bang model so that $\Omega$ today can not be far away from unity, because its initial value at the end of inflation is so accurately close to unity. Thus we solve the flatness problem. A crucial point to notice here is that not far away from the end of inflation, the Universe should be so flat ($\Omega \simeq 1$) that in equation (2.9) the curvature term, $k/a^2$, is negligible. This can be made more explicit in the rewritten Friedmann equation

$$H^2 + \frac{k}{a^2} = \Omega H^2 \tag{2.14}$$

Notice that $\Omega = 1$ is equivalent to $k = 0$. Without a specific announcement, we shall neglect the curvature term throughout this paper and refer to (2.9) with $k = 0$ and (2.10) as the "flat Friedmann model". From (2.14), we also see that if $\Omega = 1$, it will be unity forever. This indicates a division between open and closed Universes, which can never evolve from one to the other.

### 2.2.2 Solving the horizon problem

To solve the horizon problem, let's consider the evolution between the comoving horizon,[5] $H^{-1}/a$, and the size of a small thermalised patch, $d_{\rm thm}$, in the *comoving* co-ordinates. The size of this patch can only grow because at any given time $t$, the size of this patch since the creation at time $t_*$ is

$$d_{\rm thm}(t) = \int_{t_*}^{t} \frac{dt'}{a(t')} \tag{2.15}$$

which is obviously a monotonically increasing function of time. However, during inflation, according to expression (2.12), the comoving horizon kept decreasing so that it can be as small as we want in relation to $d_{\rm thm}$. Therefore, provided *cosmologically sufficient inflation* occurs, no matter how rapidly $H^{-1}/a$ has grown after inflation, its size today can still sit well below the size of $d_{\rm thm}$ at last-scattering.[6] This provides a good explanation for the observed isotropy and homogeneity in the CMBR (Cosmic Microwave Background Radiation). Thus we solve the horizon problem or, alternatively, the smoothness problem.

### 2.2.3 Solving the monopole problem

As indicated in Chapter 1, a great amount of magnetic monopoles are produced by the spontaneous symmetry breaking in the GUT scenario. Even allowing for monopole-anti-monopole annihilations, they are still inefficient in avoiding monopole domination today.

However, if inflation is inserted between the symmetry-breaking phase and the standard Big Bang era, this monopole problem can be solved as follows. During inflation, as a feature of the slow rollover process indicated on page 7, the scalar energy density $\rho_\phi$ remains almost constant, while the monopole energy density, $\rho_{\rm mon}$, dilutes as $a^{-3}$ (their comoving number density being preserved after the symmetry breaking). Eventually, $\rho_{\rm mon}$ becomes negligible compared with $\rho_\phi$, which will be converted into the radiation energy density when the standard Big Bang epoch is reached. Therefore, the monopole density today is negligible and, hence, we solve the monopole problem.

[5]This is also called "comoving Hubble length" which indicates the order of the horizon size.

[6]This is also called "decoupling", indicating the epoch when radiation decoupled from matter at T$\simeq$3000K in Hot Big Bang model.

### 2.2.4 Solving the entropy problem

In the inflationary regime, the entropy problem can be solved with the following two steps:

1. *Dramatic* expansion: Suppose a smooth patch occupies the entire horizon at the start of inflation. Its size is $H^{-1}$. During inflation, this size grows by a dramatic factor $a(t_{\rm f})/a(t_{\rm i}) \stackrel{(2.6)}{=} \exp[N(t_{\rm i}, t_{\rm f})] \gg 1$, as the patch "supercools" to a temperature $T_{\rm f} = a(t_{\rm i})/a(t_{\rm f})T_{\rm i} \ll T_{\rm i}$.

2. *Reheating* process: because the energy stored in the false vacuum is converted into ordinary matter by the "frictional" damping of $\phi$, this process must be *irreversible* and *non-adiabatic*. This non-adiabaticity results in a rise of temperature up to $T_{\rm reh}$, which has almost the same order as at the start of inflation, i.e. $T_{\rm reh} \sim T_{\rm i} \gg T_{\rm f}$. Therefore, the entropy within the patch now is given by

$$S_{\rm f} \simeq (H^{-1})^3 \exp[3N(t_{\rm i}, t_{\rm f})] T_{\rm reh}^3 \tag{2.16}$$

Provided *cosmologically sufficient inflation* occurs, we see the massive entropy production within the patch due to the combination of the dramatic increase of the patch size during inflation, and the non-adiabaticity during reheating. Therefore, the huge amount of entropy observed today can be generated from this mechanism and thus we solve the entropy problem.

### 2.2.5 How much inflation

As we have seen from subsections 2.2.1 to 2.2.4, inflation can easily solve the conundrums of the standard Big Bang model. However, the discussion above is just qualitative. For further consideration in realistic cases, we need a more precise analysis about how much inflation is needed to solve these problems. The best way to do this is to use the entropy approach since the observed number of photons today is available, i.e. $S_0 = 10^{88}$.

Let us recall (2.16). Substituting $H^{-1} \sim m_{\rm Pl}/M^2$ (by (2.2) for $k = 0$ and $\rho_{vac} \equiv M^4$) and adding a correcting factor of $(M^4/T_{\rm reh}^4)^{1/3}$ for the growth of $a(t)$ during reheating, the entropy within the smooth patch is now given by

$$S_{\rm f} \simeq \exp[3N(t_{\rm i}, t_{\rm f})] \frac{m_{\rm Pl}^3}{M^2 T_{\rm reh}} \tag{2.17}$$

Solving the horizon problem requires $S_\mathrm{f} > S_0 = 10^{88}$. This condition can be rewritten to yield

$$N(t_\mathrm{i}, t_\mathrm{f}) > N_\mathrm{min} \simeq 53 + \frac{2}{3}\ln\left(\frac{M}{10^{14}\mathrm{GeV}}\right) + \frac{1}{3}\ln\left(\frac{T_\mathrm{reh}}{10^{10}\mathrm{GeV}}\right) \tag{2.18}$$

Taking both $M$ and $T_\mathrm{reh}$ to their upper limit, i.e. $M \simeq T_\mathrm{reh} \simeq m_\mathrm{Pl} \simeq 10^{19}\mathrm{GeV}$, we have $N_\mathrm{min} \simeq \mathbf{68}$.

Now let us further consider the flatness problem. Since the scale factor at the beginning of inflation can be related to the Hubble length by equation (2.14):

$$a(t_\mathrm{i}) = \frac{H^{-1}}{|\Omega_\mathrm{i} - 1|^{1/2}} \tag{2.19}$$

where $\Omega_\mathrm{i}$ is the density parameter at that time, the entropy contained within a unit comoving volume can be given as

$$S_\mathrm{com} \equiv [a(t_\mathrm{i})]^3 T_\mathrm{reh}^3 \simeq S_\mathrm{f}|\Omega_\mathrm{i} - 1|^{-3/2} \tag{2.20}$$

Since the entropy is proportional to the comoving horizon volume (the comoving entropy density being preserved after reheating), solving the flatness problem requires $S_\mathrm{com} \geq S_0 = 10^{88}$, or alternatively

$$N(t_\mathrm{i}, t_\mathrm{f}) \geq N_\mathrm{min} + \frac{1}{2}\ln(|\Omega_\mathrm{i} - 1|) \tag{2.21}$$

Moreover, we see the present density parameter is given by [52]

$$|\Omega_0 - 1| = \exp(2[N_\mathrm{min} - N(t_\mathrm{i}, t_\mathrm{f})])|\Omega_\mathrm{i} - 1| \tag{2.22}$$

Therefore, in a successful inflationary model, $N(t_\mathrm{i}, t_\mathrm{f})$ must be sufficiently larger than $N_\mathrm{min}$ so that $|\Omega_0 - 1| \ll 1$ and $S_\mathrm{f} \gg 10^{88}$. We shall take $N(t_\mathrm{i}, t_\mathrm{f}) = \mathbf{80}$ as a minimum requirement for testing our realistic models.

## 2.3 Analysis Techniques

The study of Inflationary Cosmology is to investigate the Friedmann equation (2.9) and the equation of $\phi$-motion (2.10). To investigate them in more detail, appropriate analysing techniques are required. In this section, we are mainly concerned with **analytical** approaches to inflation, and leave the **numerical** ones to Chapter 5.

### 2.3.1 Potential-slow-roll approximation

In the inflationary scenario introduced in section 2.1, the assumption is made that, during inflation, the potential energy $V(\phi)$ is sufficiently flat (the slow-rollover process). Buying the concept from classical dynamics applied to equation (2.10), this implies that after a sufficient time the scalar field must have been *overdamped* rolling with a "terminal velocity". In this slow-rollover regime, both the acceleration term $\ddot{\phi}$ in equation (2.10) and the kinetic term $\dot{\phi}^2/2$ in equation (2.9) are negligible. This confirms the features of slow rollover introduced on page 7 and results in

$$3H\dot{\phi} \simeq -V'(\phi) \tag{2.23}$$

and

$$H^2 \simeq \frac{8\pi}{3m_{\mathrm{Pl}}^2} V(\phi) \tag{2.24}$$

where the curvature term is also dropped due to the feature of flatness during inflation.[7]

For consistency in neglecting those terms, we derive conditions as follows:

Squaring (2.23), using (2.24) to eliminate $H$, and requiring $\dot{\phi}^2/2 \ll V(\phi)$ yields

$$\epsilon_V(\phi) = \frac{m_{\mathrm{Pl}}^2}{16\pi}\left(\frac{V'(\phi)}{V(\phi)}\right)^2 \ll 1 \tag{2.25}$$

Differentiating (2.23), requiring $|\ddot{\phi}| \ll |3H\dot{\phi}|$, using (2.24) to eliminate $H$, and using (2.25) yield

$$\eta_V(\phi) = \frac{m_{\mathrm{Pl}}^2}{8\pi}\left|\frac{V''(\phi)}{V(\phi)}\right| \ll 1 \tag{2.26}$$

Here $\epsilon_V$ and $\eta_V$ are defined as potential-slow-roll parameters.[8]

The conditions (2.25) and (2.26), and the usage of (2.23) and (2.24) are "conventionally" referred to as **PSRA** (potential-slow-roll approximation) [88, 98, 56]. The reason to put the "conventionally" here is given as follows.

### Attractor solution

Originally, the smallness of $\epsilon_V$ and $\eta_V$ is used to justify the neglect of terms $\ddot{\phi}$ and $\dot{\phi}^2/2$ in (2.10) and (2.9) respectively. However, when we check our derivation above carefully, we find this derivation is irreversible because during the derivation we are using the result we want to guarantee. In other words, conditions (2.25) and (2.26) are just necessary but *not*

[7] Please see subsection 2.2.1.

[8] The conditions here are actually written as three times stronger than originally required. We shall see that this extra factor of three has in fact its advantage for analysing some realistic inflationary models and for fitting in with generic conditions of inflation.

sufficient to drop those terms. Therefore, to complete the PSRA, an extra assumption is required:

$$\dot{\phi} \simeq -\frac{V'(\phi)}{3H(\phi)} \tag{2.27}$$

since the information of the smallness of $\dot{\phi}^2/2$ in (2.9) is lost in our derivation. This is called the **attractor solution**, which should be checked during the slow rollover to make sure the appropriateness of the PSRA. In general, (2.27) is used to test if the initial $\dot{\phi}$ approaches this attractor solution, because $\dot{\phi}$ is one of the initial conditions of (2.9) ($\phi$ and $\dot{\phi}$) but ceases to be the initial condition of (2.24) (only $\phi$). Let us explore this approximation a little further.

### The comparison with *generic* condition

First, one crucial thing to investigate is how well the PSRA will work in the inflationary regime. Let us start off with the *generic* condition for inflation:

$$\ddot{a} > 0 \Leftrightarrow \frac{\ddot{a}}{a} = \dot{H} + H^2 > 0 \Leftrightarrow \frac{-\dot{H}}{H^2} < 1 \Longrightarrow \epsilon_V \stackrel{\text{def}}{=} \frac{m_{\text{Pl}}^2}{16\pi}\left(\frac{V'(\phi)}{V(\phi)}\right)^2 \stackrel{PSRA}{\simeq} \frac{-\dot{H}}{H^2} < 1 \tag{2.28}$$

This implies that the PSR conditions $\epsilon_V \ll 1$ and $\eta_V \ll 1$ guarantee inflation to happen although they are not necessary. Therefore, assuming that inflation ends shortly after slow rollover, the violation of PSR conditions provides a rough but analytically simple indicator to the end of inflation.

### The solutions

Secondly, we try to close the equations (2.10) and (2.9). We see that (2.23) and (2.24) have their obviously analytic advantage of reducing the order of these ordinary differential equations. This is of great help for tackling realistic inflationary models. Now substituting (2.24) into (2.23) to eliminate $H$, we can get

$$t(\phi) \simeq \frac{-\sqrt{24\pi}}{m_{\text{Pl}}} \int \frac{[V(\phi)]^{1/2}}{V'(\phi)} d\phi \tag{2.29}$$

Once $V(\phi)$ is specified, we can obtain $\phi(t)$ and, therefore, $V(t)$. Furthermore, (2.24) can be rearranged and then integrated to give

$$\ln a(t) \simeq \frac{\sqrt{8\pi}}{\sqrt{3} m_{\text{Pl}}} \int V(t)^{1/2} dt \tag{2.30}$$

Assuming both (2.29) and (2.30) are integrable, we have so far solved the Friedmann equation and the equation of $\phi$-motion by PSRA.

#### Number of $e$-foldings and the flatness

Another direct application of PSRA is to rewrite the number of $e$-foldings

$$N(t_{\rm i},t_{\rm f}) \overset{\phi(t)}{\equiv} N(\phi_{\rm i},\phi_{\rm f}) \equiv \int_{\phi_{\rm i}}^{\phi_{\rm f}} \frac{H}{\dot{\phi}} d\phi \overset{PSRA}{\simeq} -\frac{8\pi}{m_{\rm Pl}^2} \int_{\phi_{\rm i}}^{\phi_{\rm f}} \frac{V(\phi)}{V'(\phi)} d\phi \tag{2.31}$$

Qualitatively, a sufficiently flat $V(\phi)$ (i.e. $V'(\phi)$ sufficiently small) will give a significant rise to $N(\phi_{\rm i},\phi_{\rm f})$. More precisely, using (2.24) to eliminate $V$ in (2.26) first, and taking $1/V'' \sim \phi/V'$ for a polynomial potential, the last expression in (2.31) indicates that $N$ must be $\gg \mathcal{O}(1)$ for a non-zero interval $(\phi_{\rm i},\phi_{\rm f})$. That is, the flatness property in the slow-rollover regime implies a dramatic growth in the scale factor when $\phi$ rolls down the potential. This demonstrates the importance of flatness in $V(\phi)$ for getting *cosmologically sufficient inflation.*

### 2.3.2 Hubble-slow-roll approximation

As we see above, the PSRA only works well if the real end of inflation (indicated by (2.5)) is tolerably close to the end of the slow rollover. However, it must eventually fail if inflation is to end, since the PSR conditions are not exactly consistent with the generic condition of inflation. For some precise study, like the perturbation theory where even weak deviations from the exact condition are not allowable, a more accurate framework is desired. Moreover, for general studies, the form of potential is not specified so that PSRA is not applicable. Therefore, here is an alternative version of slow-roll approximation, which is, however, much more powerful than the PSRA—the **HSRA** (Hubble-slow-roll approximation) [59].

#### Hamilton-Jacobi formalism

The key concept of HSRA is to rewrite Friedmann equation and the equation of $\phi$-motion by using the scalar field as a time variable [88, 80, 60]. This requires a monotonic relation between $\phi$ and $t$. To do this, we shall choose $\dot{\phi} > 0$ throughout. Differentiating (2.9) with respect to $t$ (taking $k = 0$) and using (2.10) gives

$$\dot{H} = -\frac{4\pi}{m_{\rm Pl}^2}\dot{\phi}^2 \tag{2.32}$$

which implies $\dot{H} < 0$. Dividing each side by $\dot{\phi}$ to eliminate the time dependence gives

$$\dot{\phi} = -\frac{m_{\rm Pl}^2}{4\pi} H'(\phi). \tag{2.33}$$

Taking its square and using (2.9) to eliminate $\dot{\phi}$ yields

$$[H'(\phi)]^2 - \frac{12\pi}{m_{\rm Pl}^2}H^2(\phi) = -\frac{32\pi^2}{m_{\rm Pl}^4}V(\phi). \tag{2.34}$$

The rewriting of equations (2.33) and (2.34) as an alternative set of equations (2.9) and (2.10) is called the Hamilton-Jacobi formalism.

**The approximation**

As an analogue to the PSRA, we can now use $H(\phi)$ as the primary quantity instead of $V(\phi)$ to reconstruct the approximation. To drop both the acceleration term in (2.10) and the kinetic term in (2.9), we define the new HSR parameters and, therefore, the HSR conditions as

$$\epsilon_H(\phi) = \frac{m_{\rm Pl}^2}{4\pi}\left(\frac{H'(\phi)}{H(\phi)}\right)^2 = 3\frac{\dot{\phi}^2/2}{V+\dot{\phi}^2/2} \ll 1 \tag{2.35}$$

$$\eta_H(\phi) = \frac{m_{\rm Pl}^2}{4\pi}\frac{H''(\phi)}{H(\phi)} = 3\frac{\ddot{\phi}}{3H\dot{\phi}} \ll 1 \tag{2.36}$$

where (2.33) and (2.34) have been used to eliminate $H$, $H'$ and $H''$. Obviously, the HSR conditions preserve the information of the smallness of the acceleration term in (2.10) and the kinetic term in (2.9) exactly, unlike PSRA in which we need an extra assumption, the attractor solution. Therefore, all the necessary dynamical information is encoded in the HSR parameters. This is called the Hubble-slow-roll approximation.

**Inflationary attractor**

Let us explore the dynamical property of the inflaton further by using Hamilton-Jacobi formalism. Suppose $H_0(\phi)$ is a solution to (2.34). Consider a *linear* perturbation $\delta H(\phi)$. Assuming again that the perturbation does not change the sign of $\dot{\phi}$ gives

$$H_0'\delta H' \simeq \frac{12\pi}{m_{\rm Pl}^2}H_0\delta H \tag{2.37}$$

which has the general solution

$$\delta H(\phi) = \delta H(\phi_{\rm i})\exp\left(\frac{12}{m_{\rm Pl}^2}\int_{\phi_{\rm i}}^{\phi}\frac{H_0}{H_0'}d\phi\right) = \delta H(\phi_{\rm i})\exp\left(\frac{6\sqrt{\pi}}{m_{\rm Pl}}\int_{\phi_{\rm i}}^{\phi}\frac{-d\phi}{\sqrt{\epsilon_H(\phi)}}\right) \tag{2.38}$$

where a negative sign is put since $H_0'$ and $d\phi$ have opposite signs by (2.33). Therefore, the perturbation is always decaying, whether or not inflation is occurring. Notice that even if $\dot{\phi}$ changes sign somewhere, as long as $\delta H$ is insufficient to bring $\phi$ over a maximum of

$H(\phi)$ (if any), $\delta H$ will inevitably reverse and finally pass through $\phi_{\rm i}$ again. Then it can be treated as a perturbation with the same sign of $\dot{\phi}$ as the original solution.

Now supposing a inflationary universe, the decay is particularly dramatic because $\epsilon_H < 1$ guarantees that the decay is at least exponential. This illustrates the importance of the **inflationary attractor**, which guarantees the at least exponential approach between inflationary solutions, regardless of how different the initial conditions are. Therefore, when $H(\phi)$ converges asymptotically, the approach to the PSRA attractor solution is assured. This is a crucial feature of inflation in the application of the slow-roll approximation.

### The comparison with *generic* condition

Let us consider again, like in PSRA, how well the HSRA will work in the inflationary regime. Start off with the *generic* condition for inflation:

$$\ddot{a} > 0 \Longleftrightarrow \epsilon_H \stackrel{\rm def}{=} \left(\frac{m_{\rm Pl}^2}{4\pi}H'\right)\left(\frac{H'}{H^2}\right) \stackrel{(2.33)}{=} -\dot{\phi}\left(\frac{H'}{H^2}\right) = \frac{\dot{H}}{H^2} = -\frac{\ddot{a}a}{\dot{a}^2} + 1 < 1 \tag{2.39}$$

This indicates that the HSR condition $\epsilon_H < 1$ is identical to the generic condition of inflation $\ddot{a} > 0$, unlike PSRA where $\ddot{a} > 0 \Rightarrow \epsilon_V < 1$. Therefore, without needing any further assumption, the violation of the HSR condition $\epsilon_H < 1$ provides the *precise* indicator for the end of inflation. This is a vital feature of the HSRA overriding the PSRA.

### Number of $e$-foldings

Now we can use HSRA to rewrite the number of $e$-foldings

$$N(\phi_{\rm i}, \phi_{\rm f}) \equiv \int_{\phi_{\rm i}}^{\phi_{\rm f}} \frac{H}{\dot{\phi}} d\phi \stackrel{(2.33)}{=} -\frac{4\pi}{m_{\rm Pl}^2}\int_{\phi_{\rm i}}^{\phi_{\rm f}} \frac{H(\phi)}{H'(\phi)} d\phi \stackrel{(2.35)}{=} \frac{\sqrt{4\pi}}{m_{\rm Pl}}\int_{\phi_{\rm i}}^{\phi_{\rm f}} \frac{1}{\sqrt{\epsilon_H(\phi)}} d\phi \tag{2.40}$$

These expressions are *precisely* identical to the definition of the number of $e$-foldings. Once again, this shows another vital feature of the HSRA overriding the PSRA, where the number of $e$-foldings can be only *approximated* by $V$ and $V'$, or, alternatively, $\epsilon_V$ (c.f. (2.31)). Obviously, the extreme HSR condition $\epsilon_H \ll 1$ automatically guarantees a large number of $e$-foldings when $\phi$ evolves. Thus, we can easily get *cosmologically sufficient inflation* in this regime.

### PSR and HSR parameters

One interesting thing to demonstrate is the relation between $\epsilon_V, \eta_V, \epsilon_H$ and $\eta_H$. By using their definitions and differentiating (2.34), one can easily derive

$$\epsilon_V = \epsilon_H \left(\frac{1-\eta_H/3}{1-\epsilon_H/3}\right)^2 \tag{2.41}$$

and

$$\eta_V = (\epsilon_H + \eta_H)\left(\frac{1-\eta_H/3}{1-\epsilon_H/3}\right) + \frac{m_{\rm Pl}}{\sqrt{4\pi}}\frac{\sqrt{\epsilon_H}\eta'_H}{3-\epsilon_H} \tag{2.42}$$

To the lowest order, we have $\epsilon_V \simeq \epsilon_H$ and $\eta_V \simeq \eta_H + \epsilon_H$.

Actually, a hierarchy system exists for these slow-roll parameters. It was first introduced by Liddle, Parsons and Barrow in 1994 [59]:

$$^n\beta_H \equiv \left[\prod_{i=1}^{n}\left(-\frac{d\ln H^{(i)}}{d\ln a}\right)\right]^{\frac{1}{n}} = \frac{m_{\rm Pl}^2}{4\pi}\left(\frac{[H']^{n-1}H^{(n+1)}}{H^n}\right)^{\frac{1}{n}} \tag{2.43}$$

$$^n\beta_V \equiv \frac{m_{\rm Pl}^2}{8\pi}\left(\frac{d\ln V}{d\phi}\right)\left[\prod_{i=1}^{n}\left(\frac{d\ln V^{(i)}}{d\phi}\right)\right]^{\frac{1}{n}} = \frac{m_{\rm Pl}^2}{8\pi}\left(\frac{[V']^{n-1}V^{(n+1)}}{V^n}\right)^{\frac{1}{n}} \tag{2.44}$$

where $^n\beta_H$ denotes the hierarchy HSR parameters ($\epsilon_H, \eta_H, \xi_H \ldots$ for $n = 0, 1, 2, \ldots$); $^n\beta_V$ denotes the hierarchy PSR parameters ($\epsilon_V, \eta_V, \xi_V \ldots$ for $n = 0, 1, 2, \ldots$)[9]; and the superscripts $(i)$ and $(n)$ indicate the $i$th and $n$th derivatives, respectively, with respect to $\phi$. This system has two main vital applications. The first is, by using Taylor expansion up to order $m$, we can express $H(\phi)$ in terms of $(^n\beta_H)^n$ with integer power, where $n < m$, i.e. only a finite number of HSR parameters can appear. The second is the case when the form of $V(\phi)$ is specified but $H(\phi)$ is unknown. In this case, we can recast (2.34) as

$$[H(\phi)]^2 = \frac{8\pi}{3m_{\rm Pl}^2}V(\phi)\left(1-\frac{1}{3}\epsilon_H(\phi)\right)^{-1} \tag{2.45}$$

Since the PSRA and HSRA parameters are related as in (2.41) and (2.42), we can expand $\epsilon_H$ in terms of PSR parameters of ascending order. This step has to be achieved iteratively order by order and is somewhat tedious. However, the crucial thing is that, having this done, the value of $H(\phi)$ is approximated since all the PSR parameters are calculable when $V(\phi)$ is specified. The only defect is for arbitrary $V(\phi)$, we don't know how many orders are needed for the series to converge, or if it never converges.

[9] Here we retain the standard definitions of $\epsilon_H$ and $\epsilon_V$ from (2.35) and (2.25), escaping from the hierarchy system here.

## 2.4 Realistic Models

Before we go too far, we have to doubt the nature of the scalar field. In section 2.1.1, the scalar field is thought of as a new type of particle which is spinless in terms of quantum field theory. In the literature of particle physics, the concept of such particles is introduced to cause a spontaneous symmetry breaking—the "Higgs field" in the Glashow-Weinberg-Salam model of the electroweak interactions. Grand Unified Theories also make use of similar Higgs fields but at a much higher mass scale, as briefly discussed in subsection 2.1.2. Even in modern work of current interest like superstring theories, a large number of scalar fields are found. Therefore, the particle physics motivation for believing the existence of scalar fields is quite strong, although they have yet to be found.

Unlike the electromagnetic field, the potential energy density of the scalar field $V(\phi)$ has a wider range of possibilities. Different choices of $V(\phi)$ raise various inflationary models. In this section, we will start off with a quick review of a scalar field commonly used in particle physics, the Higgs field, and then move on to introduce various inflationary models specified by different forms of $V(\phi)$.

### 2.4.1 Higgs field and topological defects

At very early times in the universe, the Higgs field is in the symmetric "false vacuum" at $\phi = 0$ as mentioned in section 2.1.2. The real process to develop the two true vacua [52] is far more complicated than we can derive here [30] and let us just consider a simple form for the effective potential which can demonstrate the conceptual features

$$V_{\text{eff}}(\phi, T) = \frac{\lambda}{4}(\phi^2 - M^2)^2 + \frac{\alpha}{2}T^2\phi^2 \tag{2.46}$$

where $\lambda$ is a dimensionless coupling constant and $M$ is the mass of the field with the GUT scale (see Figure 2.2 (a)).

This effective potential has a global minimum at $\phi = 0$ while $T > T_{\text{c}} = \sqrt{\lambda/\alpha}M$. Once $T$ falls below $T_{\text{c}}$, two global minima form at $\phi^{\pm}_{\text{min}} = \pm\sqrt{M^2 - \alpha T^2/\lambda}$. As $T \ll T_{\text{c}}$, $\phi$ must roll down to one of the two true vacua at $\phi = \pm M$ so that $\langle\phi^2\rangle = M^2 \neq 0$, i.e. the symmetry of the physical state no longer exists. This is called "**spontaneous symmetry breaking**". The smooth transition from $\phi = 0$ to $\phi = \pm M$ introduced here is generally referred to as a **second order** phase transition. This is indicated as path (a2) in Figure 2.1. Another case in which potential barriers can exist between the true vacua

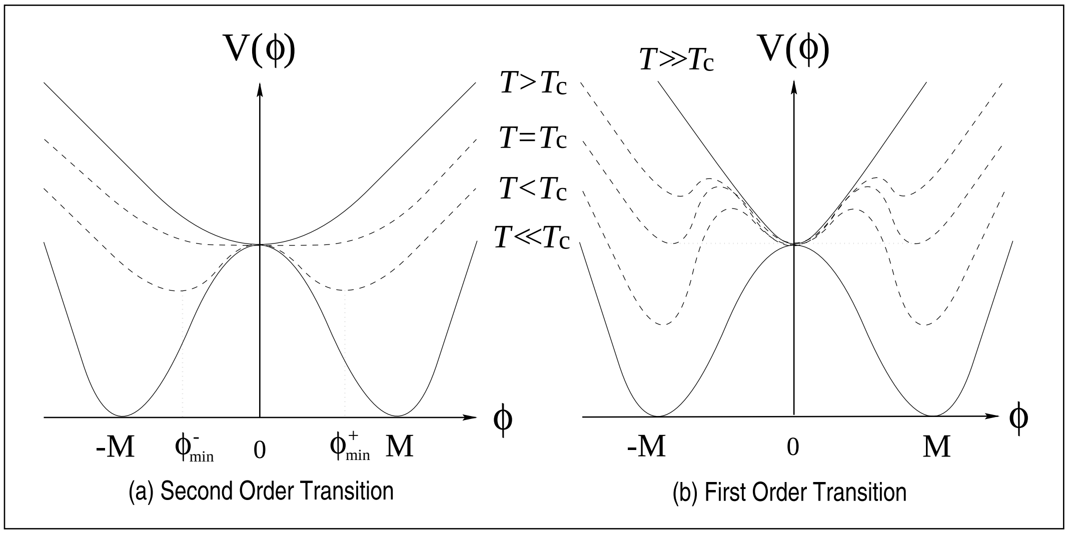


Figure 2.2: (a) Second order transition: the effective potential with a simple form $V_{\text{eff}}(\phi, T) = \lambda(\phi^2 - M^2)^2/4 + \alpha T^2\phi^2/2$; (b) First order transition: two barriers exist between the true vacua and the false vacuum. The barriers can be negotiated either by quantum/thermal tunnelling or by the disappearance of the barrier at some $T < T_{\text{c}}$.

and the false vacuum is known as a **first order** phase transition [22]. This is indicated as path (a1) in Figure 2.1. Figure 2.2 shows the forms of $V(\phi)$ for both cases.

A by-product of the spontaneous symmetry breaking is "**topological defects**," which are expected to form between the different true vacua, depending on the topology of the "vacuum manifold". The defects associated with the potential form introduced above are called **domain walls**, since they are two dimensional with a point like manifold, i.e. a 0-sphere.[10] Similarly, for manifolds with higher dimension, we have: **cosmic strings** for a manifold of a 1-sphere, **monopoles** for a manifold of a 2-sphere, **textures** for a manifold of a 3-sphere, etc. Their existence and evolution have the importance that they may be responsible for the structure formation in the universe and, hopefully, providing the evidence of spontaneous symmetry breaking.

### 2.4.2 De Sitter expansion

In Subsection 2.1.2 and 2.3.1, we have seen the importance of flatness of a potential for inflation. Now let us consider a extreme case, $V = V_0 =$ positive constant. By equation (2.10), we know that the frictional damping from the Hubble expansion will

[10] A $n$-sphere is referred to as a $n$ dimensional sphere: 0 for a point, 1 for a circle, 2 for a sphere, etc.

finally bring the scalar field to rest. By equation (2.7), we have $\rho_\phi = V_0$ which shows a thoroughly $V(\phi)$-dominated energy density. Combined with equation (2.8), we also have $p_\phi = -\rho_\phi$ which indicates a barotropic fluid with barotropic index $\gamma = 0$. By using this result, we can easily integrate the *full* Friedmann equation (2.2) with respect to $t$, to yield the exact solution for scale factor

$$a(t) = \begin{cases} a(t,k{=}{+1}) = & H_\infty^{-1}\cosh[H_\infty(t-t_0)] & \text{for a closed universe} \\ a(t,k{=}0) = & a_0\exp[H_\infty(t-t_0)] & \text{for a flat universe} \\ a(t,k{=}{-1}) = & H_\infty^{-1}\sinh[H_\infty(t-t_0)] & \text{for an open universe} \end{cases} \tag{2.47}$$

where $H_\infty^2 = 8\pi V_0/3m_{\rm Pl}^2$. As $t \to \infty$, we have $a(t,k{=}{+1}), a(t,k{=}{-1}) \to a(t,k{=}0)$ and $H \to H_\infty$, which indicates an *exponential* expansion. Moreover, the acceleration of the scale factor $\ddot{a}(t) = H_\infty^2 a(t) > 0$, which guarantees inflation to occur. This exponential expansion is known as the "**de Sitter expansion**". It is the extreme case of inflation and was first derived by de Sitter for a vacuum universe with a cosmological constant $\Lambda \equiv 8\pi V_0/m_{\rm Pl}^2 = 8\pi G V_0$. Because of its neat form and its assurance of inflation, the features of de Sitter epoch described above are commonly used for roughly describing the characteristics of inflation.

### 2.4.3 Power-law inflation

Another example in which the flat Friedmann model ((2.9) with $k = 0$ and (2.10)) can be solved exactly is the power-law inflation. Its potential takes the form

$$V(\phi) = V_0 \exp\left(-\sqrt{\frac{16\pi}{p}}\frac{\phi}{m_{\rm Pl}}\right) \tag{2.48}$$

where $V_0$ and $p$ are constant. It possesses an *exact* solution to the flat Friedmann model as

$$\phi(t) = \sqrt{\frac{p}{4\pi}}m_{\rm Pl}\ln\left(\sqrt{\frac{8\pi V_0}{p(3p-1)}}\frac{t}{m_{\rm Pl}}\right) \tag{2.49}$$

$$a(t) = a_p t^p \tag{2.50}$$

where $a_p$ is an arbitrary constant. From (2.49) and (2.50), one also have

$$H(\phi) = \sqrt{\frac{8\pi V_0 p}{3p-1}}m_{\rm Pl}\exp\left(-\sqrt{\frac{4\pi}{p}}\frac{\phi}{m_{\rm Pl}}\right) \tag{2.51}$$

For inflation to happen, we require

$$\ddot{a}(t) = a_p p(p-1)t^{p-2} > 0 \Longleftrightarrow p < 0 \;\; or \;\; p > 1 \tag{2.52}$$

Because the universe is expanding now, i.e. $\dot{a}(t) = a_p p t^{p-1} > 0$, the condition for inflation to occur is just $\underline{p > 1}$. This is called the "**power-law inflation**" since the solution of the scale factor possesses a power form [70, 11, 15, 55, 14]. Notice that if $p > 1$, $\ddot{a} > 0$ will hold true forever and inflation will continue indefinitely. However, in practice we usually use this model only in some limited regions of the potential and this requires further modification to the model to specify the end of inflation [55]. Once this step has been achieved, number of $e$-foldings can be given by

$$N(t_{\mathrm{i}}, t_{\mathrm{f}}) \equiv \ln\left(\frac{a(t_{\mathrm{f}})}{a(t_{\mathrm{i}})}\right) \overset{(2.50)}{=} p \ln\left(\frac{t_{\mathrm{f}}}{t_{\mathrm{i}}}\right) \overset{(2.49)}{=} \frac{\sqrt{4\pi p}}{m_{\mathrm{Pl}}}(\phi_{\mathrm{f}} - \phi_{\mathrm{i}}) \tag{2.53}$$

Another feature of this model is that the ratio of the potential energy $V(\phi)$ to the kinetic energy $\dot{\phi}^2/2$ is a constant. This can be seen by substituting (2.49) into (2.48) to yield $V \propto t^{-2}$, and by differentiating (2.49) with respect to $t$ to yield $\dot{\phi} \propto t^{-1}$.

Let us further consider the slow-roll approximation. Substituting (2.48) into (2.25) and (2.26) gives $\epsilon_V = 1/p \ll 1$ and $\eta_V = 2/p \ll 1$, i.e. $p \gg 1$ and $p \gg 2$ respectively. This confirms that the PSR conditions are sufficient but not necessary for inflation. Moreover, substituting (2.48) into (2.29) and (2.30) gives

$$\phi(t) = \sqrt{\frac{p}{4\pi}} m_{\mathrm{Pl}} \ln\left(\sqrt{\frac{8\pi V_0}{3p^2}} \frac{t}{m_{\mathrm{Pl}}}\right) \tag{2.54}$$

$$a(t) = a'_p t^p \tag{2.55}$$

respectively, where $a'_p$ is an arbitrary constant. This demonstrates the suitability and power of PSRA for analysing realistic models.

### 2.4.4 Intermediate inflation

The models which can be solved exactly are relatively few, although they are usually of special interest to cosmologists. A series of this sort of models was demonstrated by Barrow in 1990 [11]. His analysis was based on the following model equation of state:

$$\rho + p = \gamma \rho^{\lambda} \tag{2.56}$$

where $\gamma$ and $\lambda$ are constants. Substituting this into the flat Friedmann model gives

$$3H^2 = \rho \tag{2.57}$$

where $8\pi/m_{\mathrm{Pl}}^2$ has been normalized to unity for the convenience of later analysis, and

$$\dot{\rho} + 3\gamma H \rho^{\lambda} = 0 \tag{2.58}$$

Substituting (2.57) into (2.58) to eliminate $H$ and then integrating it with respect to $t$ yields

$$\rho(t) = \begin{cases} \rho_0 & \text{for} \quad \gamma = 0 \\ \rho_2 \exp(-\sqrt{3}\gamma\, t) & \text{for} \quad \lambda = \frac{1}{2},\ \gamma \neq 0 \\ \left[\sqrt{3}\gamma(\lambda - \frac{1}{2})\, t\right]^{2/(1-2\lambda)} & \text{for} \quad \lambda \neq \frac{1}{2},\ \gamma \neq 0 \end{cases} \tag{2.59}$$

where $\rho_0$ and $\rho_2$ are constants and an arbitrary integration constant has been removed by a translation of the time coordinate. Substituting this into (2.57) and then integrating it with respect to $t$ yields

$$a(t) = \begin{cases} a_0 \exp(\sqrt{\frac{\rho_0}{3}}\, t) & \text{for} \quad \gamma = 0 \\ a_1 t^{2/3\gamma} & \text{for} \quad \lambda = 1,\ \gamma \neq 0 \\ a_2 \exp[-\frac{2}{3}\rho_2^{1/2} \exp(-\frac{\sqrt{3}}{2}\gamma\, t)] & \text{for} \quad \lambda = \frac{1}{2},\ \gamma \neq 0 \\ a_3 \exp[(3^{\lambda}\gamma\frac{(\lambda-\frac{1}{2})^{2(1-\lambda)}}{(\lambda-1)^{1-2\lambda}} t^{2(1-\lambda)})^{1/(1-2\lambda)}] & \text{for} \quad \lambda \neq \frac{1}{2} \text{ or } 1,\ \gamma \neq 0 \end{cases} \tag{2.60}$$

where $a_0$, $a_1$, $a_2$ and $a_3$ are constants. This solution contains a wide range of behaviours parametrised by $\lambda$ and $\gamma$ [11]. Of particular interest are the following cases:

1. $\lambda = 1$, $\gamma = 0$: This solution is nothing but de Sitter expansion as introduced in subsection (2.4.2).

2. $\lambda = 1$, $2/3 > \gamma > 0$: The second case of (2.60) is just identical to power-law inflation as introduced in subsection (2.4.3).

3. $\lambda > 1$, $\gamma > 0$: The last case of (2.60) has the form $a(t) \propto \exp(At^f)$ with $A$ and $f$ constants. In general, we can rescale it to

$$a(t) = \exp(At^f) \tag{2.61}$$

   where

$$1 > f \equiv \frac{2(1-\lambda)}{1-2\lambda} > 0 \tag{2.62}$$

   This indicates a behaviour with expansion proceeding at a rate between de Sitter and power-law inflation. Therefore, it is the so-called "**intermediate inflation**" [11, 15, 13, 80].

Let us investigate intermediate inflation as follows. For $\rho \equiv \rho_\phi = \dot{\phi}^2/2 + V(\phi)$, by differentiating (2.57) and using (2.10) to eliminate the terms involving $V'(\phi)$ and $\ddot{\phi}$, we

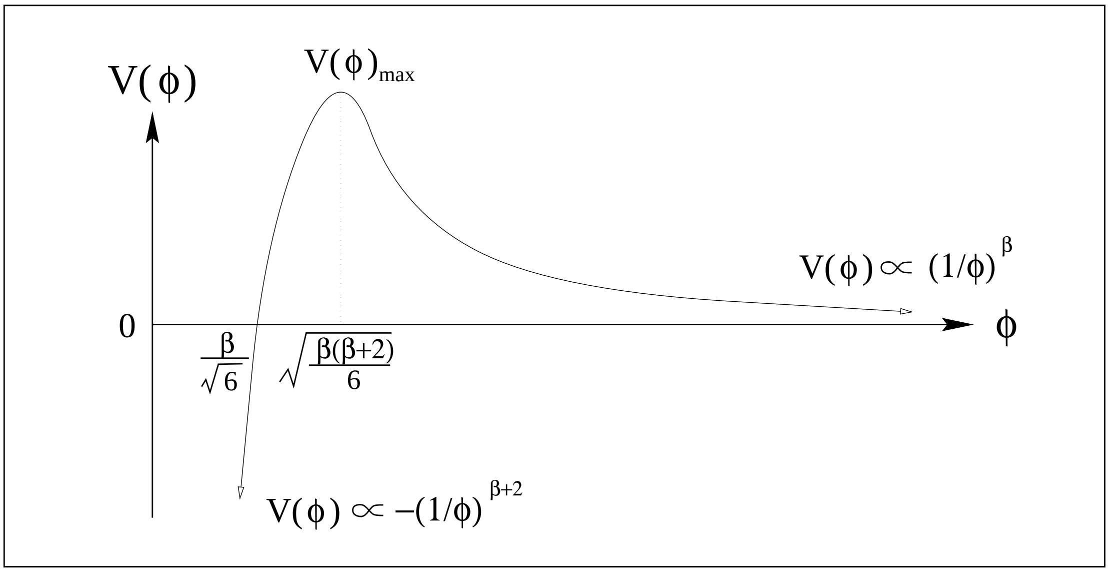


Figure 2.3: The potential form of intermediate inflation: It has a solution anywhere for $\phi > 0$. In this region, the potential approaches $-\infty$ as $\phi \to 0$, is negative for $0 < \phi^2 < \beta^2/6$, increases to a maximum at $\phi^2 = \beta(\beta+2)/6$ and then falls to zero as $1/\phi^\beta$ as $\phi \to \infty$.

obtain $2\dot{H} = -\dot{\phi}^2$. Since $\dot{H}$ can be calculated by using (2.61), we can assume $\dot{\phi} > 0$ and then integrate the last equation we obtain to yield

$$\phi(t) = \sqrt{2A\beta}\, t^{f/2} \tag{2.63}$$

where $\beta = 4(f^{-1} - 1) > 0$ and an arbitrary integration constant has been removed. Thus the Hubble parameter can be obtained by using (2.61) and (2.63):

$$H(\phi) = Af(2A\beta)^{\beta/4}\phi^{-\beta/2} \tag{2.64}$$

Substituting (2.63) and (2.64) back to (2.57) with $\rho \equiv \dot{\phi}^2/2 + V(\phi)$ yields the potential form:

$$V(\phi) = \frac{8A^2}{(\beta+4)^2}\left(\frac{\sqrt{2A\beta}}{\phi}\right)^{\beta}\left(6 - \frac{\beta^2}{\phi^2}\right) \tag{2.65}$$

It is calculable anywhere for $\phi > 0$. In this region, the potential is negative for $\beta^2/6 > \phi^2 > 0$, increases to a maximum at $\phi^2 = \beta(\beta+2)/6$ and then falls to zero as $\phi \to \infty$ (see Figure 2.3).

Furthermore, by substituting (2.61) and (2.63) into (2.5), the condition for inflation can be given exactly as

$$\ddot{a} > 0 \quad \Longleftrightarrow \quad t > \left(\frac{\beta}{4A}\right)^{1/f} \quad \Longleftrightarrow \quad \phi^2 > \frac{\beta^2}{2} \tag{2.66}$$

Comparing this with the analysis after (2.65), we see: for $\beta < 1$, inflation can occur on the left-hand side of the maximum of the potential. Notice that (2.63) does not guarantee a monotonic relation between $\phi$ and $t$ since the assumption $\dot{\phi} > 0$ has been used to derive (2.63). Therefore, inflation can last a long time only if the initial $\dot{\phi}$ is large enough to bring the inflaton across over the maximum to its right-hand side, which avoids the change of the sign of $\dot{\phi}$; for $\beta > 1$, inflation can only occur beyond the maximum. In this case, since we see no natural end to inflation from (2.66), as with power-law inflation we need further assumption [12, 14] to specify the end of inflation. Having this done, number of $e$-foldings can be calculated as

$$N(t_{\rm i}, t_{\rm f}) \equiv \ln\left(\frac{a(t_{\rm f})}{a(t_{\rm i})}\right) \overset{(2.61)}{=} A(t_{\rm f}^f - t_{\rm i}^f) \overset{(2.63)}{=} \frac{1}{2\beta}(\phi_{\rm f}^2 - \phi_{\rm i}^2) \tag{2.67}$$

Notice that since the form of the Hubble parameter (2.64) is available, we can alternatively use the definition of $\epsilon_H$ in (2.35) and (2.40) to yield exactly the same results as in (2.66) and (2.67) apart from a factor normalized in (2.57).

Once again, we solved this model exactly without using any approximation. However, the models introduced since subsection 2.4.2 are amongst the few examples solved exactly in the literature. Other models must be solved with recourse to some approximation like PSRA or HSRA. More examples are given as follows.

### 2.4.5 Chaotic inflation

In the historic development of inflation, a very simple and elegant model that successfully implements inflation was introduced by Linde in 1983—"**chaotic inflation**" [66]. There is no concept of spontaneous symmetry breaking in this model and the scalar field here is not necessarily part of any unified theory. The term "chaotic" refers to the initial distribution of the scalar field being chaotic due to wild thermal and quantum fluctuations. Therefore, the only constraint to this model is that the scalar energy density $\rho_\phi$ is less than the Planck density $m_{\rm Pl}^4$. Its potential takes the simple form:

$$V(\phi) = \frac{1}{2}m^2\phi^2 \tag{2.68}$$

which corresponds to a massive scalar field with no interaction. Even for such a simple model, the Friedmann equation and the equation of $\phi$-motion are still difficult to solve. However, if we use **PSRA**, the equations can be rewritten as

$$H^2 = \frac{4\pi m^2\phi^2}{3m_{\rm Pl}^2} \tag{2.69}$$

$$3H\dot{\phi} + m^2\phi = 0 \tag{2.70}$$

Supposing inflation starts at $t_{\rm i} = 0$ with an initial value of the scalar field $\phi_{\rm i} > 0$ rolling towards $\phi = 0$, recalling (2.29) and (2.30) yields

$$t(\phi) = \frac{\sqrt{12\pi}}{m m_{\rm Pl}}(\phi_{\rm i} - \phi) \tag{2.71}$$

and

$$a(t) = a(0) \exp\left[\sqrt{\frac{4\pi}{3}}\frac{m}{m_{\rm Pl}}\left(\phi_{\rm i} - \frac{m m_{\rm Pl}}{\sqrt{48\pi}}t\right)t\right] \tag{2.72}$$

We see at the beginning the expansion is exponential and, therefore, inflationary.

Now we take the equality in the PSR conditions (2.25) and (2.26) as an indicator of the end of inflation and find these two conditions yield the same result

$$\phi_{\rm f} = \frac{m_{\rm Pl}}{\sqrt{4\pi}} \tag{2.73}$$

so that by (2.71)

$$t_{\rm f} = \frac{\sqrt{12\pi}}{m m_{\rm Pl}}\phi_{\rm i} - \frac{\sqrt{3}}{m} \tag{2.74}$$

Therefore, the number of $e$-foldings can be calculated by using (2.73) and (2.31) as

$$N(t_{\rm i}, t_{\rm f}) \overset{PSRA}{\simeq} -\frac{8\pi}{m_{\rm Pl}^2}\int_{\phi_{\rm i}}^{\phi_{\rm f}} \frac{V(\phi)}{V'(\phi)}d\phi = \frac{2\pi}{m_{\rm Pl}^2}\phi_{\rm i}^2 - \frac{1}{2} \tag{2.75}$$

which is independent of $m$. Its maximum value is taken when $\phi$ starts from rest at a potential around Planck scale, i.e. $\rho_{\phi_{\rm i}} \equiv V(\phi_{\rm i}) = m^2\phi_{\rm i}^2/2 \simeq m_{\rm Pl}^4$. This gives $\phi_{\rm i(max)} \simeq \sqrt{2}m_{\rm Pl}^2/m$ and

$$N(t_{\rm i}, t_{\rm f})_{\rm max} \simeq 4\pi\frac{m_{\rm Pl}^2}{m^2} - \frac{1}{2} \tag{2.76}$$

As we suggest in subsection (2.2.5), $N(t_{\rm i}, t_{\rm f})_{\rm max}$ should be at least 80. This yields the condition

$$m \leq 0.4 m_{\rm Pl} \tag{2.77}$$

which indicates that sufficient inflation is easily provided. The lighter the mass of the scalar field, the larger the maximum amount of chaotic inflation will be. So far, we have obtained the relevant features of the chaotic inflationary model by using PSRA.

### 2.4.6 Self-coupling inflation

In addition to the potential form introduced above, chaotic inflation also refers to models based on other simple forms. Another example is taken as

$$V(\phi) = \frac{\lambda}{4}\phi^4 \tag{2.78}$$

where $\lambda$ is a dimensionless constant. This is usually referred to as "**self-coupling inflation**". Now using **PSRA** and following the same logical sequence as in subsection 2.4.5, we investigate this model as follows.

Using PSRA gives the Friedmann equation and the equation of $\phi$-motion as

$$H^2 = \frac{2\pi\lambda\phi^4}{3m_{\rm Pl}^2} \tag{2.79}$$

$$3H\dot{\phi} + \lambda\phi^3 = 0 \tag{2.80}$$

Supposing inflation starts at $t_{\rm i} = 0$ with $\phi_{\rm i} > 0$ rolling towards $\phi = 0$, recalling (2.29) and (2.30) yields

$$t(\phi) = \sqrt{\frac{6\pi}{\lambda m_{\rm Pl}^2}}(\ln\phi_{\rm i} - \ln\phi) \tag{2.81}$$

and

$$a(t) = a(0)\exp\left\{\frac{\pi\phi_{\rm i}^2}{m_{\rm Pl}^2}\left[1 - \exp\left(-\sqrt{\frac{2\lambda m_{\rm Pl}^2}{3\pi}}\,t\right)\right]\right\} \tag{2.82}$$

We see that, at the beginning when $t^2 \ll 3\pi/2\lambda m_{Pl}^2$, expanding the internal exponent of (2.82) yields

$$a(t) \simeq a(0)\exp\left\{\left(\frac{8\pi}{3m_{\rm Pl}^2}\frac{\lambda\phi_{\rm i}^4}{4}\right)^{1/2} t\right\} \tag{2.83}$$

This indicates an approximately exponential expansion. Comparing this with (2.47), we find (2.83) is precisely identical to a de-Sitter expansion with $V_0 = \lambda\phi_{\rm i}^4/4$.

Now taking the equality in the PSR conditions (2.25) and (2.26) gives

$$\phi_{\rm f}(\epsilon_V = 1) = \frac{m_{\rm Pl}}{\sqrt{\pi}} \tag{2.84}$$

$$\phi_{\rm f}(\eta_V = 1) = \sqrt{\frac{3}{2}}\frac{m_{\rm Pl}}{\sqrt{\pi}} \tag{2.85}$$

respectively. Since the PSR conditions are just sufficient but not necessary for inflation, we take (2.84) as a tolerable indicator of the end of inflation to obtain

$$t_{\rm f} = \sqrt{\frac{3\pi}{2\lambda m_{\rm Pl}^2}}\ln\left(\frac{\pi\phi_{\rm i}^2}{m_{\rm Pl}^2}\right) \tag{2.86}$$

Then the number of $e$-foldings can be calculated by using (2.84) and (2.31) as

$$N(t_{\rm i}, t_{\rm f}) \overset{PSRA}{\simeq} -\frac{8\pi}{m_{\rm Pl}^2}\int_{\phi_{\rm i}}^{\phi_{\rm f}}\frac{V(\phi)}{V'(\phi)}d\phi = \frac{\pi}{m_{\rm Pl}^2}\phi_{\rm i}^2 - 1 \tag{2.87}$$

which is independent of $\lambda$. Its maximum value is taken when $\rho_{\phi_{\rm i}} \equiv V(\phi_{\rm i}) = \lambda\phi_{\rm i}^4/4 \simeq m_{\rm Pl}^4$. This gives $\phi_{\rm i(max)}^2 \simeq 2m_{\rm Pl}^2/\sqrt{\lambda}$ and

$$N(t_{\rm i}, t_{\rm f})_{\max} \simeq \frac{2\pi}{\sqrt{\lambda}} - 1 \tag{2.88}$$

Getting sufficient inflation requires $N(t_{\mathrm{i}}, t_{\mathrm{f}})_{\mathrm{max}} \geq 80$. This yields the condition

$$\lambda \leq 6 \times 10^{-3} \tag{2.89}$$

The smaller the self-coupling constant is, the larger the maximum amount of self-coupling inflation will be. Again, we have solved self-coupling inflationary model by using PSRA.

### 2.4.7 Hybrid inflation

Recently a new type of inflation has been favoured because it seems to have good prospects for particle physics model building. The potential energy of this model possesses a generic form:

$$V = V(\phi, \psi) \tag{2.90}$$

where $\phi$ and $\psi$ are two interacted scalar fields: $\phi$ is the inflaton and $\psi$ is the noninflaton. This is known as "**hybrid inflation**". It possesses special distinctions to other models, such as the much lower energy scale at the end of inflation and a different predicted behaviour of the spectrum of density perturbation. The phenomenology in this regime is also more complicated than other models, including the possibility for inflation to restart after its first end. In variants of this model, neither exact analytical solution is valid nor the slow-roll approximation is sufficient. Therefore, **numerical techniques** are desired to obtain the exact solution of hybrid inflation. This model will be independently investigated in more detail in Chapter 4.

CHAPTER 3

# DENSITY PERTURBATIONS AND GRAVITATIONAL WAVES

A feature of inflation overriding the standard Hot Big Bang model is that inflation provides a mechanism to seed the density perturbation in the universe that may be responsible for the later formation of large-scale structure. In the standard Hot Big Bang model, this perturbation must be dealt as a part of its initial conditions, which is far too unnatural. In this Chapter, we shall consider the way inflation allows the generation of the perturbations in the early universe. Of particular interest is how well the form of such a perturbation can be used to interpret the observed anisotropies in the CMB. The forms generated by various inflationary models will be investigated. Comparing these forms with the observation can yield further constraints on our models. We shall also consider the possibility for inflation to generate gravitational waves, since they would hopefully be a probe into the very early universe due to their very weak coupling with ordinary matter. Let us begin by discussing the mechanical aspect of inflation that makes the generation of density perturbations possible.

## 3.1 Origin of Perturbations

As we have seen in the previous chapter, the whole point of inflation is that a patch much larger than our present horizon was in causal contact in the pre-inflationary epoch. This allows not only the overall homogeneity and isotropy of the observable universe to be explained properly, but also the fluctuations at the early time to be responsible for large-scale structure formation and the large-scale anisotropies COBE sees. This is provided by the combination of quantum fluctuations in the scalar field and the decreasing comoving horizon size during inflation.

### 3.1.1 The mechanism

As indicated in subsection 2.1.1, the only particle concerned in the inflationary regime is the inflaton $\phi$. Since its energy density will be converted into ordinary matter which is observable today, the behaviour of $\phi$ in the early universe should be responsible for the observed density perturbation. Assume that the scalar field can be decomposed into a homogeneous background and small perturbations:

$$\phi(\mathbf{x},t) = \phi_0(t) + \delta\phi(\mathbf{x},t) \tag{3.1}$$

where $\mathbf{x}$ denotes the comoving position coordinates and $t$ the cosmic time. Then we expand each perturbation into its Fourier components:

$$\delta\phi(\mathbf{x},t) = \sum_k \delta\phi_k(t)e^{i\mathbf{kx}} \simeq \frac{V}{(2\pi)^3}\int \delta\phi_k(t)e^{i\mathbf{kx}}d^3k \tag{3.2}$$

where the Fourier transform is carried out in a very large box of comoving volume $V$:

$$\delta\phi_k(t) = \frac{1}{V}\int_{\text{vol}} \delta\phi(\mathbf{x},t)e^{-i\mathbf{kx}}d^3x \tag{3.3}$$

and $k \equiv 2\pi/\lambda$ is the "comoving wave number" where $\lambda$ is the concerned comoving scale. Provided the perturbations are linear and $\phi$ is weakly coupled during the inflationary era, each comoving wave mode, $k$, evolves independently. For a massless inflaton in flat spacetime, to the lowest order, perturbing equation (2.10) gives a linear wave equation for the classical evolution of a given mode $k$:

$$\delta\ddot{\phi}_k + 3H\delta\dot{\phi}_k + \left(\frac{k}{a}\right)^2\delta\phi_k = 0 \tag{3.4}$$

Let us consider its solutions in the following two cases:

1. $k^{-1} \ll H^{-1}/a$: The solution has the form $\delta\phi_k \propto exp[\pm i(k/a)t]$. This means that the wave modes with wavelength much shorter than the comoving horizon are insensitive to the expansion and oscillate stably inside the horizon.

2. $k^{-1} \gg H^{-1}/a$: The perturbation will approach to a constant, i.e. $\delta\phi_k \to constant$ due to the frictional damping of the Hubble expansion. This means that the wave modes with wavelength much longer than the comoving horizon are "frozen in" outside the horizon.

As we know from (2.12) that during inflation the comoving horizon keeps decreasing ($H^{-1}/a$ decreases), some wave modes which are initially inside the horizon ($H^{-1}/a > k^{-1}$)

will be subsequently crossed by the horizon ($H^{-1}/a < k^{-1}$). Supposing there exists quantum fluctuations in $\phi$ for a given mode $k$, the decreasing comoving horizon causes the fluctuations, which can cancel themselves out inside the horizon, being suddenly frozen in outside the horizon since the horizon size is the measure of causally connected regions. Finally the quantum fluctuations in $\phi$ become classical perturbations $\delta\phi_k$ provided by (3.4) when $k^{-1} \gg H^{-1}/a$. The watershed between these two epochs is specified by $k = aH$. When inflation ends and rejoins the standard Big Bang evolution, the comoving horizon increases again ($H^{-1}/a$ increases) and finally re-reaches the modes it crossed during inflation. When the previously frozen perturbations re-entre the horizon, they become the origin of the large-scale structure formation and the observed anisotropies in CMB. Generally, for a given wave number $k$ the two epochs at which $k = aH$ are referred to as "**horizon crossings**". As can be clearly seen in Figure 3.1, in inflationary cosmology the scales are "first out-last in" [52]. This mechanism is a dramatic effect of inflation in the historic development of cosmology.

### 3.1.2 The epoch of horizon exit

Before we can analyse the spectrum of perturbations, we have to know *when* a given scale crosses outside the horizon during inflation, i.e. the epoch of horizon exit. This is the first epoch of horizon crossings and we shall use a subscript "*" to denote it. Thus for a given scale one has

$$k = a_* H_* \tag{3.5}$$

A convenient way to specify this epoch is by the number of $e$-foldings $N(t_\mathrm{i}, t_\mathrm{f})$. We know $t_\mathrm{f}$ is specified by (2.5); however, $t_\mathrm{i}$ can be replaced by any epoch before the end of inflation so that the number of $e$-foldings can be dealt with as an indicator of the epoch of horizon exit. By (2.6) we can define

$$N_* \equiv N(t_*, t_\mathrm{f}) \equiv \ln\left(\frac{a_\mathrm{f}}{a_*}\right) \overset{(2.40)}{=} -\frac{4\pi}{m_\mathrm{Pl}^2}\int_{\phi_*}^{\phi_\mathrm{f}} \frac{H(\phi)}{H'(\phi)} d\phi \tag{3.6}$$

From Figure 3.1, we see there are four stages between the epoch of horizon exit and present: inflation; reheating process denoted by "reh" and dominated by matter; radiation domination ended by "eq" at which the radiation density is equal to the matter density; and matter domination until present denoted by "0". We know throughout the history of the universe the radiation density $\rho_\mathrm{r} \propto a^{-4}$ and the matter density $\rho_m \propto a^{-3}$ so that (3.5)

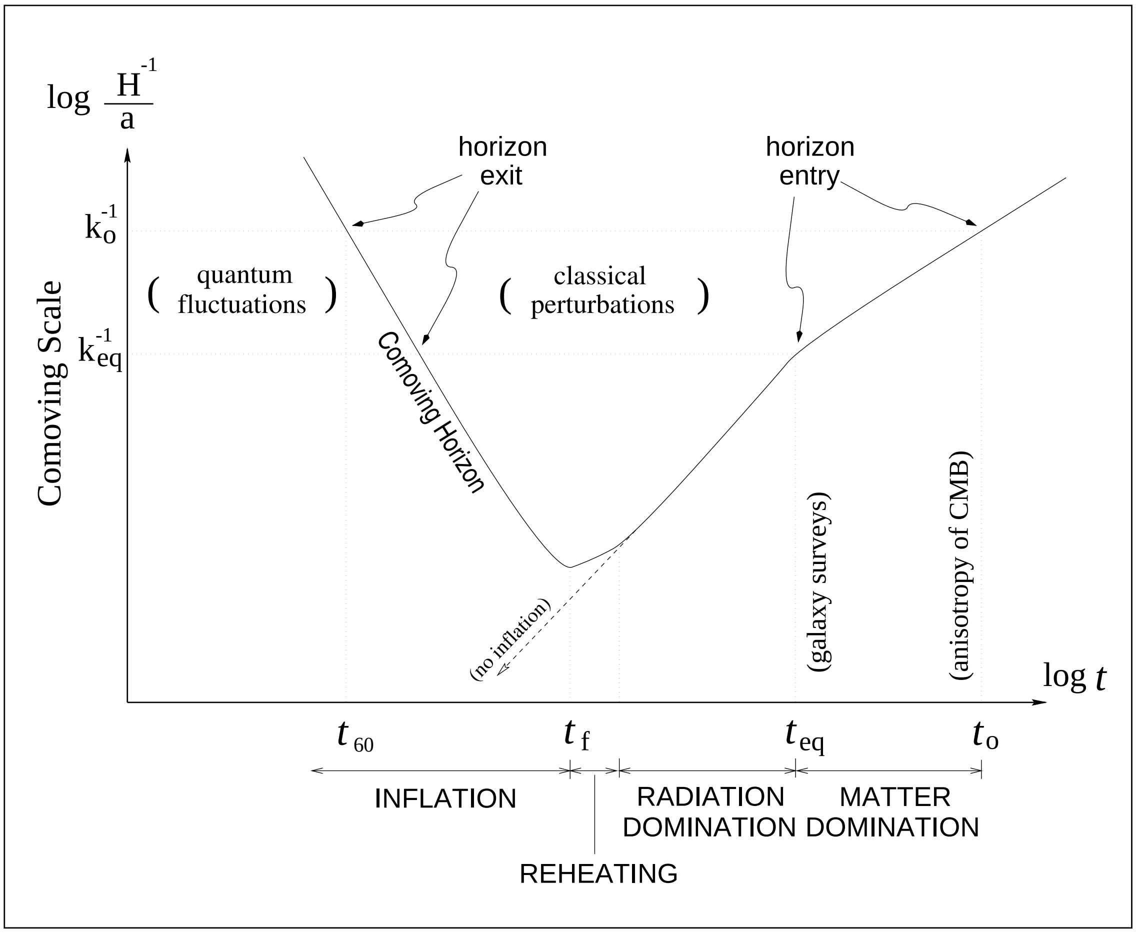


Figure 3.1: The evolution of the comoving horizon, $H^{-1}/a$, and of the wave mode with wave number $k$ in comoving space. In the standard Big Bang evolution (i.e. no inflation), a given scale can cross the horizon only once; in inflationary cosmology, the scale begins sub-horizon size, crosses outside the horizon ("horizon exit") during inflation, and re-enters it again ("horizon entry") during the post-inflationary era.

can be rearranged as

$$\frac{k}{a_0 H_0} = \frac{a_*}{a_{\rm f}}\frac{a_{\rm f}}{a_{\rm reh}}\frac{a_{\rm reh}}{a_0}\frac{H_*}{H_0} = \exp(-N_*)\left(\frac{\rho_{\rm reh}}{\rho_{\rm end}}\right)^{1/3}\left(\frac{\rho_{\rm r0}}{\rho_{\rm reh}}\right)^{1/4}\left(\frac{\rho_*}{\rho_0}\right)^{1/2} \tag{3.7}$$

where we have assumed that instantaneous transitions occur between regimes. Thus we have

$$N_* = 62 - \ln\frac{k}{a_0 H_0} - \ln\frac{10^{16}\text{GeV}}{V_*^{1/4}} + \ln\frac{V_*^{1/4}}{V_{\rm f}^{1/4}} - \frac{1}{3}\ln\frac{V_{\rm f}^{1/4}}{\rho_{\rm reh}^{1/4}} \tag{3.8}$$

Because of the "first out-last in" property of the scales, the largest one we can explore is at the present horizon crossing (or, alternatively, present "horizon entry"), i.e. $k_0 = a_* H_* = a_0 H_0$. To a reasonable degree [57, 73], by (3.8) we take $N_* = \mathbf{60}$ as the epoch at which this largest scale leaves the horizon during inflation. We shall denote this epoch by subscript "60", like $t_{60}$, rather than by subscript $*$ like $t_*$ (see Figure 3.1). This largest observable scale is also the one associated with the anisotropies COBE sees. The other observable scales are smaller and responsible for the large-scale structure formation. They leave the horizon at $N_* < 60$ during inflation (see Figure 3.1). For the convenience of later use, we shall normalize the scale factor to be unity at the present epoch, i.e. $a_0 = 1$, so that the physical coordinates now coincide with the comoving ones.

Recalling the minimum number of $e$-foldings, 80, required in subsection 2.2.5 for solving the problems of Big Bang model, we see that the epoch of $t_{60}$ is guaranteed to lie with a clear margin in the inflationary era. Thus at horizon exit $k = a_* H_*$, from (3.6) one can surely have $\ln k(\phi_*) = \ln a_{\rm f} - N_* + \ln H(\phi_*)$. Differentiating this with respect to $\phi_*$ and using (3.6) yields

$$\frac{d\ln k}{d\phi_*} = \frac{4\pi}{m_{\rm Pl}^2}\frac{H(\phi_*)}{H'(\phi_*)}(\epsilon_{H*} - 1) \tag{3.9}$$

which is a measure of how rapidly scales pass through the horizon at horizon exit as compared to the evolution of the scalar field. This will be useful in later analysis.

## 3.2 The Spectrum of Density Perturbations

### 3.2.1 Definitions

For a general inhomogeneous field, the energy density of the universe can be written as $\rho(\mathbf{x}, t)$. We define a dimensionless quantity known as the "**density contrast**":

$$\delta(\mathbf{x}, t) = \frac{\rho(\mathbf{x}, t) - \bar\rho(t)}{\bar\rho(t)} \tag{3.10}$$

where $\bar{\rho}(t)$ is the mean density. As an analogue to the analysis of $\delta\phi(\mathbf{x}, t)$ in the previous section, we can decompose $\delta(\mathbf{x}, t)$ into its Fourier series as

$$\delta(\mathbf{x}, t) = \sum_k \delta_k(t) e^{i\mathbf{kx}} \tag{3.11}$$

where the Fourier transform is carried out in a very large box of comoving volume $V$:

$$\delta_k(t) = \frac{1}{V} \int_{\text{vol}} \delta\phi(\mathbf{x}, t) e^{-i\mathbf{kx}} d^3x \tag{3.12}$$

Notice that $\delta_k(t)$ is complex because it possesses the information of both the phase and the amplitude. We can consider the normalized size of its Fourier amplitudes. This quantity evaluated at the *present* epoch (matter domination) is known as the "spectrum of the matter density contrast" [89, 74]:

$$\mathcal{P}_\delta(k) = V \left( \frac{k^3}{2\pi^2} \right) \langle |\delta_k|^2 \rangle \tag{3.13}$$

Alternatively, by considering the evolution of the spectrum from its initial form, one obtains [82, 19, 52]

$$\mathcal{P}_\delta(k) = \delta_H^2(k) T^2(k) \left( \frac{k}{H_0} \right)^4 \tag{3.14}$$

where $T(k)$ is the "transfer function" determining the evolution of the spectrum and the quantity $\delta_H^2(k)$ specifies the initial spectrum, i.e. when $T(k) = 1$. The form of $T(k)$ is model-dependent. We shall use the CDM (cold dark matter) model. In this regime, for the scales $k^{-1} > 8h^{-1}$Mpc which[1] covers the observable range today ($20h^{-1}$Mpc for IRAS/QDOT [91] and POTENT [18] galaxy surveys, $10^3h^{-1}$Mpc for COBE [94], etc.), the dependence is weak [34], i.e. $T(k) \simeq 1$ on large scales. Notice that in (3.14) the subscript $H$ of $\delta_H^2(k)$ is used because at the scale of present horizon entry, $k_0 = a_{60}H_{60} = H_0$, $\delta_H^2(k)$ is exactly equal to $\mathcal{P}_\delta(k)$. Therefore, $\delta_H(k)$ is called the "**density contrast at horizon crossing**" (cf. (3.10)) and is sometimes denoted alternatively as $(\delta\rho/\rho)|_{\text{hor}}$. As we have seen in the previous section that the comoving horizon size $H^{-1}/a$ varies across the whole range of observable scales after the end of inflation, the entire perturbation spectrum can be specified by giving the density contrast at horizon crossing, $\delta_H$, as a function of horizon size. This is more convenient than giving the density contrast on each scale, $\delta_k$, at a given epoch.

[1] Here $h$ is the present Hubble parameter $H_0$ in units of $100\text{kms}^{-1}\text{Mpc}^{-1}$, and we take $h = 0.5$.

### 3.2.2 Power spectrum

To investigate the behaviour of the spectrum, we define the "**power spectrum**" as

$$P(k) = \mathcal{P}_\delta(k)\frac{2\pi^2}{Vk^3} = \langle|\delta_k|^2\rangle \tag{3.15}$$

For the convenience of analysing its behaviour across a range of scales, we assign a power-law form for it as an approximation:

$$P(k) \propto k^n \tag{3.16}$$

where $n$ is known as the "spectral index". By comparing (3.14), (3.15) and (3.16), we yield a further relation

$$\delta_H^2(k) \propto k^{n-1} \tag{3.17}$$

Since the form (3.16) is taken as an approximation, generally we expect the spectral index to be a function of scales, i.e. $n \equiv n(k)$. However, because the range of scales of our interest is small, we expect the dependence of the index on scales could be weak. In other words, for the scales around $10^3h^{-1}\text{Mpc} \gtrsim k^{-1} \gtrsim 8h^{-1}\text{Mpc}$, $n$ can be often approximated as a constant and thus $P(k)$ indeed satisfies power-laws. This is called the "**power-law spectrum**". We shall discuss this further in subsection 3.3.1.

### 3.2.3 Scale-invariant spectrum

Let us consider the perturbations at the scale of horizon entry. Suppose the comoving radius of the horizon at a *fixed* epoch $t$ is $H^{-1}/a$ and the mass contained inside is $M$ such that we have $M \propto (H^{-1}/a)^3$. Then the density contrast $\delta(\mathbf{x}, t) \equiv \delta(\mathbf{x})$ has a mean square given by

$$\langle\delta^2(\mathbf{x})\rangle_M \equiv \sigma^2(M) = \frac{1}{2\pi^2}\int_0^\infty P(k)W(k,M)k^2dk \tag{3.18}$$

where $W(k, M)$ is a window function which describes the manner in which the fluctuations are measured. As we have seen in Section 3.1.1, fluctuations with scales well inside the horizon ($k^{-1} \ll H^{-1}/a$) will average out to zero and those with scales outside the horizon ($k^{-1} \gg H^{-1}/a$) contribute fully so that $W(k, t)$ is one. Therefore, we can take $W(k, t)$ as a step function with truncation at $k = (H^{-1}/a)^{-1}$ and substitute (3.15) into (3.18) to obtain

$$\sigma^2(M) \simeq \frac{1}{2\pi^2}\int_0^{(H^{-1}/a)^{-1}} k^{n+2}dk \propto (H^{-1}/a)^{-(n+3)} \propto M^{-(n+3)/3} \tag{3.19}$$

Putting in the time dependence $\delta_k(t) \propto t^{2/3}$ for a matter-domination regime in a flat Friedmann model [10, 52] and using $M \propto \rho H^{-3} \propto (t^{-2})(t^3) = t$ yields[2]

$$\sigma^2(M,t) \propto \left(t^{2/3}\right)^2 M^{-(n+3)/3} \propto M^{[4/3-(n+3)/3]} \tag{3.20}$$

We see if and only if n=1, the mean amplitude of the density perturbation at horizon entry maintains constant. Thus a power spectrum with $\underline{n=1}$ is called the "**scale-invariant**" spectrum, i.e. $P(k) \propto k$ or alternatively $\mathcal{P}_\delta(k) \propto k^4$. This was first advocated by Harrison and by Zel'dovich in 1970 [44, 107] and is also called Harrison-Zel'dovich spectrum. In this regime, we see from (3.17) that $\delta_H^2(k) \equiv \delta_H^2$ is k-independent and therefore specified by a single number.

The scale-invariant spectrum is of great importance when we consider the smoothness problem of the Big Bang model. In that case we require a particular form of initial density perturbation spectrum to produce structure across a wide range of scales and the overall homogeneities on the microwave sky. In order to solve the smoothness problem, this scale-invariant spectrum becomes a *required* feature of inflation and was widely assumed before the 1990's. However, from recent investigation of the spectrum with increasing precision [36, 102, 58, 57, 56], a distinguishable deviation from scale invariance can be important. In this case, a more precise framework is required. We shall see this in the next Section.

## 3.3 Inflationary Perturbations

Before we explore the spectrum of perturbations, we have to consider the origin of "perturbations" in cosmology. Assuming that in the early universe departures from homogeneities and isotropies are small, we can apply cosmological perturbation theory to develop *linear* equations for the perturbations which are valid to first order. Following Lifshitz's analysis in 1946 [63] using the metric perturbation approach, the perturbations associated with the energy-momentum tensor of a perfect fluid form can be divided into three *independent* modes: "density perturbation", "gravitational waves" and "vorticity". Because the last one has been shown to decay significantly with time [104, 79], by the present epoch we concern ourselves only with the first two modes. In the inflationary regime, the density is specified by a scalar field and therefore its perturbations have scalar forms. We shall use "$A_S(k)$" to denote its contribution to the full spectrum of perturbations for a given

[2] $\rho \propto t^{-2}$ holds true for all barotropic fluid in a flat Friedmann model. For details see Sections 2.1 and 2.2.1 in Chapter 2; $H^{-1}$ is the physical horizon size which grows proportional to $t$.

scale $k^{-1}$. For the same reason, because the graviton possesses a tensor form, we shall use "$A_T(k)$" to denote the contribution from gravitational waves.

Before the 1990's, because of limitations of observational techniques, only a fairly limited range of scales could be observed to constrain the spectrum of perturbation. Therefore, it was satisfactory at that time to treat inflation as a mechanism of generating scale-invariant spectrum of density perturbations with a negligible gravitational waves. However, after COBE detection [17, 94, 106], a much wider range of scales were covered so that the tilt from scale invariance was constrained and a number of authors reexamined the spectra contributed by not only density perturbation but also gravitational waves [3, 29, 32, 54, 56, 61, 71, 87, 95]. We shall explore both cases.

### 3.3.1 Density perturbation

Qualitatively, fluctuations in the scalar field $\phi$ arise from the fact that the field reaches the true vacuum at different time in different places in the universe. This causes a non-uniform distribution in density $\rho$ due to different $\dot{\phi}$ in different regions for a given time. As we have seen in subsection 3.1.1 that the microphysics of quantum fluctuations in $\phi$ is frozen in after horizon exit and reentres the horizon at horizon entry. Thus the condition $k \ll aH$ determines the form of the spectrum of density perturbation we are to derive. In addition, the density perturbation we are to consider here is adiabatic. It has been shown that, in the inflationary regime, even the isocurvature density perturbation arising from the axion could not survive [76]. We shall ignore the isocurvature perturbation from now on.[3]

An analysis of the spectrum of density perturbations was provided by Lyth & Stewart in 1992 [75]. They used linear scalar metric perturbation formulae provided by Bardeen [10] and by Kodama & Sasaki [48] to calculate the curvature perturbation $\mathcal{R}$ [90]. Since $\phi$ is considered as matter, following the matter sector $S_M$ of the full Einstein action [79] and applying quantum theory yields the form of the curvature perturbation and thus the form of the spectrum $\mathcal{P}_{\mathcal{R}}$. However, this form is not calculable in general circumstances. By applying the power-law inflationary model in this final form and taking $k \ll aH$,

[3] In the literature, the axion field is the only potential candidate to generate an isocurvature perturbation; even if we consider more generally the effect arising from an isocurvature perturbation in the CMB anisotropy, we find the isocurvature density perturbation can be only a small fraction of the total density perturbation [35, 49].

they found an exact solution. In a slightly different way, Stewart & Lyth [101] expanded the HSR parameters ($\epsilon_H - \eta_H$) instead of treating them as constant in the power-law inflationary regime (see subsection 2.4.3) and yielded a solution which is true for *general* inflation potentials. To the next order, this spectrum is given by

$$\mathcal{P}_{\mathcal{R}}^{1/2}(k) \simeq \frac{2}{m_{\rm Pl}^2}[1-(2C+1)\epsilon_H + C\eta_H]\left.\frac{H^2}{|H'|}\right|_* \tag{3.21}$$

where $C \simeq -0.73$. Notice here that the calculated value of $\mathcal{P}_{\mathcal{R}}^{1/2}(k)$ is the asymptotic value when $k \ll aH$, but expressed in terms of the quantities at horizon exit. Because in a matter-dominated universe the spectrum of the initial curvature perturbation is related to the density contrast at horizon crossing (in (3.14)) due to Bardeen [10] (in which we take $p/\rho = 0$):

$$\frac{2}{5}\mathcal{P}_{\mathcal{R}}^{1/2}(k) = \delta_H(k) \tag{3.22}$$

we shall take the rescaled spectrum of density perturbation as

$$A_S(k) = \frac{2}{5}\mathcal{P}_{\mathcal{R}}^{1/2}(k) \overset{(3.21)}{\simeq} \frac{4}{5m_{\rm Pl}^2}[1-(2C+1)\epsilon_H + C\eta_H]\left.\frac{H^2}{|H'|}\right|_* \tag{3.23}$$

so that $A_S(k)$ coincides with $\delta_H(k)$.

Actually, soon after inflation was proposed [40], $\delta_H(k)$ was calculated in terms of the inflationary potential by several people [42, 45, 96, 9]. An approximated result is [9, 90]

$$\delta_H(k) = \left.\frac{H^2}{5\pi|\dot{\phi}|}\right|_* \tag{3.24}$$

By using PSRA (2.23) and (2.24) to eliminate $H$ and $\dot{\phi}$, (3.24) can be rewritten as

$$\delta_H(k) \overset{PSRA}{\simeq} \sqrt{\frac{512\pi}{75}}\left.\frac{V^{3/2}}{m_{\rm Pl}^3|V'|}\right|_* = \sqrt{\frac{32}{75}}\left.\frac{V^{1/2}}{m_{\rm Pl}^2\epsilon_V^{1/2}}\right|_* \tag{3.25}$$

This result was first obtained by Lyth in 1985 [72]. Instead of PSRA, we can also use Hamilton-Jacobi formalism (2.33) to eliminate $\dot{\phi}$ in (3.24). This yields the same result as (3.23) but only to its lowest order. The reason is in the original derivation yielding (3.24) an approximation $\delta\rho \simeq \delta\phi(\partial V/\partial\phi)$ was made. This approximation is intrinsically identical to the slow-roll approximation in which we require the slow-roll parameters to be sufficiently small so that the kinetic term can be dropped when compared with the potential. In a theoretical work requiring higher precision, (3.23) is preferred. However, not all inflationary models have a specified form for $H(\phi)$. Thus we also need (3.25) when only the form of $V(\phi)$ is known in our model and this is typically the case.

### The spectral index

As an approximation, we take the spectrum of density perturbation to be a power-law form. Since $A_S(k)$ is identical to $\delta_H(k)$ now, from (3.17) we can assign an amplitude to $A_S(k)$ so that it takes the form

$$A_S^2(k) = A_S^2(k_A)\left(\frac{k}{k_A}\right)^{n(k)-1} \tag{3.26}$$

where $k_A$ is a specified scale. Thus by differentiating (3.23) with respect to $k$ and employing (3.9), one can have

$$n(k) - 1 = \frac{d\ln A_S^2(k)}{d\ln k} \simeq 2\eta_{H*} - 4\epsilon_{H*} - \left[8(1+C)\epsilon_{H*}^2 - (6+10C)\epsilon_{H*}\eta_{H*} + 2C\xi_{H*}^2\right] \tag{3.27}$$

where $\xi_H$ is the third HSR parameter as defined in (2.43). From (2.41) and (2.42) to the lowest order, one has $\epsilon_V \simeq \epsilon_H$ and $\eta_V \simeq \eta_H + \epsilon_H$ so that (3.27) can be rewritten to the lowest order as

$$n(k) - 1 \simeq 2\eta_{V*} - 6\epsilon_{V*} \tag{3.28}$$

One subtlety to notice here is the subscript "*". Since $A_S(k)$ in (3.23) is determined in terms of the quantities at horizon exit, the assumed spectral index determined here should be also in terms of the quantities at horizon exit. This means that, for a given scale $k^{-1}$, the slow-roll parameters involved in (3.27) and (3.28) should be some fixed values at horizon exit during inflation, i.e. at $H = H_k$ or alternatively at $k = aH$. Therefore, for any given scale of our interest, the predicted spectrum of density perturbation is determinable for a specified inflationary model. This is extremely useful when testing the suitability of inflationary models by comparing their predicted spectra to the observations. However, as we mentioned earlier in subsection 3.2.2, spectral indices are generally scale-dependent. If we are to fit inflationary models into the observed spectrum, we have to consider this dependence [21, 53]:

$$\left.\frac{dn(k)}{d\ln k}\right|_* = -24\epsilon_{V*}^2 + 16\epsilon_{V*}\eta_{V*} - \frac{m_{\rm Pl}^4}{32\pi}\frac{V'_*V'''_*}{V_*^2} \tag{3.29}$$

Generally, because the observed range of scales for a specific experiment say COBE is quite small, as long as this quantity is not too large the dependence of $n$ on $k$ should be negligible. However, the full spectrum observed today still contains another component we haven't yet considered — the spectrum of gravitational waves. Let us move on to investigating the situation in that case.

### 3.3.2 Gravitational waves

Basically, gravitational waves are generated in a similar fashion to the density perturbation: during inflation the microphysics effectively becomes frozen outside the horizon and therefore the asymptotic state is not a zero-particle state so that particles are created by the gravitational field and the perturbations in the gravitational field are also generated. Gravitational waves can be thought of as a ripple in the background RW metric (2.1). As in the previous section [75], one starts off with linear tensor metric perturbations due to Bardeen [10] and Kodama & Sasaki [48], follows the Einstein-Hilbert sector $S_{E-H}$ of the full Einstein action [38, 39], and then applies quantum theory to yield an exact solution in the power-law inflationary regime [2]. By the slow-roll expansion to the next order due to Stewart & Lyth [101], one obtains the tensor spectrum

$$\mathcal{P}_g^{1/2}(k) \simeq [1-(C+1)\epsilon_H]\frac{4}{\sqrt{\pi}}\frac{H}{m_{\rm Pl}}\bigg|_* \tag{3.30}$$

where $C \simeq -0.73$. Then we take the rescaled spectrum of gravitational waves as

$$A_T(k) = \frac{1}{10}\mathcal{P}_g^{1/2}(k) \overset{(3.30)}{\simeq} [1-(C+1)\epsilon_H]\frac{2}{5\sqrt{\pi}}\frac{H}{m_{\rm Pl}}\bigg|_* \tag{3.31}$$

By using PSRA (2.24) to eliminate $H$, (3.31) can be also rewritten to the lowest order as

$$A_T(k) \overset{PSRA}{\simeq} \sqrt{\frac{32}{75}}\frac{V_*^{1/2}}{m_{\rm Pl}^2} \tag{3.32}$$

Actually, before the COBE detection, gravitational waves had been studied by several authors [96, 65, 103]. The crucial conclusion is the gravitational wave amplitude satisfies the massless wave equation which is of the form (3.4). It follows that the spectrum of the gravitational waves is the same as that of any other massless scalar field [57]:

$$\mathcal{P}_g(k) = \frac{16}{\pi}\frac{H_*^2}{m_{\rm Pl}^2} \tag{3.33}$$

We see this is exactly the same as the $\mathcal{P}_g(k)$ in (3.30) to its lowest order.

**The spectral index**

As an analogue to the spectrum of density perturbation, we now take the spectrum of gravitational waves to be a power-law form [62]

$$A_T^2(k) = A_T^2(k_A)\left(\frac{k}{k_A}\right)^{n_T(k)} \tag{3.34}$$

where $k_A$ is the same as in (3.26). There is no specific reason to assign this form. It is just taken as an approximation for investigating the behaviour of the spectrum. By differentiating (3.31) with respect to $k$ and employing (3.9), one can have

$$n_T(k) = \frac{d\ln A_T^2(k)}{d\ln k} \simeq -2\epsilon_{H*}\left[1 + (3+2C)\epsilon_{H*} - 2(1+C)\eta_{H*}\right] \tag{3.35}$$

From (2.41) to its lowest order, one has $\epsilon_V \simeq \epsilon_H$ so that (3.35) can be also rewritten to the lowest order as

$$n_T(k) \simeq -2\epsilon_{V*} \tag{3.36}$$

Again, the assumed spectral index determined here should be in terms of the quantities at horizon exit. This means that (3.35) and (3.36) can be applied throughout the whole range of scales provided that for each scale the slow-roll parameters are calculated at horizon exit and therefore treated as constants. The only constraint on $n_T(k)$ is that it must be negative. Because we know the graviton is weakly coupled with other matter, gravitational waves will propagate almost freely once they are inside the horizon. Thus they can survive only at large scales and we expect their power spectrum to have negative spectral index, i.e. the smaller the scale $k^{-1}$, the smaller the amplitude of gravitational waves $A_T(k)$. Actually, in the slow-roll regime, (2.25) and (2.35) have guaranteed the negativity in (3.36) and (3.35) to its lowest order. For higher-order work, this constraint should be noticed.

Again we have to consider the $k$-dependence of $n_T$ if we are to fit inflationary models into the observed spectrum [53]:

$$\left.\frac{dn_T(k)}{d\ln k}\right|_* = -4\epsilon_{H*}(\epsilon_{H*} - \eta_{H*}) \tag{3.37}$$

As long as this quantity is not too large the dependence of $n_T$ on $k$ should be negligible.

The combination of (3.27) (or (3.28)) and (3.35) (or (3.36)) indicates one crucial advantage of assigning power-law spectra to be the forms of both density perturbation and gravitational waves. It is that the behaviour of the full spectrum is determinable in the inflationary regime. In other words, inflation predicts spectra which can be approximated as power-laws. Provided the range of observed scales is suitably small, the power-law approximation should be a good one so that we can test various inflationary scenarios. In the next subsection, we shall consider the link between the two spectra of density perturbation and gravitational waves since they have the same origin of quantum fluctuations in inflaton.

### 3.3.3 Consistency equation

Dividing (3.31) by (3.23) to next order yields

$$\frac{A_T^2(k)}{A_S^2(k)} \simeq \epsilon_{H*}\left[1 + 2C(\epsilon_{H*} - \eta_{H*})\right] \simeq \epsilon_{V*}\left[1 + 2C(2\epsilon_{V*} - \eta_{V*})\right] \tag{3.38}$$

where $C \simeq -0.73$. Substituting the first expression into (3.35), to lowest order one has

$$n_T(k) = -2\frac{A_T^2(k)}{A_S^2(k)} \tag{3.39}$$

This implies that the two spectra are not independent. From a physical point of view, this is not surprising since density perturbations and gravitational waves correspond to two continuous functions that have an origin in the single scalar field potential which is also continuous. Thus (3.39) is called the "consistency equation" because the link between the spectra of density perturbation and gravitational waves is expected to be a differential equation although here (3.39) is just a lowest-order result. This was first pointed out by Liddle & Lyth [56]. The crucial thing is such a link is unlikely to be obtained from any other mechanism. Further investigation was carried out by Copeland *et al.* [24, 25] and a second consistency equation was derived by Kosowsky & Turner [53]. Unfortunately, due to the limitation of accuracy in observation this second equation is unlikely to be testable. Even (3.39) is also difficult to test since the two contributions from density perturbations and gravitational waves in the full spectrum are difficult to be distinguished by observation. Nevertheless, (3.39) still holds its own importance in theoretical work.

In practical applications, (3.38) is useful for investigating inflationary models because different models will predict different ratios of the two contributions from density perturbation and gravitational waves in the full observed spectrum. Instead of treating the full spectrum as arising only from density perturbation, this will strengthen the constraint on the form of the spectrum of density perturbation. Generally, due to the weak coupling of the graviton with other matter, gravitational waves redshift away once they entre the horizon (i.e. after horizon entry) and hence can be seen only at large scales. This causes their effect to be significant as we look at large angles on the CMB sky but not at smaller scales. Therefore, as long as the accuracy of the CMB observation is improved, we should be able to distinguish the viability of different inflationary models with more confidence.

**The order**

In the derivation of $n$, $n_T$ and $A_T^2/A_S^2$ above, we use either the lowest-order or the next-order result in different places. Let me clarify:

1. Theoretical analysis vs. observational work: To the presently desired accuracy limited by observations, lowest-order results will be adequate for probing the observed spectrum. For example, we use only the lowest-order result for (3.39). In the future, once higher resolution CMB anisotropy experiments are available, lowest-order results may be insufficient and if so we will need higher order results. Actually, from (2.43) and (2.44) we know that a hierarchy system exists for HSR parameters. This makes higher-order expansions of $\mathcal{P}_{\mathcal{R}}^{1/2}(k)$ and $\mathcal{P}_g^{1/2}(k)$ in terms of slow-roll parameters possible and we may need it some day for observational work. On the other hand, for theoretical analysis, the next or higher order results may be desired since we tend to make our theoretical predictions as accurate as possible so that they can be confirmed or disproved as the observations progress.

2. HSRA vs. PSRA: In the derivation, we generally use next-order results for quantities in HSR version but only the lowest-order results when converting these quantities into their PSRA version. The reason is that for models in which only the form of $V(\phi)$ is known and not $H(\phi)$, we generally use slow-roll approximation to analyse the scenarios so that their slow-roll parameters are considered small at the epoch corresponding to large scales (eg. $t_{60}$ for the present horizon scale) and thus the lowest-order results will be adequate. However, for those which possess exact solutions like power-law or intermediate inflation, the slow-roll parameters are not necessarily small and thus the next-order results are more appropriate since in this case $H(\phi)$ is generally solved. So we use next-order results for HSR version.

So far, we have reached the limit of analytic progress for determining the generic behaviour of inflationary models. Equations (3.27) (or (3.28)), (3.35) (or (3.36))and (3.38) provide us with all the information we are to apply in our models. Under the status of current accuracy of observation, their lowest-order results will be sufficient for probing large scale structure or the CMB anisotropy. In the following section, we are to investigate the realistic spectrum observed from CMB sky so that one can have some constraints on inflationary models and, hopefully, rule out some of them.

### 3.3.4 The CMB anisotropies

The sources of the CMB anisotropies are a combination of both intrinsic and extrinsic effects [105]. Having subtracted the monopole and dipole terms, it is conventional in CMB work to expand the temperature fluctuations in spherical harmonics [62, 105]:

$$\frac{\Delta T}{T_0}(\theta,\varphi)=\sum_{l=2}^{\infty}\sum_{m=-l}^{l}a_{lm}Y_{lm}(\theta,\varphi) \tag{3.40}$$

where $a_{lm}$ are the multipoles and $T_0 = 2.726\text{K}$ is the present mean background temperature. To investigate the composition of the fluctuation, we take the moments of the random variables $a_{lm}$ over positions (the mean square multipoles)

$$C_l=\left\langle |a_{lm}|^2\right\rangle_{\text{position}} \tag{3.41}$$

which is a rotationally symmetric quantity and treated as a continuous function of $l$. Thus for a randomly placed observer the mean square anisotropy is expressed as

$$\left\langle\left\langle\left(\frac{\Delta T}{T_0}\right)^2\right\rangle\right\rangle_{\text{position}}=\left\langle\frac{1}{4\pi}\sum_{l=2}^{\infty}\sum_{m=-l}^{l}|a_{lm}|^2\right\rangle_{\text{position}}\simeq\frac{1}{4\pi}\int_2^{\infty}l(2l+1)C_l\frac{dl}{l} \tag{3.42}$$

which implies the angular size of a feature in the sky and the order $l$ of the multipoles have a relation at large $l$ as $\theta\sim(60/l)^\circ$. According to cosmological perturbation theory, $C_l$ can be decomposed into two parts contributed by density perturbation and gravitational waves as

$$C_l=C_l^{\text{S}}+C_l^{\text{T}} \tag{3.43}$$

The theoretical prediction of these two components requires numerical simulation [20]. However, to the present observational accuracy, analytic approaches will be adequate. In the literature, this was carried out with increasing precision by many authors. Here we shall just briefly analyse it.

For a power spectrum with a spectral index $n$, due to Scaramella & Vittorio [92] the first (scalar) component in a purely matter-dominated universe is given as

$$C_l^{\text{S}}=\frac{\pi}{2}\left[\frac{\sqrt{\pi}}{2}l(l+1)\frac{\Gamma((3-n)/2)}{\Gamma((4-n)/2)}\frac{\Gamma(l+(n-1)/2)}{\Gamma(l+(5-n)/2)}\right]\frac{\delta_H^2(H_0/2)}{l(l+1)} \tag{3.44}$$

For $n=1$ the square bracket is 1; for $l\gg 1$ and $l\gg|n|$ it can be replaced by 1 if $\delta_H$ is to be evaluated on the scale $k\simeq lH_0/2$ which dominates the integral.[4] On the other

[4] $\Gamma(1/2)=\sqrt{\pi}$; $\Gamma(z+1)=z\Gamma(z)$.

hand, due to Starobinsky [97] when $\mathcal{P}_g(k)$ is weakly $k$-dependent ($n_T(k) \simeq 0$), the second (tensor) component in $C_l$ is given as

$$C_l^{\mathrm{T}} = \frac{\pi}{36}\left(1 + \frac{48\pi^2}{385}\right)\frac{\mathcal{P}_g D_l}{l(l+1)} \tag{3.45}$$

where the $D_l$ are constants close to 1. Thus from (3.44) and (3.45) we see $\delta_H^2$ and $\mathcal{P}_g$ both have the form $l(l+1)C_l$ so we define the observed power spectrum as $l(l+1)C_l$. In the case of a scale-invariant spectrum of density perturbation ($n = 1$ in (3.17)), we see from (3.44) that $l(l+1)C_l^{\mathrm{S}}$ is a constant. Dividing (3.45) by (3.44) for $\delta_H = A_S$ and $\mathcal{P}_g^{1/2} = 10A_T$) yields the theoretical ratio of the two spectra contributed by gravitational waves and density perturbation:

$$R_0 = \frac{l(l+1)C_l^{\mathrm{T}}}{l(l+1)C_l^{\mathrm{S}}} \simeq 12.4 D_l \frac{A_T^2(k)}{A_S^2(k)} \simeq 12.4\frac{A_T^2(k)}{A_S^2(k)} \tag{3.46}$$

where $A_T^2(k)/A_S^2(k)$ is given by (3.38). In the derivation of this result, a perfectly matter-dominated universe has been assumed. However, a deviation should be expected if the universe is not to be fully matter-dominated. This is indeed the case when one is looking at the CMB sky since the universe at last-scattering was not purely matter-dominated. Thus a correction factor of 0.75 is used by Bunn, Liddle & White [21] in the study of four-year COBE normalization in 1996. Therefore, we shall take the corrected ratio as

$$\begin{aligned} R &= 0.75R_0 = 9.3\frac{A_T^2(k)}{A_S^2(k)} && (3.47)\\ &\overset{(3.38)}{\simeq} 9.3\epsilon_{H*}\left[1 - 1.46\epsilon_{H*} - 1.46\eta_{H*}\right] && (3.48)\\ &\simeq 9.3\epsilon_{V*} && (3.49)\end{aligned}$$

for later analysis. The usage of $R$ is to tighten the amplitude of density perturbation from the observed spectrum by a factor $\sqrt{1+R}$, i.e. $C_l^{S\,1/2} = C_l^{1/2}/\sqrt{1+R}$ or $\delta_H = \delta_{H(\mathrm{obs})}/\sqrt{1+R}$. Since the observed spectrum will have included both contributions from density perturbation and gravitational waves, the real amplitude of the spectrum of density perturbation should be less than the observed one under the assumption that the anisotropies were caused by density perturbations alone. If we are to consider other contributions like isocurvature density perturbation or topological defects [4], the net value of the amplitude of the density perturbation will again be smaller.

For most inflationary models, because the slow-roll approximation is usually a good description of inflationary scenarios, the slow-roll parameters are very small, especially at $t_{60}$ which corresponds to the CMB scale. Therefore, in most models, from (3.48) we see that gravitational waves are negligible in CMB sky. However, three exceptions are the power-law (see subsection 2.4.3 [70, 11, 15, 55, 14]) intermediate (see subsection 2.4.4 [11, 15, 13, 80]) and extended [55, 51] inflation. In these cases, slow-roll parameters are not necessary small, so the ratio $R$ can be of order one or higher. We shall examine the first two cases briefly in subsection 3.4.1 and 3.4.2.

Theoretically, in the regime of power spectrum, one can use the CMB spectrum accompanied with other observations at smaller scales to explore the behaviour of the spectrum of density perturbation. The observations at smaller scales are used to normalise the spectrum since at smaller scales gravitational waves have already redshifted away. Then one can use the CMB spectrum predicted by different inflationary models, which give different predictions of the ratio $R$, to investigate the spectral index. An example was provided by Liddle & Lyth [56] who showed that many versions of extended inflation were ruled out.

### Four-year COBE normalization

Recently the four-year COBE normalization has been obtained [17]. By using these data, Bunn, Liddle & White obtained the normalization in the inflationary regime [21]. Their result is

$$\delta_{H_0} = \delta_H(a_0 H_0) \simeq 1.91 \times 10^{-5} \; \frac{\exp[1.01(1-n)]}{\sqrt{1+0.75r}} \tag{3.50}$$

where

$$r = -6.2 n_T \left(1 - \frac{n_T}{2} + (n-1)\right) \tag{3.51}$$

is the uncorrected[5] ratio of the two contributions from gravitational waves and density perturbation. Within the region $|n-1| \leq 0.3$ and $-0.3 \leq n_T \leq 0$, this fitting function is good to 1.5% when ignoring other effects. Actually this $r$ is identical to our $R_0$ in (3.46), if we substitute (3.38) into (3.35) to eliminate $C$ and then use the lowest-order results of (3.27) and (3.35) to replace slow-roll parameters. Two subtle points in (3.50) to notice are:

1. The $n$ and $r$ dependence of $\delta_H(a_0 H_0)$ in (3.50): because $\delta_H(a_0 H_0)$ is the normalized amplitude of $\delta_H(k)$ at a fixed scale, i.e.

$$\delta_H^2(k) \overset{(3.17)}{=} \delta_H^2(a_0 H_0) \left(\frac{k}{a_0 H_0}\right)^{n-1} \tag{3.52}$$

[5] "Uncorrected" refers to the correction factor 0.75 which appeared in (3.50) and was mentioned in subsection 3.3.4.

and $r$ determines the portion of density perturbation in the observed spectrum, one certainly expects different $\delta_H(a_0H_0)$ for different presumed $n$ or $r$.

2. The scale of horizon crossing: the presumed power spectrum is normalized to cross at the centre of the COBE data whose scale is around $k_* = a_*H_* = 7a_0H_0$, but expressed as at the scale of present horizon entry $k = a_0H_0$. Therefore, when we use this result for testing our inflationary models, we have to fit our epoch $t_{60}$ to the scale $k_* = k_{60} = 7a_0H_0$, rather than the present horizon scale. Therefore, according to (3.17) the corresponding density contrast at this scale will be

$$\begin{aligned} \delta_{H60} &\overset{(3.52)}{=} \left(7^{n-1}\delta_H^2(a_0H_0)\right)^{1/2} \\ &\overset{(3.50)}{=} 7^{(n-1)/2} \times 1.91 \times 10^{-5} \ \frac{\exp[1.01(1-n)]}{\sqrt{1+0.75r}} && (3.53) \\ &\simeq 1.91 \times 10^{-5}\,(1 - 4.50\epsilon_{H60} - 0.07\eta_{H60}) && (3.54) \\ &\simeq 1.91 \times 10^{-5}\,(1 - 4.43\epsilon_{V60} - 0.07\eta_{V60}) && (3.55) \end{aligned}$$

where we have employed (3.51) and the lowest-order results of (3.27) and (3.35) to carry out the parameter expansion.

Since the epoch of $t_{60}$ corresponds to $k_* = 7a_0H_0$, combining (3.53) and (3.23) and carrying out the parameter expansion as in (3.54) yields the expansion time scale at $t_{60}$ as

$$\begin{aligned} H_{60}^{-1} &\simeq (1.18 \times 10^4 m_{\rm Pl}^{-1})\ \epsilon_{H60}^{-1/2}\,(1 + 4.96\epsilon_{H60} - 0.66\eta_{H60}) && (3.56) \\ &\simeq (1.18 \times 10^4 m_{\rm Pl}^{-1})\ \epsilon_{V60}^{-1/2}\,(1 + 5.62\epsilon_{V60} - 0.66\eta_{V60}) && (3.57) \\ &\simeq (6.37 \times 10^{-40}{\rm sec})\ \epsilon_{V60}^{-1/2}\,(1 + 5.62\epsilon_{V60} - 0.66\eta_{V60}) && (3.58) \end{aligned}$$

As an analogue to this, Ref. [21] used a next-order version of (3.25) [101] to calculate the energy scale at $t_{60}$ and yielded

$$\begin{aligned} V_{60}^{1/4} &\simeq (5.40 \times 10^{-3} m_{\rm Pl})\ \epsilon_{V60}^{1/4}\,(1 - 3.2\epsilon_{V60} + 0.5\eta_{V60}) && (3.59) \\ &\simeq (6.60 \times 10^{16}{\rm GeV})\ \epsilon_{V60}^{1/4}\,(1 - 3.2\epsilon_{V60} + 0.5\eta_{V60}) && (3.60) \end{aligned}$$

We shall use all these results for our later analysis. In the next section, we shall examine some realistic inflationary models by applying the perturbation theory introduced so far.

## 3.4 Realistic Models

### 3.4.1 Power-law inflation

From (2.48), (2.49), (2.50) and (2.51) we can derive HSR and PSR parameters defined by (2.43) and (2.44) as

$$ {}^{n}\beta_{H} = \frac{1}{p} \qquad ; \qquad {}^{n}\beta_{V} = \begin{cases} \frac{1}{p} & n = 0 \\ \frac{2}{p} & n \geq 1 \end{cases} \tag{3.61} $$

which are all constants. Instead of truncating the expansion at the next order when deriving (3.27) and (3.35), we expand it into infinite order with respect to ${}^{n}\beta_{H}$ and find

$$ n_T = n - 1 = \lim_{n\to\infty} \left( -2 \sum_{i=1}^{n} \frac{1}{p^i} \right) = \frac{-2}{p-1} \tag{3.62} $$

This is the exact solution for $n$ and $n_k$ and indicates that both are constants specified by the parameter $p$. The condition for inflation $p > 1$ leads to $n - 1 < 0$ and $n_T < 0$. This implies that the amplitudes of both density perturbations and gravitational waves decrease with scale. Actually, the decrease of $A_T$ with scale is as we expected in subsection 3.3.2. Moreover, Ref. [2] gives an exact relation $\mathcal{P}_g^{1/2}/\mathcal{P}_{\mathcal{R}}^{1/2} = 4/\sqrt{p}$ for the power-law inflation so that

$$ R \overset{(3.46)}{=} 9.3\frac{A_T^2}{A_S^2} = \frac{9.3}{p} \tag{3.63} $$

which is also a constant. From (3.62) and (3.63) we see for a larger value of $p$, the spectrum is closer to scale-invariant and gravitational waves are more negligible. Substituting (3.62) and (3.63) into (3.53) yields

$$ \delta_{H_{60}} = 1.91 \times 10^{-5} \times 7^{[-1/(p-1)]} \, \frac{\exp\left[2.02/(p-1)\right]}{\sqrt{1 + 9.3/p}} \tag{3.64} $$

We see the value of $p$ could not be too close to unity. Otherwise the good fit of this function to the COBE data would be violated. For a good fit within 1.5% mentioned after (3.50), this fitting function can work well only within the range of $p \gtrsim 8$. More specifically, direct limits from COBE do not permit a very small $p$. Thus we have approximately

$$ -0.3 \lesssim n - 1 = n_T < 0 \tag{3.65} $$

$$ 0 < R \lesssim 1.2 \tag{3.66} $$

### 3.4.2 Intermediate inflation

As introduced in subsection 2.4.4, we normalize $8\pi/m_{\rm Pl}^2$ to unity in (2.57) so here we also have to normalize the HSR parameters from (2.43) as

$$\epsilon_H(\phi) = 2\left(\frac{H'(\phi)}{H(\phi)}\right)^2 \quad ; \quad \eta_H(\phi) = 2\frac{H''(\phi)}{H(\phi)} \quad ; \quad \xi_H(\phi) = 2\left(\frac{H'(\phi)H'''(\phi)}{H^2(\phi)}\right)^{1/2} \tag{3.67}$$

in order that we can use them accompanied with all the equations derived in subsection 2.4.4. Thus by (2.64) one has

$$\epsilon_H(\phi) = \frac{\beta^2}{2\phi^2} \quad ; \quad \eta_H(\phi) = \frac{\beta(\beta+2)}{2\phi^2} \quad ; \quad \xi_H(\phi) = \frac{\beta\sqrt{(\beta+2)(\beta+4)}}{2\phi^2} \tag{3.68}$$

Substituting all these into (3.27), (3.35) and (3.48) yields the next-order results:

$$n - 1 = -\frac{\beta(\beta-2)}{\phi^2} - \frac{\beta^2}{2\phi^4}(\beta^2 - 3.08\beta - 5.84) \tag{3.69}$$

$$n_T = -\frac{\beta^2}{\phi^2} - \frac{\beta^3}{2\phi^4}(\beta - 1.08) \tag{3.70}$$

$$R = \frac{4.65\beta^2}{\phi^2} - \frac{6.789\beta^3}{\phi^4}(\beta + 1) \tag{3.71}$$

We see the only possibilities to have an approximate scale-invariant spectrum are $\beta \to 0$ or $\phi \gg \beta$. In both cases gravitational waves are also negligible. Recalling (2.66) for the condition of inflation $\phi^2 > \beta^2/2$, one finds further conditions for $n$ and $n_T$:

$$n - 1 \quad > \quad -4 + \frac{10.16}{\beta} + \frac{11.68}{\beta^2} \quad > \quad -4 \tag{3.72}$$

$$n_T \quad > \quad -4 + \frac{2.16}{\beta} \quad > \quad -4 \tag{3.73}$$

These conditions are actually very weak to specify the behaviour of the spectrum predicted by the intermediate inflation. However, they at least show that it is possible for this model to produce a scale-invariant spectrum of density perturbations. For the choice of $\beta = 2$ corresponding to $f = 2/3$, we have

$$n - 1 = \frac{16}{\phi^4} \quad ; \quad n_T = -\frac{4}{\phi^2} - \frac{3.68}{\phi^4} \quad ; \quad R = \frac{18.6}{\phi^2} - \frac{162.936}{\phi^4} \tag{3.74}$$

which implies that only when $\phi \to \infty$ can we have a scale-invariant spectrum. This result differs from that of Ref. [13] in which the authors advocated $\beta = 2$ as a choice to produce a scale-invariant spectrum by using only the lowest-order version of $n$ and $R$. Therefore, because of the strong parameter-dependence of this model, it is unlikely for it to be tested by using observational results without requiring other assumptions.

### 3.4.3 Chaotic inflation

In subsection 2.4.5 we used slow-roll approximation to solve the chaotic inflation whose potential is $V(\phi) = m^2\phi^2/2$. By employing PSR conditions $\epsilon_V < 1$ and $\eta_V < 1$ one finds the end of inflation $\phi_{\rm f} = m_{\rm Pl}/\sqrt{4\pi}$. Now setting (2.75) to be 60 yields

$$\phi_{60} = \phi_{\rm i} \simeq 3.10 \;\; m_{\rm Pl} \tag{3.75}$$

Then one has

$$\epsilon_{V_{60}} = \eta_{V_{60}} \simeq 8.28 \times 10^{-3} \tag{3.76}$$

Substituting this into (3.28), (3.29), (3.36), (3.37) and (3.49) gives

$$n \simeq 0.967 \quad ; \quad \left.\frac{dn(k)}{d\ln k}\right|_{60} \simeq -5.5 \times 10^{-4} \tag{3.77}$$

$$n_T \simeq -0.017 \quad ; \quad \left.\frac{dn_T(k)}{d\ln k}\right|_{60} \simeq -2.8 \times 10^{-4} \tag{3.78}$$

$$R \simeq 0.077 \tag{3.79}$$

We recall $\epsilon_V \simeq \epsilon_H$ and $\eta_V \simeq \eta_H + \epsilon_H$ for those appropriate. This shows this model is very close to scale-invariant limit with a reasonably negative $n_T$. Furthermore, substituting (3.76) into (3.50), (3.55), (3.57) and (3.59) yields

$$\delta_{H_0} = 1.90 \times 10^{-5} \tag{3.80}$$

$$\delta_{H60} = 1.84 \times 10^{-5} \tag{3.81}$$

$$H_{60}^{-1} = 1.36 \times 10^5 \; m_{\rm Pl}^{-1} = 7.29 \times 10^{-39}{\rm sec} \tag{3.82}$$

$$V_{60}^{1/4} = 1.59 \times 10^{-3} \; m_{\rm Pl} = 1.95 \times 10^{16}{\rm GeV} \tag{3.83}$$

Combining (3.83) with (3.75) gives

$$m = 1.15 \times 10^{-6} m_{\rm Pl} = 1.41 \times 10^{13}{\rm GeV} \tag{3.84}$$

This is between the Axion and the GUT scales. Comparing this with (2.77) implies that the chaotic model can easily provide sufficient inflation to solve the problems with the standard Big Bang model.

### 3.4.4 Polynomial chaotic inflation

Instead of $V(\phi) = m^2\phi^2/2$ or $V(\phi) = \lambda\phi^4/4$, let us consider a generic form for the chaotic inflation:

$$V(\phi) = \chi\phi^\alpha \tag{3.85}$$

whose first two PSR parameters are

$$\epsilon_V = \frac{m_{\rm Pl}^2 \alpha^2}{16\pi\phi^2} \qquad ; \qquad \eta_V = \frac{m_{\rm Pl}^2 \alpha(\alpha-1)}{8\pi\phi^2} \tag{3.86}$$

Because $\eta_V \geq \epsilon_V$ for $\alpha \geq 2$, one should use $\eta_V = 1$ as an indicator of the end of inflation, so that

$$\phi_{\rm f}^2 = \frac{\alpha(\alpha-1)}{8\pi} m_{\rm Pl}^2 \tag{3.87}$$

Substituting (3.85) and (3.87) into (2.31) gives

$$\phi_{60}^2 = \frac{m_{\rm Pl}^2}{8\pi}\alpha(119+\alpha) \tag{3.88}$$

so that

$$\epsilon_{V_{60}} = \frac{\alpha}{2(119+\alpha)} \qquad ; \qquad \eta_{V_{60}} = \frac{\alpha-1}{119+\alpha} \tag{3.89}$$

Thus by (3.28), (3.36) and (3.49) we obtain

$$n = \frac{117}{119+\alpha} < 1 \tag{3.90}$$

$$n_T = \frac{-\alpha}{119+\alpha} < 0 \tag{3.91}$$

$$0.077 \overset{(\alpha\geq 2)}{\lesssim} R = \frac{4.65\alpha}{119+\alpha} < 4.65 \tag{3.92}$$

(3.90) implies that, as long as $\alpha$ is not too large, the spectrum of density perturbations predicted by this model is close to scale-invariant; (3.91) guarantees that the amplitude of gravitational waves decreases with scale as we expected earlier; (3.92) shows that the predicted portion of gravitational waves in the full spectrum has a maximum of around 82% and a minimum of around 7% if $\alpha \geq 2$. Moreover, by (3.50), (3.55), (3.57) and (3.59) one obtains

$$\delta_{H_0} = 1.91 \times 10^{-5} \times \frac{121.02 - 0.32\alpha}{119+\alpha} \tag{3.93}$$

$$\delta_{H60} = 1.91 \times 10^{-5} \times \frac{119.07 - 1.29\alpha}{119+\alpha} \tag{3.94}$$

$$H_{60}^{-1} = (6.37 \times 10^{-40}\ \text{sec})\, \frac{\sqrt{2}(119.66 + 3.15\alpha)}{\sqrt{\alpha(119+\alpha)}} \tag{3.95}$$

$$V_{60}^{1/4} = (6.60 \times 10^{16}\text{GeV})\, \frac{\alpha^{1/4}(118.5 - 0.1\alpha)}{\sqrt[4]{2}(119+\alpha)^{5/4}} \tag{3.96}$$

We see the expansion time scale and the energy scale for this model are typically of the order $10^{-40}$ sec and $10^{16}$ GeV respectively. Finally, combining (3.96) with (3.88) gives

$$\chi = 8.5 \times 10^{-10}\, m_{\rm Pl}^{(4-\alpha)}\, \frac{(8\pi)^{\alpha/2}\alpha^{(2-\alpha)/2}(117 - 3.4\alpha)}{2(119+\alpha)^{(4+\alpha)/2}} \tag{3.97}$$

By using all these, we can immediately obtain the desired quantity whenever $\alpha$ is specified. For example, $\alpha = 2$ reproduces the same result as in the previous section. When $\alpha = 4$, we get the result for our self-coupling inflation introduced in subsection 2.4.6:

$$
\begin{aligned}
n &= 0.951 && (3.98)\\
nT &= -0.033 && (3.99)\\
R &= 0.151 && (3.100)\\
\delta_{H_0} &= 1.86 \times 10^{-5} && (3.101)\\
\delta_{H_{60}} &= 1.77 \times 10^{-5} && (3.102)\\
H_{60}^{-1} &= 5.37 \times 10^{-39}\mathrm{sec} && (3.103)\\
V_{60}^{1/4} &= 2.26 \times 10^{16}\mathrm{GeV} && (3.104)\\
\lambda = 4\chi &= 1.21 \times 10^{-13} && (3.105)
\end{aligned}
$$

CHAPTER 4

# HYBRID INFLATION

As we noted in Section 2.4, the particle physics motivation for believing the existence of scalar fields is quite strong and in modern work of current interest like superstring theories a large number of scalar fields are found. To build up these models in the inflationary regime, we assume that in the early universe the noninflaton fields quickly settle down to their minimum at fixed $\phi$, after which inflation occurs as the inflaton field rolls slowly down its potential. This can be thought of as a chaotic inflation model which features more than one scalar field such that one field (the inflaton $\phi$) rolls while the others are trapped in their vacuum states. Two possibilities exist concerning these vacuum states. The simplest one is they are *true* vacua so that those noninflaton fields have the same values as in the present universe. In this case the inflationary scenario is not much different from the chaotic inflation model as introduced in subsection 2.4.5. It follows the standard process of inflation in which inflation ends while $\phi$ rolls down its potential and the reheating ensues when $\phi$ starts to execute decaying oscillations around its own true vacuum. This is the usually considered case and has been widely investigated in the literature. However, the other possibility is that those vacuum states of noninflaton fields are *false* ones, whose energy density is not zero while inflation occurs. It is generally called the "**false-vacuum inflation**". In this case, if the false-vacuum energy is negligible compared with the inflaton energy, the scenario is similar to the true-vacuum case apart from exotic effects due to the coupling of $\phi$ with noninflaton fields. On the other hand, if the false-vacuum energy dominates while inflation occurs, it can significantly affect the dynamics of inflation and this was first termed as "**hybrid inflation**" by Linde [69]. Because the distinction of the false-vacuum inflation to other traditional models is featured by its non-negligible false-vacuum energy, it is also generally referred to as hybrid inflation. In this chapter, we shall investigate a sample model in this regime and conclude with one of its variants.

## 4.1 A Sample Model

Generally hybrid inflation refers to a wide range of variants possessing the property mentioned above. To investigate its main features, we pick a second-order model whose potential energy takes the form [50, 69, 26]:

$$V(\phi,\psi) = \frac{1}{4}\lambda\left(\psi^2 - M^2\right)^2 + \frac{1}{2}m^2\phi^2 + \frac{1}{2}\lambda'\phi^2\psi^2 \tag{4.1}$$

where $\lambda$ is the self-coupling constant of $\psi$, $M$ the true-vacuum scale of $\psi$, $m$ the inflaton mass and $\lambda'$ the coupling constant of the two scalar fields. In the context of particle physics, one generally requires $1 \gtrsim \lambda, \lambda' > 0$, $M \lesssim m_{\rm Pl}/\sqrt{8\pi} = 2.4 \times 10^{18}$ GeV and $m \gtrsim 100$ GeV which corresponds to the soft supersymmetry-breaking scale of the vacuum. Let us investigate the form of this potential as follows (see Figure 4.1):

1. From (4.1) we see this potential possesses the symmetries $\phi \leftrightarrow \phi$ and $\psi \leftrightarrow \psi$. Because of this symmetry, we shall concentrate ourselves within only the region $\phi > 0$.

2. By differentiating it with respect to $\phi$, one finds $V \equiv V(\phi)$ always has a minimum at $\phi = 0$.

3. By differentiating it with respect to $\psi$, one finds $V \equiv V(\psi)$ possesses

   (a) one minimum at $\psi = 0$ when $\phi^2 > \lambda M^2/\lambda'$.

   (b) two minima at $\psi^2 = M^2 - \lambda'\phi^2/\lambda$ when $\phi^2 < \lambda M^2/\lambda'$.

   Thus we define

   $$\phi^2_{\rm inst} = \frac{\lambda}{\lambda'}M^2 \tag{4.2}$$

   as the division of these two cases.

4. Combining 2 and 3 together, we see $V(\phi,\psi)$ has global minima at $(\phi,\psi) = (0, \pm M)$.

Our false-vacuum inflation model is based on the assumption that inflation occurs at the region $\phi > \phi_{\rm inst}$, since this is the only region allowed for maintaining the false-vacuum state of the noninflaton field $\psi$. Because in this region $\psi = 0$ is always the minimum of the potential for a fixed $\phi$, provided that the potential along the $\phi$ direction is flat enough, we can assume that soon after the initial state the noninflaton field $\psi$ settles down to $\psi = 0$ while $\phi$ could not have changed too much. Therefore the effective potential which dominates the evolution of $\phi$ afterwards becomes

$$V(\phi) \equiv V(\phi,0) = \frac{1}{4}\lambda M^4 + \frac{1}{2}m^2\phi^2 \tag{4.3}$$

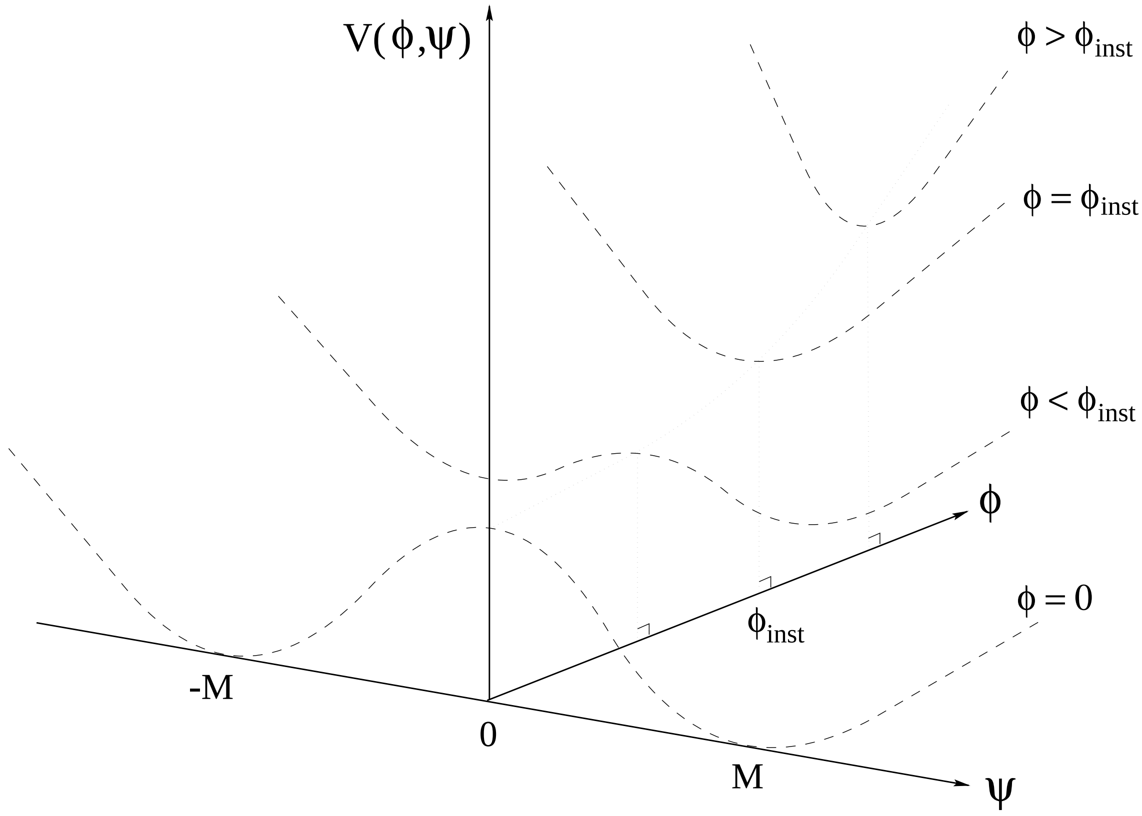


Figure 4.1: A sample model of false-vacuum inflation whose potential takes the form $V(\phi,\psi) = \lambda\left(\psi^2 - M^2\right)^2/4 + m^2\phi^2/2 + \lambda'\phi^2\psi^2/2$ within the region $\phi > 0$. This is a 3-dimensional diagram of $(\psi,\phi,V)$ with the $\phi$ direction pointing backwards. The dashed lines are drawn on the $(\psi,V)$ plane and the dotted lines are on the $(\phi,V)$ plane: (1) When $\phi > \phi_{\rm inst}$, $V \equiv V(\psi)$ has only one minimum at $\psi = 0$; (2) $\phi = \phi_{\rm inst}$ is the critical point beyond which the symmetry (the false vacuum) is restored; (3) When $\phi < \phi_{\rm inst}$, $V \equiv V(\psi)$ has two minima at $\psi = (M^2 - \lambda'\phi^2/\lambda)^{1/2}$; (4) The global minima are at $(\phi,\psi) = (0,\pm M)$.

i.e. the inflaton rolls down towards its minimum at $\phi = 0$ along the trajectory of $\psi = 0$. By comparing the two terms on the right-hand side of (4.3), one finds two different ways for $\phi$ to evolve. The first is when the second term is much larger than the first one, the evolution of the inflaton is similar to the chaotic inflation featuring only one scalar field since the false-vacuum energy $M$ is considerably negligible. This case is referred to as "inflaton-dominated" inflation. It was first considered by Kofman & Linde [50], who pointed out that it might produce cosmic strings with enough energy per unit length to form the structure of the universe. The second is when the first term of (4.3) is much larger than the second, inflation could be terminated by a prompt phase transition once $\phi \lesssim \phi_{\rm inst}$. This case is referred to as "vacuum-dominated" inflation and was termed "hybrid inflation" [69]; it is our focus.

In the conventional scenario of inflation which involves only one scalar field $\phi$, the end of inflation is generally signalled by the violation of $\max\{\epsilon_V(\phi), \eta_V(\phi)\} \lesssim 1$, or more precisely by $\epsilon_H(\phi) < 1$. However, in the regime of false-vacuum inflation, both $\epsilon_H(\phi) = 1$ and $\phi = \phi_{\rm inst}$ could trigger the end of inflation, depending on how flat the potential is along the $\phi$ direction. If the potential is flat enough, the second condition could be achieved while $\epsilon_H(\phi)$ is still less than unity. In this situation, because of the instability at $\phi_{\rm inst}$ a prompt phase transition will be carried out and then cause the prompt reheating. This phase transition may be either first [68] or second [69, 57] order. Finally the scalar fields roll down to one of their global minima at $(\phi, \psi) = (0, \pm M)$. To analyse these ideas concretely, a dynamical system is required and we shall assume the flat Friedmann model as introduced in Chapter 2.

## 4.2 The Dynamics

### 4.2.1 Conventional Analysis

For the convenience of our later analysis, we shall normalize $m_{\rm Pl}$ to be unity so that $\phi$, $\psi$, $M$ and $m$ are all in the unit of Planck mass. Recalling (2.9) and (2.10) for scalar field dynamics in a flat Friedmann model, we have equations governing the false-vacuum inflation as

$$H^2 = \frac{8\pi}{3}\left[\frac{1}{2}\dot{\phi}^2 + \frac{1}{2}\dot{\psi}^2 + V(\phi, \psi)\right] \tag{4.4}$$

$$\ddot{\phi} + 3H\dot{\phi} = -\frac{\partial V(\phi, \psi)}{\partial \phi} \tag{4.5}$$

$$\ddot{\psi} + 3H\dot{\psi} = -\frac{\partial V(\phi,\psi)}{\partial \psi} \tag{4.6}$$

As we mentioned in the previous section, the noninflaton field $\psi$ rolls down to $\psi = 0$ from whatever its initial value may have been and then the inflaton $\phi > 0$ proceeds towards $\phi = 0$ along the $\psi = 0$ channel so that the effective potential becomes the form of (4.3). Thus we can consider the scenario as if there is only one scalar field—the inflaton. For the convenience of our later analysis, we rewrite (4.3) as

$$V(\phi) = \frac{\lambda}{4}M^4(1 + B\phi^2) \tag{4.7}$$

where

$$B = \frac{2m^2}{\lambda M^4} \tag{4.8}$$

By observing (4.4) through (4.6), we see that these equations are invariant under a rescaling of the potential and the time variable, $V \to \alpha V$ and $t \to t/\sqrt{\alpha}$. So now $B$ is the only effective parameter in the situation of our current consideration. We can hence define the inflaton-dominated regime as when $B\phi^2 \gg 1$ and the vacuum-domination regime as when $B\phi^2 \ll 1$. Substituting (4.7) into (4.4) and (4.5) gives

$$H^2 = \frac{8\pi}{3}\left[\frac{1}{2}\dot{\phi}^2 + \frac{\lambda}{4}M^4(1 + B\phi^2)\right] \tag{4.9}$$

$$\ddot{\phi} + 3H\dot{\phi} = -\frac{\lambda}{2}M^4 B\phi \tag{4.10}$$

Obviously, these are nonlinear differential equations with no explicit solutions. However, by using PSRA, we obtain a solution

$$\begin{aligned}
t &= \frac{-\sqrt{6\pi\lambda}M^2}{m^2}\left[\left(1 + \frac{2m^2\phi^2}{\lambda M^4}\right)^{1/2} + \ln\frac{\left(\frac{2m^2\phi^2}{\lambda M^4}\right)^{1/2}}{\left(1 + \frac{2m^2\phi^2}{\lambda M^4}\right)^{1/2} + 1}\right] && (4.11)\\
&= \frac{-\sqrt{6\pi\lambda}M^2}{m^2}\left\{\sqrt{\frac{4}{\lambda M^4}}V^{1/2} + \ln\frac{\left[\frac{2}{m^2}\left(V - \frac{\lambda}{4}M^4\right)\right]^{1/2}}{\sqrt{\frac{4}{\lambda M^4}}V^{1/2} + 1}\right\} && (4.12)\\
a(\phi) &= \phi^{-2\pi\lambda M^4/m^2}\exp(-2\pi\phi^2) && (4.13)
\end{aligned}$$

Since the exact solution is not available, we cannot provide a conventional indicator of the end of inflation like $\epsilon_H(\phi) = 1$. Instead, we consider the PSR parameters. Substituting (4.7) into (2.25) and (2.26) gives

$$\epsilon_V(\phi) = \frac{B^2\phi^2}{4\pi(1 + B\phi^2)^2} \tag{4.14}$$

$$\eta_V(\phi) = \frac{B}{4\pi(1+B\phi^2)} \tag{4.15}$$

By comparing these two parameters, one obtains

$$\frac{\eta_V(\phi)}{\epsilon_V(\phi)} = \frac{1+B\phi^2}{B\phi^2} > 1 \tag{4.16}$$

Since $\eta_V(\phi)$ is always the larger of the two parameters we shall concentrate on its value. From (4.15) it can be clearly seen that $\eta_V(\phi)$ keeps increasing as $\phi$ rolls towards $\phi = 0$. Therefore, we can define a quantity by setting (4.15) to be unity

$$\phi_\eta = \sqrt{\frac{1}{4\pi} - \frac{1}{B}} \tag{4.17}$$

which characterizes a proper indicator of the end of inflation in the PSRA regime. This is dramatically different from Ref. [26] in which $\epsilon_V(\phi) = 1$ was used for specifying the end of inflation and the restart of inflation in the PSRA regime became possible. Actually, the smallness of both parameters is just sufficient but not necessary to have inflation so that we could not say specifically which one is better to specify the end of inflation. Fortunately, in this second-order model under investigating, it has been verified by numerical simulation across a wide range of $B$ from zero to a few billions that the restart of inflation has never happened and the end of inflation is not far behind this predicted $\phi_\eta$. Thus (4.17) could be a good choice for purely analytical work. However, this is just the conventional result which involves only one scalar field. In our model we still have another possibility to terminate inflation—the instability of the fields once $\phi < \phi_{\text{inst}}$ as mentioned in the previous section.

### 4.2.2 The instability

The above analysis is valid only if the vacuum energy $M$ is negligible, since in that case the scenario is similar to chaotic inflation featuring only a single scalar field and we have no worry about the breaking point of symmetry at $\phi_{\text{inst}}$ introduced in section 4.1. However, in the vacuum-dominated case ($B\phi^2 \ll 1$), from (4.15) one can see that $\eta_V(\phi)$ can be treated as a constant and once given $\eta_V(\phi) < 1$ it always grows too slowly to violate the inequality. This implies that the potential in this case must be quite flat in the $\phi$ direction so that it can maintain inflation all the time. Therefore, we have to consider the other possible way to terminate inflation when the inflaton reaches $\phi_{\text{inst}}$.

Because of quantum fluctuation, once the inflaton rolls down passing through $\phi_{\text{inst}}$ it must be unstable and finally falls down to one of the global minima at $(0, \pm M)$. Assuming that the friction of the Hubble expansion is negligible and that the potential is still sufficiently flat along the $\phi$ direction when the $\psi$ leaves $\psi = 0$, from (4.6) we know the noninflaton field $\psi$ will easily roll down to one of the degenerate local minima while $\phi$ will not change much. Thus according to 3b in section 4.1 we have the value of $\psi$ when $\phi < \phi_{\rm inst}$ as

$$\psi^2 \simeq \psi^2_{\rm min}(\phi) = M^2(1 - \frac{\phi^2}{\phi^2_{\rm inst}}) \tag{4.18}$$

Substituting this into (4.1) to eliminate $\psi$ and $\lambda'$ yields

$$\begin{aligned} V(\phi) &= \frac{\lambda}{4}M^4\left[1 + B\phi^2 - \left(1 - \frac{\phi^2}{\phi^2_{\rm inst}}\right)^2\right] \\ V'(\phi) &= \frac{\lambda}{2}M^4\phi\left[B + \frac{2}{\phi^2_{\rm inst}}\left(1 - \frac{\phi^2}{\phi^2_{\rm inst}}\right)\right] \\ V''(\phi) &= \frac{\lambda}{2}M^4\left[B + \frac{2}{\phi^2_{\rm inst}}\left(1 - 3\frac{\phi^2}{\phi^2_{\rm inst}}\right)\right] \end{aligned} \tag{4.19}$$

Using these to recalculate $\epsilon_V$ and $\eta_V$ by their definitions, one finds in the vacuum-dominated regime ($B\phi^2 \ll 1$) at the initial stage when $\psi$ departs from its false vacuum $\psi = 0$:

$$\epsilon_V(\phi) \gtrsim \frac{1}{4\pi}\phi^2_{\rm inst}B^2 \tag{4.20}$$

$$\eta_V(\phi) \gtrsim \frac{1}{\pi}\phi^{-2}_{\rm inst} \tag{4.21}$$

To terminate inflation after the departure from the symmetric point at $\psi = 0$, we just simply require

$$\phi^2_{\rm inst} \lesssim \frac{1}{\pi} \tag{4.22}$$

Since the vacuum domination condition may be written as $\phi^2_{\rm inst} \ll B^{-1}$, condition (4.22) is redundant unless $B$ is extremely small. In practice, if the potential along the $\psi$ direction at $\phi < \phi_{\rm inst}$ is still sufficiently flat, inflation is possible to continue. However, we shall just assume that inflation cannot proceed once the inflaton has passed through the critical point $\phi_{\rm inst}$. It follows that a phase transition is triggered and causes prompt reheating.

Actually the nature of the phase transition occurring at $\phi = \phi_{\rm inst}$ is far more complicated than we can study here. It includes the first-order [68] and second-order [69, 57] transitions. In a general case, both $\phi$ and $\psi$ are inhomogeneous and the phenomena are unlikely to be as simple as those described above. Nevertheless, we shall just use $\phi = \phi_{\rm inst}$ as an indicator of the end of inflation if it is still proceeding when passing through this point. Thus combining (4.2) and (4.17), we define the end of inflation in the regime of the false-vacuum inflation as

$$\phi_{\mathrm{f}} = \max\{\phi_\eta, \phi_{\mathrm{inst}}\} \tag{4.23}$$

### 4.2.3 Number of $e$-foldings

Before the end of the false-vacuum inflation, the scenario can be considered as if only the inflaton field is involved since the noninflaton field is trapped in its false vacuum. Thus we can use the conventional techniques developed in Chapter 2 to analyse the events of inflation with an end specified by (4.23). The first thing to consider is the amount of inflation. Because of the existence of attractor solution of inflation as introduced in subsection 2.3.2, this can be specified by number of $e$-foldings using PSRA:

$$N(\phi_{\mathrm{i}}, \phi_{\mathrm{f}}) \equiv \ln \frac{a(\phi_{\mathrm{f}})}{a(\phi_{\mathrm{i}})} \overset{PSRA}{\simeq} -8\pi \int_{\phi_{\mathrm{i}}}^{\phi_{\mathrm{f}}} \frac{V(\phi)}{V'(\phi)} d\phi \tag{4.24}$$

where the Planck mass has been normalized to unity.

In order to link the theoretical side to the observations, especially the CMB detection, one is generally interested in the epoch of $t_{60}$. In the previous chapter, we used (3.8) and assigned $N_* = 60$ to indicate this epoch. However, we shall see that in the regime of false-vacuum inflation the energy scale $V_{60}^{1/4}$ could be as low as $10^{11}$ GeV, rather than the typical value $10^{16}$ GeV as we estimated in (3.96). This could have reduced our $N_{60}$ from 60 to about 50. Nevertheless, we only need a rough estimate of $N$ for most purposes because the potential varies slowly and for simplicity we shall just use $N_* = 60$ to specify the cosmologically interesting scale. Thus in order to obtain $\phi_{60}$, we substitute (4.7) into (4.24) and use $\phi_{60}$ and (4.23) for $\phi_{\mathrm{i}}$ and $\phi_{\mathrm{f}}$ respectively to yield

$$60 = -4\pi \int_{\phi_{60}}^{\phi_{\mathrm{f}}} \frac{1 + B\phi^2}{B\phi} d\phi \tag{4.25}$$

$$= \frac{4\pi}{B}(\ln \phi_{60} - \ln \phi_{\mathrm{f}}) + 2\pi(\phi_{60}^2 - \phi_{\mathrm{f}}^2) \tag{4.26}$$

We see the analytical difficulty to get $\phi_{60}$ is to pick up $\phi_{\mathrm{f}}$ between $\phi_\eta$ and $\phi_{\mathrm{inst}}$ for various parameter values. Figure 4.2 illustrates this point. It can be overcome by employing numerical simulation as we shall use in the next chapter. In the later section of this chapter, we shall investigate two extreme cases in which this quantity can be approached analytically.

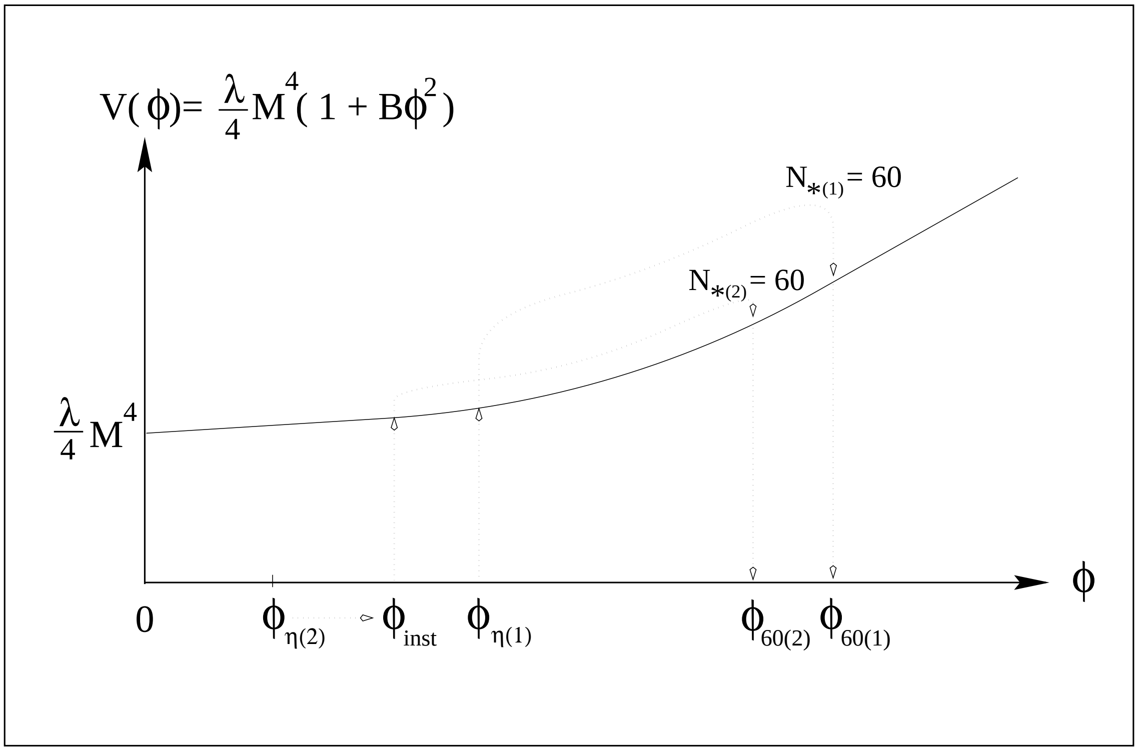


Figure 4.2: The scheme to obtain $\phi_{60}$. Assuming $\lambda$, $\lambda'$ and $M$ are specified so that we have a fixed $\phi_{\rm inst} = M(\lambda/\lambda')^{1/2}$: (1) When $\phi_{\eta(1)} > \phi_{\rm inst}$, $\phi_{\eta(1)}$ is the end of inflation and we trace from it back to 60 $e$-foldings to get $\phi_{60(1)}$; (2) When $\phi_{\eta(2)} < \phi_{\rm inst}$, $\phi_{\rm inst}$ is the end of inflation and we trace from it back to 60 $e$-foldings to get $\phi_{60(2)}$.

### 4.2.4 Density perturbations and gravitational waves

With recourse to the observational result introduced in subsection 3.3.4, we can apply some constraints on the parameter set of our false-vacuum inflationary model. For simplicity we shall use the lowest results developed in the previous chapter.

#### Density perturbations

As we developed in the previous chapter, it is the size of density perturbations that is the most important constraint placed on the parameter set of inflationary models. According to (3.25), for adiabatic density perturbations the spectrum predicted by false-vacuum inflationary model can be calculated as

$$\delta_H^2(k) \overset{PSRA}{\simeq} \frac{512\pi}{75} \frac{V^3}{V'^2}\bigg|_* = \frac{32\pi}{75} \frac{\lambda M^4(1+B\phi_*^2)^3}{B^2\phi_*^2} \tag{4.27}$$

To link this predicted quantity to observations, we have to evaluate it at the epoch of $t_{60}$ so that it corresponds to the value COBE sees. Thus combining this with (3.55) to its lowest order, one obtains

$$2.72 \times 10^{-10} \simeq \frac{\lambda M^4(1+B\phi_{60}^2)^3}{B^2\phi_{60}^2} \tag{4.28}$$

$$= \frac{(\lambda M^4 + 2m^2\phi_{60}^2)^3}{4m^4\phi_{60}^2} \tag{4.29}$$

This is the condition which constrains our parameter space. The assignment of $B$ is initially for the convenience of our analytical consideration. Here it should be returned to its origin since only the parameter set $(\lambda, \lambda', M, m)$ makes sense from a physical point of view. Because the calculation of $\phi_{60}$ involves both $\phi_\eta$, which is associated with $B \equiv B(\lambda, m, M)$, and $\phi_{\rm inst}$, which is associated with $(\lambda, \lambda', M)$, it cannot be carried out without employing numerical simulations. Even if we set $\lambda \sim \lambda' \sim 1$ as a reasonable choice in the context of particle physics, the whole story is still complicated enough. Later in this chapter, we shall examine this situation in two extreme regimes which make the constraints more explicit.

Nevertheless, ignoring the difficulty of obtaining $\phi_{60}$, we can still find a strong constraint on the parameters just by considering the form of the right-hand side of (4.28). It can be treated as a function of $\phi_{60}$. If we calculate its first and second derivatives with respect to $\phi_{60}$, we find this function of $\phi_{60}$ has positive curvature and a minimum at

$$2B\phi_{60}^2 = 1 \tag{4.30}$$

This means that the value of the right-hand side of (4.28) at $\phi_{60}^2 = 1/2B$ must be less than the value given by its left-hand side, otherwise (4.28) will have no solution for $\phi_{60}$. This leads to a very neat result:

$$\frac{\lambda M^4}{B} \lesssim 4.03 \times 10^{-11} \tag{4.31}$$

or alternatively

$$\frac{\lambda M^4}{m} \lesssim 8.98 \times 10^{-6} \tag{4.32}$$

Without employing any assumption or approximation, we find a strong constraint which should be obeyed by these parameters throughout. This condition will be very useful when one considers further approaches including numerical simulations. Furthermore, we see if the minimum value of the right-hand-side function of (4.28) is less than the left-hand-side value, (4.28) should possess two solutions for $\phi_{60}$. One is in the region $\phi_{60} > 1/\sqrt{2B}$ and the other in the region $\phi_{60} < 1/\sqrt{2B}$. Since $\phi_{60} = 1/\sqrt{2B}$ is exactly the division of the inflaton-dominated and vacuum-dominated regimes (apart from a factor of 2), it implies that in the parameter space the hypersurfaces of these two regimes reproducing the COBE result should merge with each other somewhere on the hypersurface defined by the equality of (4.32). Although this property is not very useful at the present stage, it can be used to check if the results of our analytical approaches or numerical simulations are reasonable.

Derived from the observed spectrum of density perturbations, two by-products are the estimated time scale ($H_*^{-1}$) and energy scale ($V_*^{1/4}$) at the epoch of $t_{60}$. Employing (3.58) and (3.60) to their lowest order, we have

$$H_{60}^{-1} \simeq (2.26 \times 10^{-39}\mathrm{sec}) \left(\frac{1 + B\phi_{60}^2}{B\phi_{60}}\right) \tag{4.33}$$

$$V_{60}^{1/4} \simeq (3.51 \times 10^{16}\mathrm{GeV}) \left(\frac{B\phi_{60}}{1 + B\phi_{60}^2}\right)^{1/2} \tag{4.34}$$

From (4.34), we see that an energy scale which is much less than $10^{16}$ GeV is possible, provided that $\phi_{60}$ is large in the inflaton-dominated ($B\phi^2 \gg 1$) regime or that $B\phi_{60}$ is small in the vacuum-dominated regime ($B\phi^2 \ll 1$).

Let us now consider the spectral index. Substituting (4.14) and (4.15) into (3.28) yields

$$n - 1 \simeq 2\eta_{V60} - 6\epsilon_{V60} = \frac{B(1 - 2B\phi_{60}^2)}{2\pi(1 + B\phi_{60}^2)^2} \tag{4.35}$$

This form is quite unusual, because the spectral index $n$ could be either larger or smaller than unity. In the regime of the chaotic inflation with polynomial potentials, one learns from (3.90) that the spectral index $n$ is always less than unity. We shall investigate this in more detail later.

### Gravitational waves

Another interesting quantity to estimate is the contribution of gravitational waves. First we investigate the behaviour of the spectrum of gravitational waves. Substituting (4.14) into (3.36) yields

$$n_T(k) \simeq -2\epsilon_{V60} = \frac{-B^2\phi_{60}^2}{2\pi(1+B\phi_{60}^2)^2} \tag{4.36}$$

which is always negative. However, this spectral index is not guaranteed to be as small as usually seen in the regime of polynomial chaotic inflation (see (3.91)).

Returning to the ratio of the amplitudes of gravitational waves and density perturbation, we substitute (4.14) into (3.49) to get

$$R \simeq 9.3\epsilon_{V60} = \frac{0.74B^2\phi^2}{(1+B\phi^2)^2} \tag{4.37}$$

Again this ratio is strongly parameter-dependent. At least it is not necessarily small as in the usual case. This means the portion of gravitational waves predicted by the false-vacuum inflationary model needs not be negligible. Compare this with (3.92), we see again that this result is different from inflation with polynomial potentials, in which the ratio $R$ is always expected to be small.

## 4.3 Two Extreme Regimes

As we have seen that the behaviour of false-vacuum inflation is strongly parameter-dependent, we shall consider two extreme cases in which analytical approaches are possible. One is the inflaton-dominated regime in which the second term on the right-hand side of (4.3) dominates the potential. This case is expected to be similar to chaotic inflation involving only a single scalar field as introduced at the end of the previous two chapters. The condition to specify this regime is $B\phi^2 \gg 1$ as mentioned in section 4.1. The other case is the vacuum-dominated regime whose condition is $B\phi^2 \ll 1$. It means the false-vacuum energy of the noninflaton field dominates the potential. Let us investigate these two regimes separately.

### 4.3.1 The inflaton-dominated regime

With the condition $B\phi^2 \gg 1$, or equivalently

$$\frac{2m^2\phi^2}{\lambda M^4} \gg 1 \tag{4.38}$$

we recalculate the relevant quantities derived earlier in this chapter. According to (4.14), (4.15), (4.25), (4.29), (4.33), (4.34), (4.35), (4.36), and (4.37), one obtains

$$\begin{aligned}
\epsilon_V \simeq \eta_V &\simeq \frac{1}{4\pi\phi^2} && (4.39)\\
\phi_{60}^2 &\simeq \phi_{\rm f}^2 + \frac{30}{\pi} && (4.40)\\
m\phi_{60}^2 &\simeq 1.17\times 10^{-5} && (4.41)\\
H_{60}^{-1} &\simeq (2.26\times 10^{-39}\mathrm{sec})\,\phi_{60} && (4.42)\\
V_{60}^{1/4} &\simeq (3.51\times 10^{16}\mathrm{GeV})\frac{1}{\sqrt{\phi_{60}}} && (4.43)\\
n-1 \simeq 2n_T &\simeq \frac{-1}{\pi\phi_{60}^2} && (4.44)\\
R &\simeq \frac{0.74}{\phi_{60}^2} && (4.45)
\end{aligned}$$

Obviously, all the quantities are given via $\phi_{60}$ in this regime. Therefore the evaluation of $\phi_{\rm f}$ appearing in (4.40) becomes significant. Before proceeding to further analysis about $\phi_{\rm f}$, we can still get some useful information from these results. First, from (4.40) we know $\phi_{60}^2 > 30/\pi$ so that from (4.44) the spectral index of density perturbation must satisfy $1 > n \gtrsim 0.96$ which is very close to scale-invariant. We also have $0 > n_T \gtrsim -0.017$. Pushing the same into (4.45) one gets $0.078 \gtrsim R > 0$ which implies that the contribution from gravitational waves in the full spectrum is very small. Thus all these quantities are limited to a very narrow band and are very close to the results of the chaotic inflation investigated in subsection 3.4.3, no matter how different $\phi_{\rm f}$ will be. The change in $\phi_{\rm f}$ can only affect the mass of the inflaton $m$, the time scale $H_{60}^{-1}$, and the energy scale $V_{60}^{1/4}$ at the epoch of $t_{60}$.

By (4.39), one has $\phi_\eta = 1/\sqrt{4\pi}$. With the selection rule (4.23), we consider the following two cases to calculate $\phi_{\rm f}$:

1. When $\phi_\eta > \phi_{\rm inst}$: $\phi_{\rm f} \equiv \phi_\eta$. This case is exactly the same as chaotic inflation since the end of inflation is determined by slow-roll parameters and the form of the potential is exactly the same as that of chaotic inflation. Thus the relevant quantities should be the same as those given in subsection 3.4.3, eg. $\phi_{60} \simeq 3.1$. The only thing to

notice is the constraints on our parameters in this situation. Since now $\phi_{\rm f} = 1/\sqrt{4\pi}$ and $m \simeq 1.2 \times 10^{-6}$ from (3.84), (4.38) becomes

$$\frac{\lambda}{4} M^4 \ll 5.8 \times 10^{-14} \Longleftrightarrow \sqrt[4]{\lambda} M \ll 6.9 \times 10^{-4} \tag{4.46}$$

which is the condition for the validity of this approximation. Moreover, using $\phi_\eta > \phi_{\rm inst}$ yields

$$M \lesssim 0.28 \sqrt{\frac{\lambda'}{\lambda}} \Longleftrightarrow \frac{\lambda}{4} M^4 \lesssim 1.6 \times 10^{-3} \frac{\lambda'^2}{\lambda} \tag{4.47}$$

This condition should be obeyed when $\phi_\eta$ is used as the end of inflation instead of $\phi_{\rm inst}$. For a typical choice of $\lambda = \lambda' = 1$ in the context of particle physics, this second condition is less constraining than the first one.

2. When $\phi_\eta < \phi_{\rm inst}$: $\phi_{\rm f} \equiv \phi_{\rm inst}$. By (4.40), one has

$$\phi_{60}^2 = \frac{30}{\pi} + \frac{\lambda}{\lambda'} M^2 \tag{4.48}$$

so that (4.41) gives

$$1.17 \times 10^{-5} = m \left( \frac{30}{\pi} + \frac{\lambda}{\lambda'} M^2 \right) > \frac{30}{\pi}\, m \tag{4.49}$$

In the regime $\lambda \sim \lambda' \sim 1$, this condition can be dramatically simplified. Since $m^{1/2} \lesssim 10^{-3}$ from this condition, with recourse to (4.32) one has $M^2 \lesssim 10^{-3} m^{1/2}$ so that $M^2 < 10^{-6}$, which is negligible in (4.49). Thus (4.49) gives us $m \simeq 1.2 \times 10^{-6}$ and $\phi_{60} \simeq 3.1$, which are the same as case 1. Once again it is similar to chaotic inflation and the relevant quantities are the same as those given in subsection 3.4.3. Returning to the condition for the validity of this approximation, by the inequality of (4.49) and $\phi_{\rm f}^2 \equiv \phi_{\rm inst}^2 = M^2 \lambda/\lambda'$ we can rewrite (4.38) as

$$\lambda' M^2 \ll 3 \times 10^{-12} \tag{4.50}$$

However, in the regime $\lambda \sim \lambda' \sim 1$ this condition is impossible to be satisfied since from (4.47) we see that when $M \lesssim 0.28$, $\phi_\eta$ is always larger than $\phi_{\rm inst}$. This implies that, in the inflaton-dominated regime, the end of inflation is always specified by $\phi_\eta$ rather than $\phi_{\rm inst}$.

One thing to point out is that the mass of inflaton in both cases is always a constant

$$m \simeq 1.2 \times 10^{-6} \tag{4.51}$$

With the COBE constraint (4.32), this line will be truncated on the $(M, m)$ plane with $\lambda = \lambda' = 1$ at around

$$M \sim 1.8 \times 10^{-3} \tag{4.52}$$

Comparing this with (4.47), we see that with the choice of $\lambda = \lambda' = 1$ the end of inflation is always triggered by $\phi_\eta$. Comparing (4.52) further with (4.46), we see that the predicted behaviour of $m$ as a constant should be a good approximation until it approaches one order below the truncation point. After this, it will deviate from $1.2 \times 10^{-6}$ and we require numerical simulations to get the exact solution, as we shall see in the next chapter.

### 4.3.2 The vacuum-dominated regime

Since the inflaton-dominated regime is not much different from chaotic inflation, it is the vacuum-dominated regime that is our main focus. In this regime, with the condition $B\phi^2 \ll 1$ or alternatively

$$\frac{2m^2\phi^2}{\lambda M^4} \ll 1 \tag{4.53}$$

we recalculate the relevant quantities. By (4.14) and (4.15) one has

$$\epsilon_V \simeq \frac{B^2\phi^2}{4\pi} \tag{4.54}$$

$$\eta_V \simeq \frac{B}{4\pi} \tag{4.55}$$

Since $\eta_V/\epsilon_V = 1/B\phi^2 \gg 1$ and $\eta_V$ behaves as a constant, to have inflation one requires, from (4.55) combined with $B\phi^2 \ll 1$, that

$$B^2\phi^2 \ll B < 4\pi \Longrightarrow B\phi \ll \sqrt{4\pi} \tag{4.56}$$

Once this is satisfied, it will be satisfied forever because $\phi$ keeps decreasing. Thus the end of inflation must be triggered by the instability at $\phi_{\mathrm{inst}}$, ie. $\phi_{\mathrm{f}} = \phi_{\mathrm{inst}} = M\sqrt{\lambda/\lambda'}$. Furthermore, according to (4.25), (4.29), (4.33), (4.34), (4.35), (4.36), and (4.37), we obtain

$$\phi_{60} \simeq \phi_{\mathrm{f}} e^{15B/\pi} = \sqrt{\frac{\lambda}{\lambda'}} M e^{15B/\pi} \tag{4.57}$$

$$\frac{\lambda M^4}{B^2\phi_{60}^2} \simeq 2.72 \times 10^{-10} \tag{4.58}$$

$$H_{60}^{-1} \simeq (2.26 \times 10^{-39}\mathrm{sec})\,\frac{1}{B\phi_{60}} \tag{4.59}$$

$$V_{60}^{1/4} \simeq (3.51 \times 10^{16}\mathrm{GeV})\,(B\phi_{60})^{1/2} \tag{4.60}$$

$$\begin{aligned} n-1 &\simeq \frac{B}{2\pi} && (4.61)\\ n_T &\simeq \frac{-B^2\phi_{60}^2}{2\pi} && (4.62)\\ R &\simeq 0.74\, B^2\phi_{60}^2 && (4.63)\end{aligned}$$

Let us consider first the condition for the validity of the vacuum-dominated regime. With the help of (4.58), (4.56) can be rewritten as

$$\frac{\lambda}{4}M^4 \ll 8.5\times 10^{-10} \Longleftrightarrow \sqrt[4]{\lambda}M \ll 7.6\times 10^{-3} \tag{4.64}$$

Combining (4.56) with (4.31), we get the condition to have solution for $\phi_{60}$ in (4.28):

$$\frac{\lambda}{4}M^4 < 1.27\times 10^{-10} \tag{4.65}$$

The comparison of (4.64) and (4.65) tells us that in the vacuum-dominated regime $\phi_{60}$ always exists so that we can proceed with our analysis.

With (4.56), we see the timescale at $t_{60}$ in (4.59) must be at least a few orders larger than $10^{-39}$ sec and the energy scale $V_{60}^{1/4}$ in (4.60) must be also at least a few orders less than $10^{16}$ GeV. Since $\phi$ keeps decreasing, the energy scale at the end of inflation must be much less than $10^{16}$ GeV. Such an unusual smallness of the energy scale could reduce our $N_{60}$ from 60 to be much smaller as mentioned earlier (see (3.8)). This is dramatically different from the chaotic inflation in which the energy scale at the end of inflation is typically around $10^{16}$ GeV (see subsections 3.4.3 and 3.4.4). This low energy scale can also result in an unusually low reheating temperature that is very helpful for building up the gravitino model. In that model the reheating temperature scale is required to be less than $10^{11}$ GeV [37, 47] and within the regime of the vacuum-dominated inflation this condition could be achieved easily.

For density perturbations, combining (4.61) with (4.56) we have

$$1 < n < 2 \tag{4.66}$$

which is also dramatically different from polynomial chaotic inflation in which we expect $n$ to be always less than unity. This implies the amplitude of density perturbations predicted by the vacuum-dominated inflation grows with scale. For gravitational waves, putting (4.56) into (4.62) gives

$$|n_T| \ll \frac{B}{2\pi} < 2, \quad n_T < 0 \tag{4.67}$$

The negativity is reasonable and the smallness is the same as that predicted by polynomial chaotic inflation (see (3.91)). Applying (4.56) for (4.63) we see

$$R \ll 0.74B < 9.3 \tag{4.68}$$

This means gravitational waves could have a significant contribution to the full spectrum but not necessarily.

To have more explicit constraints on our parameters, we now set $\lambda \sim \lambda' \sim 1$ as a typical choice in the context of particle physics. This choice enables us to simplify our situation greatly. Starting with the constraint on $B$ in the vacuum-dominated regime, we substitute (4.57) into (4.58) and employ (4.64) to get

$$2.72 \times 10^{-10}\ B^2 e^{30B/\pi} = M^2 \overset{(4.64)}{\ll} 5.8 \times 10^{-5} \tag{4.69}$$

This condition leads to a neat constraint on $B$ as

$$B \ll 1.24 \tag{4.70}$$

so that from (4.57) we have $372\phi_{\rm f} \gg \phi_{60} > \phi_{\rm f}$. This allows us to assign $\phi_{60} \simeq \phi_{\rm f} \equiv M$ since the error will be approximately within the level of unity. Thus, using this for the COBE constraint (4.58) yields

$$\frac{M^5}{m^2} \simeq 3.3 \times 10^{-5} \Longleftrightarrow \log_{10} m = \frac{5}{2}\log_{10} M + \frac{9}{4} \tag{4.71}$$

This represents a straight line on the $(M, m)$ with logarithmic coordinates and will be truncated at around

$$M \sim 10^{-2} \tag{4.72}$$

according to (4.32). Comparing this with (4.64), we see this line will be a good approximation until $M$ grows to around one order below the truncation point. Now combining (4.71) with (4.51), we have built up a clear picture keeping in mind that, on the $(M, m)$ plane with logarithmic coordinates, the horizontal line predicted by the inflaton-dominated regime and the line with a slope of 2.5 predicted by the vacuum-dominated regime will merge with each other at around

$$(M, m) \sim (10^{-3}, 10^{-6}) \tag{4.73}$$

and this approximation should work well until around one order below this point. Thus we have obtained the constraints on our parameters $(M, m)$ in the regime $\lambda \sim \lambda' \sim 1$ for the full false-vacuum inflation model. Furthermore, substituting (4.70) into (4.59), (4.60), (4.61), (4.62) and (4.63) yields

$$\begin{aligned} H_{60}^{-1} &\gg 2.4 \times 10^{-37}\mathrm{sec} && (4.74)\\ V_{60}^{1/4} &\ll 3.4 \times 10^{15}\mathrm{GeV} && (4.75)\\ 1 < n &\lesssim 1.19 && (4.76)\\ n_T &\ll 0.2 && (4.77)\\ R &\ll 0.9 && (4.78) \end{aligned}$$

which provides us with a very clear picture for the characteristics of the vacuum-dominated inflation within the regime of $\lambda \sim \lambda' \sim 1$. Notice that the upper limit of $n = 1.19$ is very close to the numerical result of $n_{\max} = 1.14$ given in Ref. [26]. This also implies a nearly scale-invariant spectrum of density perturbations, although with a spectral index greater than unity. The predicted contribution from gravitational waves is also small.

As we have seen, the behaviour of false-vacuum inflation and the phenomena it causes is quite different from any conventional inflationary model. This includes the interruption of inflation due to the instability at $\phi_{\mathrm{inst}}$, the unusually low energy scale, the large time scale, the excess of the spectral index of density perturbations over unity, etc. These distinctions to other models arise from the existence of the false vacuum, since in the inflaton-dominated regime we see not much difference from the chaotic inflation but in the vacuum-dominated regime the properties are all changed. Actually, the existence of the false vacuum has enabled a linking of this model into the demanding context of superstring motivated supergravity [26]. Very few inflationary models possess this feature. To close our investigation of false-vacuum inflation, we shall briefly introduce another model, in which inflation may restart after its first end.

## 4.4 A Model With a Quartic Potential

Instead of the quadratic term which appeared in (4.1), a quartic potential was used by Roberts *et al.* in Ref. [85]. In that paper they investigated the false-vacuum inflation whose potential took the form

$$V(\phi,\psi) = \frac{1}{4}\lambda\left(\psi^2 - M^2\right)^2 + \frac{\lambda'}{2}\phi^2\psi^2 + \frac{\lambda''}{4}\phi^4 \qquad (4.79)$$

As before, when inflation occurs the noninflaton field is trapped in its false-vacuum state so that the effective potential at this stage becomes

$$V(\phi) = \frac{\lambda}{4}M^4(1 + B'\phi^4) \tag{4.80}$$

where

$$B' = \frac{\lambda''}{\lambda M^4} \tag{4.81}$$

The corresponding slow-roll parameters, and the critical point beyond which the symmetry is restored, are therefore

$$\epsilon_V(\phi) = \frac{1}{2}\left(\frac{4B'\phi^3}{1 + B'\phi^4}\right)^2 \tag{4.82}$$

$$\eta_V(\phi) = \frac{12B'\phi^2}{1 + B'\phi^4} \tag{4.83}$$

$$\phi^2_{\text{inst}} = M^2\frac{\lambda}{\lambda'} \tag{4.84}$$

where again $m^2_{\text{Pl}}/8\pi$ has been normalized to unity. By comparing these two parameters, one obtains

$$\frac{\eta_V(\phi)}{\epsilon_V(\phi)} = \frac{3}{2}\frac{1 + B'\phi^4}{B'\phi^4} > \frac{3}{2} \tag{4.85}$$

Since $\eta_V(\phi)$ is always the larger of the two parameters, we can define quantities by setting (4.83) to be unity

$$\phi_\pm = \sqrt{6}\left(1 \pm \sqrt{1 - \frac{1}{36B'}}\right)^{1/2} \tag{4.86}$$

which indicates the critical values for the slow-roll condition to hold in the $\phi > 0$ region. Theoretically, ignoring $\phi_{\text{inst}}$ as long as $B' > 1/36 \sim 0.03$ there should be two stages for inflation to occur: when the inflaton field rolls down the potential from somewhere at $\phi > \phi_+$, inflation will be suspended at $\phi_+$ and then reoccur when $\phi$ reaches $\phi_-$. This is because the value of $\eta_V$ is less than unity within the regions $\phi > \phi_+$ and $\phi < \phi_-$ but greater than unity when $\phi_+ > \phi > \phi_-$. However, numerical simulation shows that, ignoring the instability at $\phi_{\text{inst}}$, there are three regimes of behaviour [85]:

1. $0 < B' \lesssim 0.19$: Inflation proceeds as a single phase no matter if $\epsilon_V$ or $\eta_V$ temporarily exceeds unity.

2. $0.19 \lesssim B' \lesssim 2$: Inflation stops at $\phi \simeq \sqrt{12}$ and then restarts, giving two separate stages.

3. $2 \lesssim B$: Inflation stops at $\phi \simeq \sqrt{12}$ and never restarts.

| DYNAMICAL REGIMES | | | |
|---|---|---|---|
| | $\phi^2_{\rm inst} > \phi^2_{\rm stop}$ | $\phi^2_{\rm stop} > \phi^2_{\rm inst} > \phi^2_{\rm restart}$ | $\phi^2_{\rm restart} > \phi^2_{\rm inst}$ |
| $B \lesssim 0.19$ | $\phi_{\rm inst}$ | No regime | No regime |
| $0.19 \lesssim B \lesssim 2$ | $\phi_{\rm inst}$ | $\phi_{\rm stop}$ | $\phi_{\rm stop}$, $\phi_{\rm inst}$ |
| $2 \lesssim B$ | $\phi_{\rm inst}$ | $\phi_{\rm stop}$ | No regime |

Table 4.1: The different dynamical regimes. In each column, each $\phi$ represents an epoch of inflation which ends at that location. In the first row $\phi_{\rm stop}$ does not exist and in the last row $\phi_{\rm restart}$ does not exist.

If combined with the instability at $\phi_{\rm inst}$, the dynamics of this model becomes more complicated. Suppose when ignoring $\phi_{\rm inst}$ the precise location at which inflation stops is denoted by $\phi_{\rm stop}$ and the precise location at which inflation restarts (if it does) is denoted by $\phi_{\rm restart}$. Thus, the possible regimes of behaviour combined with $\phi_{\rm inst}$ can be summarised as in Table 4.1. Notice that when $0.19 \lesssim B \lesssim 2$ and $\phi^2_{\rm restart} > \phi^2_{\rm inst}$ the two-epoch inflation does exist in this model. Such a dynamics can cause some intriguing phenomena, like the horizon exit of the cosmologically interesting scale during the first epoch, the reentry and then exit of it during the second epoch of inflation. It will affect the usual form of density perturbations since the first epoch also contributes perturbations of the inflaton field to the full spectrum. Thus we see that false-vacuum inflation with a quartic term of inflaton has complicated both the dynamics of inflation and its phenomenology. Other variants of hybrid inflation also possess their own distinctions from the traditional models and they are of particular interest in the current literature [100, 77, 84].

CHAPTER 5

# NUMERICAL SIMULATION

In the regime of inflation, only a few models can be exactly solved analytically. The well known ones are de Sitter expansion, power-law inflation and intermediate inflation, as we have seen in Chapter 2. In that chapter, we developed a standard analytical scheme to approach those models for which exact solutions do not exist. That is the slow-roll approximation, which includes the PSRA and the HSRA, depending on whether $V(\phi)$ or $H(\phi)$ is our primary quantity. However, analytical approaches have their limit in accuracy and we know the slow-roll approximation is necessarily a poor guide of when inflation is to end. For more precise work, such as the comparison of $\phi_\eta$ and $\phi_{\rm inst}$ as we had in the hybrid model, numerical simulations that can yield the exact solution of any model are therefore desired. In this chapter, we shall use this technique to solve not only the flat Friedmann model ($k = 0$) but also the full set of Friedmann equation (2.9) and the equation of $\phi$-motion (2.10). Then we shall also use numerical simulation to analyse the parameter space of hybrid inflation.

## 5.1 Friedmann Equation and the Equation of $\phi$-Motion

In this section, our aim is to solve the full Friedmann equation (2.9) and the equation of $\phi$-motion (2.10). We shall develop several methods based on different formalisms to do this and finally favour Proty's method to deal with various models.

### 5.1.1 The techniques

The main tool we use to solve the differential equations in our model is the NAG routine D02CBF of Fortran 77. It enables one to solve simultaneous differential equations whose form is

$$y_i' = f_i(x, y_1, y_2, ..., y_n), \qquad i = 1 \sim n \tag{5.1}$$

where the prime denotes the derivative with respect to $x$. The standard output of this routine is $(x, y_1, \ldots, y_n)$ at each $x$ increased by an interval specified by the user. In our case $n = 2$, since we have only two relevant differential equations. Different formalisms of our model will enable us to have different choice of the primary quantities $x$ and $y_i$ in (5.1). Here are three different methods using different formalism to solve the equations. We shall assume the form of the potential $V(\phi)$ has been specified by some model.

### The Hamilton-Jacobi formalism

This is the simplest case in which one can obtain the solutions of the Hubble parameter $H(\phi)$ and the number of $e$-foldings $N(\phi)$. By using (2.33) and (2.34), one can have

$$H'(\phi) = \left[12\pi H^2(\phi) - 32\pi^2 V(\phi)\right]^{1/2} \tag{5.2}$$

$$N'(\phi) = -4\pi \frac{H(\phi)}{H'(\phi)} \tag{5.3}$$

where the Planck mass has been normalised to unity. Thus $\phi$ corresponds to $x$, $H(\phi)$ to $y_1(x)$ and $N(\phi)$ to $y_2(x)$. Furthermore, by (2.35) we can have the slow-roll parameter

$$\epsilon_H(\phi) = 3 - \frac{8\pi V(\phi)}{H^2(\phi)} \tag{5.4}$$

This quantity is useful because $\epsilon_H(\phi) = 1$ gives us the indicator of the end of inflation.

Program 1 attached in Appendix A was written by Liddle using this formalism. Its advantage is its neat form and high efficiency. Its direct output $(\phi, H, N)$ enable us to easily find $\phi_{60}$ which corresponds to the cosmologically interested scale. Therefore this method is sufficient for testing our models with the COBE constraint. However, it has two defects. One is what if the quantity inside the square root on the right-hand side of (5.2) is negative? If this happens there must be a discontinuity to deal with in our program. The other problem is the Hamilton-Jacobi formalism has assumed a flat universe ($k = 0$) so that we could not get a general solution to the non-flat Friedmann model ($k \neq 0$), although in the regime of inflation the curvature term is generally negligible as we have seen in subsection 2.2.1.

### The Lidsey formalism

This method is based on the change of variable:

$$\chi(\phi) = a^2(\phi) \tag{5.5}$$

which was used by Lidsey in Ref. [60] to yield a solution to the non-flat Friedmann model. With this transformation, we can have

$$\chi'(\phi) = \left(\frac{2\chi(\phi)\,[3k - \rho(\phi)\chi(\phi)]}{-3[\rho(\phi) - V(\phi)]}\right)^{1/2} \tag{5.6}$$

$$\rho'(\phi) = \frac{-3\chi'(\phi)}{\chi(\phi)}[\rho(\phi) - V(\phi)] \tag{5.7}$$

where $k = \pm 1, 0$ is the curvature and $8\pi/m_{\rm Pl}^2$ has been normalised to unity. Thus $\phi$ corresponds to $x$, $\chi(\phi)$ to $y_1(x)$ and $\rho(\phi)$ to $y_2(x)$. Furthermore, employing (5.5) to determine the Hubble parameter and the slow-roll parameter yields

$$H(\phi) = \left[\frac{\rho'(\phi)\chi'(\phi)}{-6\chi(\phi)}\right]^{1/2} \tag{5.8}$$

$$\epsilon_H(\phi) = 3 + 6\frac{V(\phi)\chi(\phi)}{\rho'(\phi)\chi'(\phi)} \tag{5.9}$$

We have used this formalism to write Program 2 attached in Appendix A. Its advantage is now the curvature term is included. However, due to the dramatic increase of the scale factor $a$ during inflation, from (5.5) we see that $\chi$ must have increased more quickly. This is easy to exceed the allow range of values by computer and we can expect the program will be interrupted or lose its accuracy sometimes. Thus we need another better method.

### The Proty formalism

This method uses $N(\phi) \equiv \ln a(\phi)$ as $y_1(x)$ and $\rho(\phi)$ as $y_2(x)$. This yields

$$N'(\phi) = \left\{\frac{1}{2[\rho(\phi) - V(\phi)]}\left[\frac{8\pi}{3}\rho(\phi) - \frac{k}{\exp[2N(\phi)]}\right]\right\}^{1/2} \tag{5.10}$$

$$\rho'(\phi) = -6N'(\phi)[\rho(\phi) - V(\phi)] \tag{5.11}$$

where the Planck mass has been normalised to unity. Comparing this with the Hamilton-Jacobi formalism, we find this formalism has two distinctions. One is here we use $\rho(\phi)$ instead of $H(\phi)$ as a primary quantity. This avoids the possibility to have negativity inside the square root. About (5.10), because $\rho(\phi)$ is always larger than $V(\phi)$ and the quantity inside the second square bracket is just the square Hubble parameter, we have no worry about a negativity inside the square root. The other advantage is that this formalism has included the curvature term, although it is generally negligible in the inflationary regime.

Moreover, based on these two primary quantities, we can have

$$H = \left[\frac{\rho'(\phi)N'(\phi)}{-3}\right]^{1/2} \tag{5.12}$$

$$\begin{aligned}
\Omega &= 1 - \frac{3k}{\exp[2N(\phi)]\rho'(\phi)N'(\phi)} && (5.13)\\
\ln\left(\frac{H^{-1}(\phi)}{a(\phi)}\right) &= -\frac{1}{2}\ln\frac{\rho'(\phi)N'(\phi)}{-3} - N(\phi) && (5.14)\\
\epsilon_H(\phi) &= 3 + \frac{24\pi V(\phi)}{\rho'(\phi)N'(\phi)} && (5.15)\\
\dot{\phi}(\phi) &= [2(\rho(\phi) - V(\phi))]^{1/2} && (5.16)\\
t(\phi) &= \int [2(\rho(\phi) - V(\phi))]^{-1/2}\, d\phi && (5.17)
\end{aligned}$$

Thus most of the relevant quantities can be evaluated numerically. We have used this formalism to write Program 3 attached in Appendix A. Because of its distinctions mentioned above, in the following subsection we shall make use of this program to investigate various inflationary models.

### 5.1.2 Power-law inflation

In subsection 2.4.3, power-law inflation was exactly solved analytically. Here we shall use numerical simulations to solve it so that we can compare the difference between them. In addition, because the analytical solution obtained in subsection 2.4.3 is based on the *flat* Friedmann model ($k = 0$), here we shall also consider the non-flat cases ($k \neq 0$) by using numerical simulations and investigate the significance of this deviation.

For convenience, we choose $p = \pi$ and $V_0 = 1$ in the model and normalise $\phi_{\rm i}$ to be the origin. Recalling (2.48), (2.51), (2.53) and (2.35) yields

$$\begin{aligned}
V(\phi) &= \exp(-4\phi) && (5.18)\\
H(\phi) &= \sqrt{\frac{8\pi^2}{3\pi - 1}}\exp(-2\phi) && (5.19)\\
N(\phi) &= 2\pi\phi && (5.20)\\
\epsilon_H(\phi) &= \frac{1}{\pi} && (5.21)
\end{aligned}$$

where the Planck mass has been normalised to unity. (5.19), (5.20) and (5.21) are the analytical solutions to the flat Friedmann model with the potential given by (5.18). They are plotted as the dot-dashed lines in Figure 5.1. To do the numerical simulation, we substitute (5.18) into our program. This yields three solutions to the flat ($k = 0$), open ($k = -1$) and closed ($k = 1$) Friedmann models. They are plotted as solid, dashed and dotted lines respectively in Figure 5.1. From this figure, we obtain:

1. Analytical solution vs. numerical solution: By comparing the dot-dashed line with

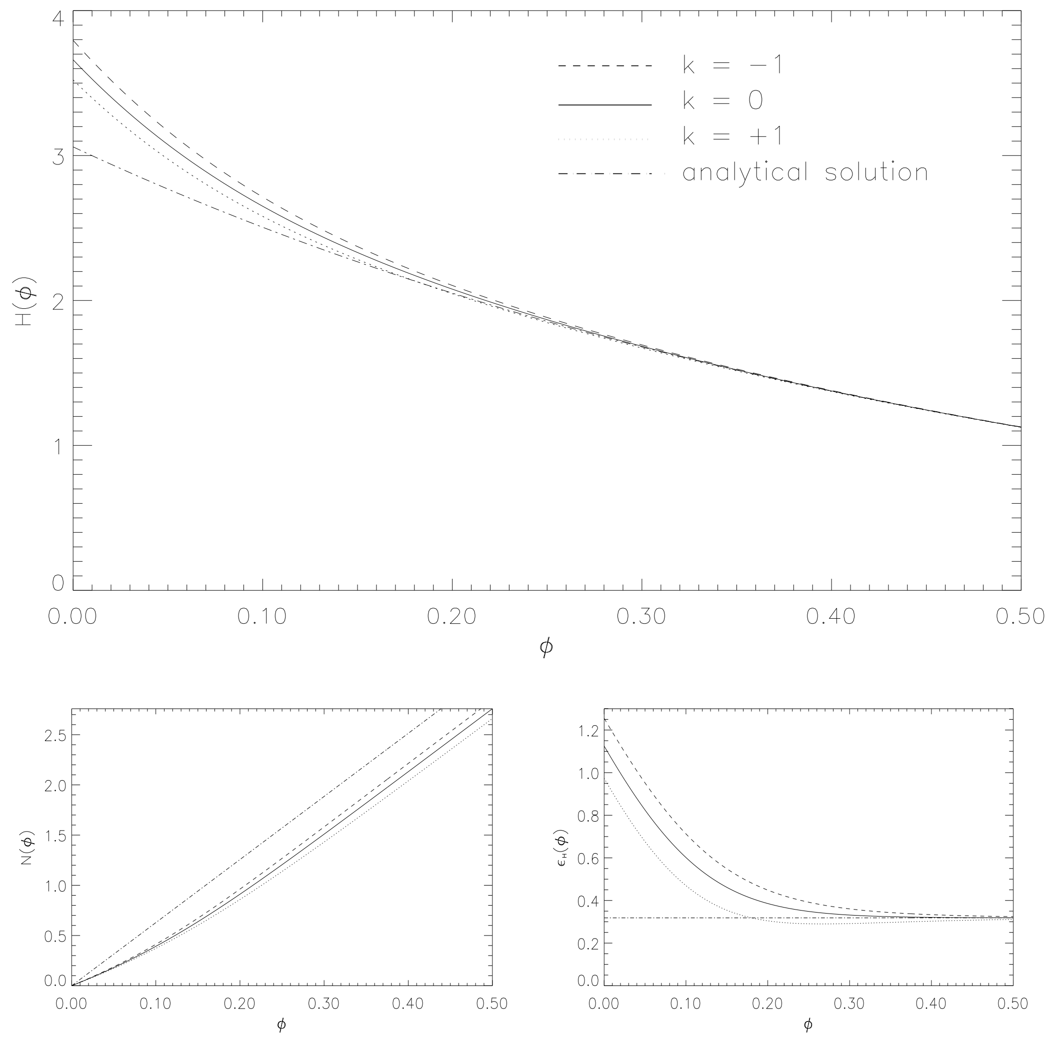


Figure 5.1: The solid lines show the numerical solution of the power-law inflation with $p = \pi$ and $V_0 = 1$ in the flat ($k = 0$) Friedmann model; the dashed and dotted lines indicate the solutions in the open ($k = -1$) and closed ($k = +1$) models respectively; the analytical solution is plotted as the dot-dashed lines. The upper figure shows how the numerical solutions approach to the analytical one; the lower left figure indicates the epoch since the beginning in terms of the number of $e$-foldings; the lower right figure shows when inflation commences.

the solid line in the $(\phi, H)$ diagram, we see that, in the flat Friedmann model, the analytical and numerical solutions approach each other very quickly. Combined with the $(\phi, N)$ diagram, we see that, despite of the initial perturbation set in the numerical simulation, its solution settles down efficiently to the analytical one within the first few $e$-foldings. This confirms the property of inflationary attractor introduced in subsection 2.3.2. From the $(\phi, \epsilon_H)$ diagram, we also find that even if the initial condition is non-inflationary, the inflationary attractor can damp it to the inflationary epoch very quickly. All these illustrate that the existence of the inflationary attractor enables us to use the analytical solution for investigating the general features of the power-law inflation with $p = \pi$.

2. Flat vs. non-flat models: By comparing the solid line ($k = 0$) with the dashed ($k = -1$) and dotted ($k = +1$) lines in the $(\phi, H)$ diagram, we see that they approach each other very quickly and the deviation of the non-flat solutions from the flat one vanishes within the first few $e$-foldings (see also the $(\phi, N)$ diagram). Since the total number of $e$-foldings for solving the Big Bang model is supposed to be around 80 (see subsection 2.2.5), the deviation arising from the curvature term in the initial stage is absolutely negligible. Conceptually, the vanishing of the deviation can be interpreted as that when inflation starts to proceed, the curvature term in the Friedmann equation is diluted efficiently due to the dramatic increase of the scale factor while the density cannot change much. More precisely, from the analysis in subsection 2.2.1, we have seen that the condition of inflation $\ddot{a} > 0$ has automatically guaranteed this to happen. This is why we can drop the curvature term throughout.

From (2.9) and (2.10), we know that the dynamics is invariant under a rescaling of the potential and the time variable, $V \to \alpha V$ and $t \to t/\sqrt{\alpha}$. So actually $p$ is the only effective parameter in the power-law inflation model. Therefore, we can conclude that, for power-law inflation with $p = \pi$, its analytical solution to the flat Friedmann model is sufficient for coping with the investigation of this model, in spite of the existence of the initial perturbation and the deviation arising from the curvature term.

### 5.1.3 Intermediate inflation

In subsection 2.4.3, we solved the intermediate inflation analytically. As an analogue to the analysis in the previous subsection, we first assign $A = 1$ and $\beta = 2$ (or equivalently

$f = 2/3$) for the intermediate inflation. According to (2.65), (2.64), (2.67) and (2.35), one has

$$V(\phi) = \frac{16}{9}\left(\frac{3}{\phi^2} - \frac{2}{\phi^4}\right) \tag{5.22}$$

$$H(\phi) = \frac{4}{3\phi} \tag{5.23}$$

$$N(\phi) = \frac{1}{4}\left(\phi^2 - \phi_{\mathrm{i}}^2\right) \tag{5.24}$$

$$\epsilon_H(\phi) = \frac{2}{\phi^2} \tag{5.25}$$

where $8\pi/m_{\mathrm{Pl}}^2$ has been normalised to unity. (5.23), (5.24) and (5.25) are the analytical solutions to the flat Friedmann model with the potential given by (5.22). They are plotted as the dot-dashed lines in Figure 5.2. According to (2.66), the theoretical condition to have inflation for $\beta = 2$ is just simply $\phi > \sqrt{2}$, which is confirmed in the $(\phi, \epsilon_H)$ diagram of Figure 5.2. Thus we choose $\phi_{\mathrm{i}} = 1.2$ to start the simulation so that we can see practically how inflation is triggered around $\phi = \sqrt{2}$. The numerical solutions for $k = -1, 0, +1$ are plotted as dashed, solid and dotted lines respectively in Figure 5.2. From this figure, we obtain

1. The numerical solutions to the non-flat models accurately coincide with that of the flat model. Compared with Figure 5.1, this implies that the curvature term in the Friedmann equation is diluted by intermediate inflation in a more efficient way than by power-law inflation.

2. Combining the $(\phi, H)$ diagram with the $(\phi, N)$ diagram, we see again that, due to the inflationary attractor, the deviation of the numerical solutions from the analytical one vanishes within the first few $e$-foldings.

3. From the $(\phi, \epsilon_H)$ diagram, we find that the numerically simulated inflation is triggered at around $\phi = 1.6$, which is later than the theoretical value $\sqrt{2}$. This implies that the initial perturbation does take time to settle down to the analytical solution, although the time is not much.

These results confirm again that the analytical solution to the *flat* Friedmann model is sufficient to feature an inflationary model, at least in the regimes of both the power-law inflation with $p = \pi$ and the intermediate inflation with $\beta = 2$ ($f = 2/3$) and $A = 1$. However, due to the difficulty of specifying the end of inflation in the slow-roll regime

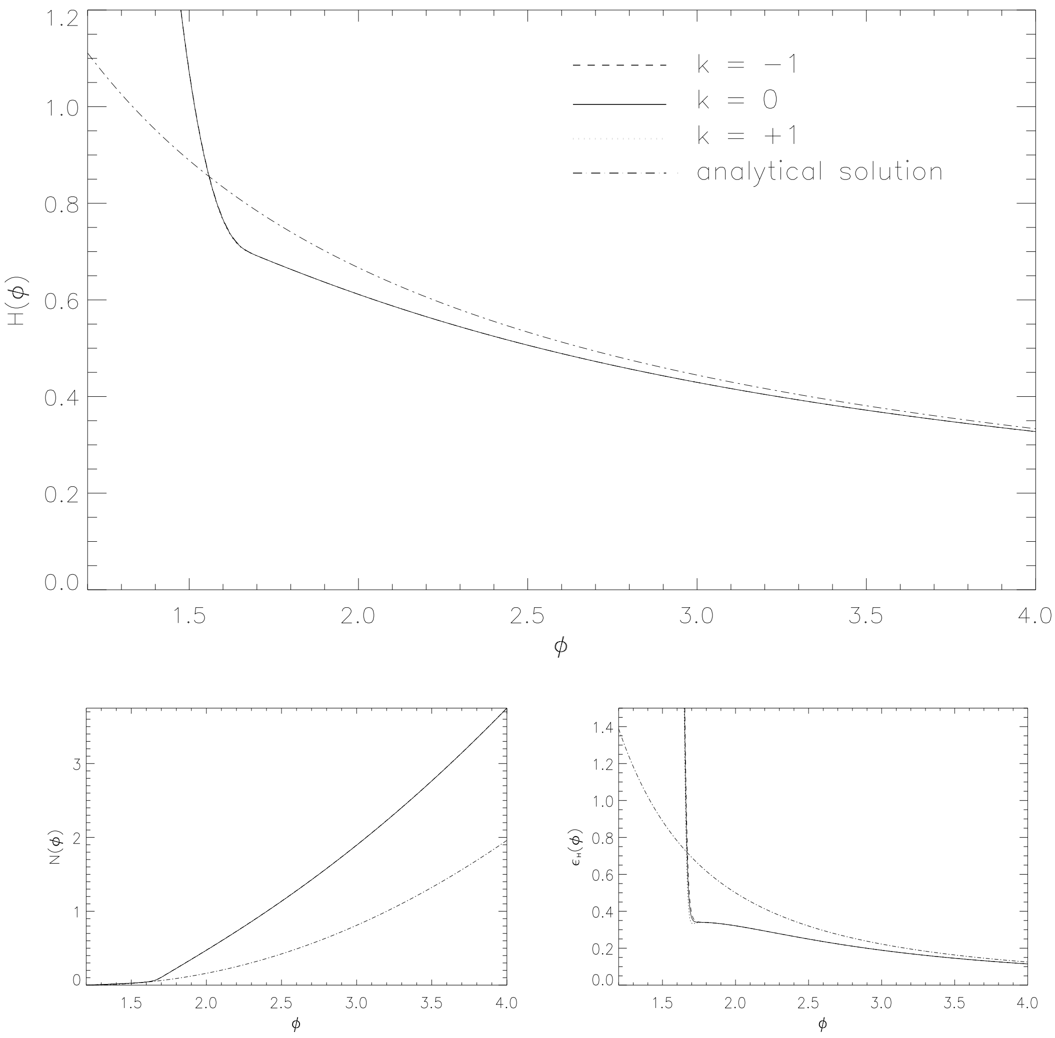


Figure 5.2: The solid lines show the numerical solution of the intermediate inflation with $A = 1$ and $\beta = 2$ ($f = 2/3$) in the flat ($k = 0$) Friedmann model; the dashed and dotted lines indicate the solutions in the open ($k = -1$) and closed ($k = +1$) models respectively, although they accurately coincide with the solution to the flat model (the solid line); the analytical solution is plotted as the dot-dashed lines. The upper figure shows how the numerical solutions approach to the analytical one; the lower left figure indicates the epoch since the beginning in terms of the number of $e$-foldings; the lower right figure shows when inflation starts to proceed.

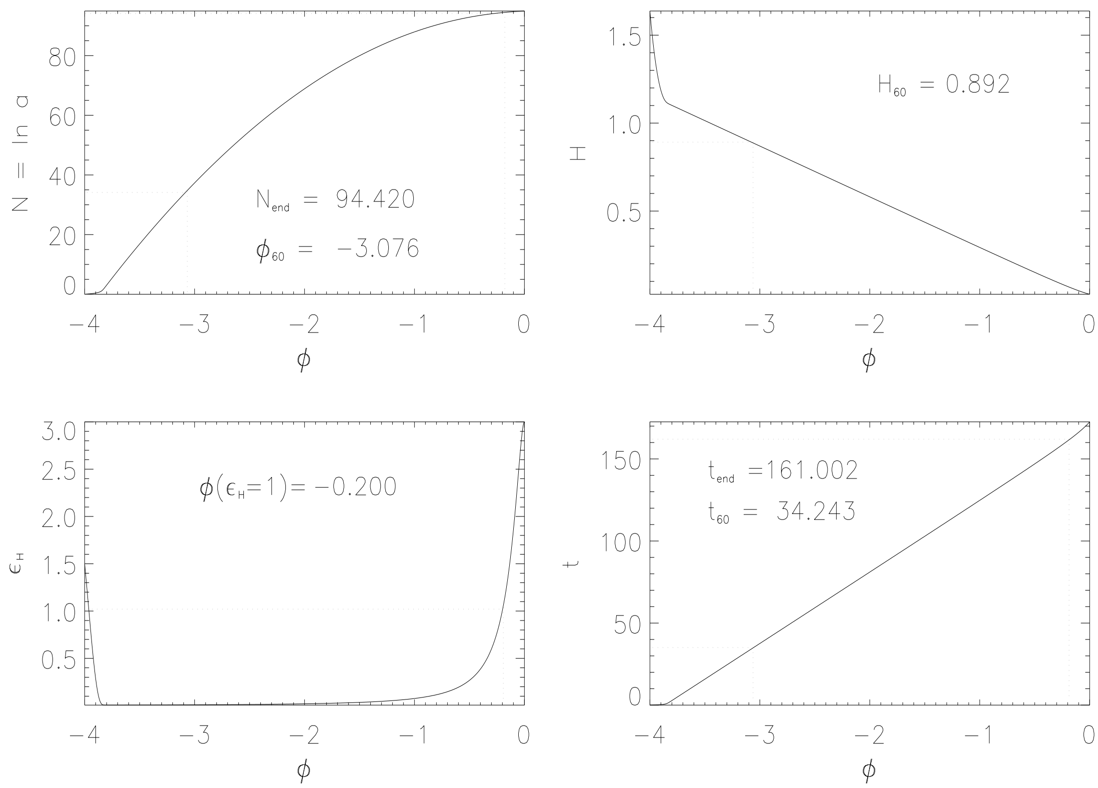


Figure 5.3: The numerical solution of the chaotic inflation with a potential $V(\phi) = 10^{-2}\phi^2$. The simulation starts from $\phi = -4$ and stops at $\phi = 0$: (1) The lower left diagram shows inflation ends at $\phi = -0.200$; (2) From this value, using the upper left diagram to trace back 60 $e$-foldings gives $\phi_{60} = -3.076$; (3) The upper right diagram shows the Hubble parameter at this epoch is 0.892; (4) The lower right diagram gives the corresponding $t_{\rm end} = 161.002$ and $t_{60} = 34.243$.

(see subsections 2.4.3 and 2.4.4), these models are hardly to be tested by observations (see subsections 3.4.1 and 3.4.2). In the following two subsections, we shall use numerical simulation to investigate the chaotic and self-coupled inflationary models, in which the end of inflation is well specified and we can thus employ observations to constrain our models.

### 5.1.4 Chaotic inflation

This model was solved by PSRA in subsection 2.4.5. Now we use numerical simulation to solve it. In the simulation, $m_{\rm Pl} \equiv 1$ and $m^2/2 = 10^{-2}$ are used and the flat Friedmann model is assumed. The results are shown in Figure 5.3. It gives

$$\phi_{60} = -3.076 \tag{5.26}$$

which is in units of Planck mass. Employing (3.28), (3.29), (3.36), (3.37) and (3.49) yields

$$n \simeq 0.966 \quad ; \quad \left.\frac{dn(k)}{d\ln k}\right|_{60} \simeq -5.659 \times 10^{-4} \tag{5.27}$$

$$n_T \simeq -0.0168 \quad ; \quad \left.\frac{dn_T(k)}{d\ln k}\right|_{60} \simeq -2.829 \times 10^{-4} \tag{5.28}$$

$$R \simeq 0.0782 \tag{5.29}$$

Using the COBE normalization (3.59) gives

$$V_{60}^{1/4} \;=\; 1.598 \times 10^{-3}\, m_{\rm Pl} \;=\; 1.953 \times 10^{16}\ \text{GeV} \tag{5.30}$$

Combining this with (5.26) yields the constraint on the mass of inflaton

$$m = 1.174 \times 10^{-6}\, m_{\rm Pl} = 1.436 \times 10^{13}\ \text{GeV} \tag{5.31}$$

All these results are very close to those obtained by using PSRA in subsection 3.4.3. This verifies that the PSRA is indeed a good approximation for this model.

Furthermore, because we know the dynamics of the Friedmann equation and the equation of $\phi$-motion is invariant under a rescaling of variables

$$V \to \alpha V, \quad t \to \frac{1}{\sqrt{\alpha}}\ t, \quad H \to \sqrt{\alpha} H \tag{5.32}$$

we can calculate the expansion time scale at $t_{60}$ from the numerical result $H_{60}$=0.892 ($m_{\rm Pl}$) shown in Figure 5.3 as

$$H_{60}^{-1} = \left[\frac{(1.174 \times 10^{-6})^2/2}{10^{-2}}\right]^{-1/2} (0.892)^{-1}\ m_{\rm Pl}^{-1} = 7.280 \times 10^{-39}\ \text{sec} \tag{5.33}$$

The time taken from the horizon exit of the cosmologically interesting scale to the end of inflation can be also obtained from Figure 5.3 as

$$\Delta t \;=\; \left[\frac{(1.174 \times 10^{-6})^2/2}{10^{-2}}\right]^{-1/2} (161.002 - 34.243)\ m_{\rm Pl}^{-1} \tag{5.34}$$

$$\equiv\; 8.231 \times 10^{-37}\ \text{sec} \;\simeq\; 100\ H_{60}^{-1} \tag{5.35}$$

This verifies the "slow" rollover, the key feature of inflation. While a roll-down time of $10^{-36}$ sec may not seem that slow, compared to the expansion time scale of the universe $10^{-38}$ sec, it is.

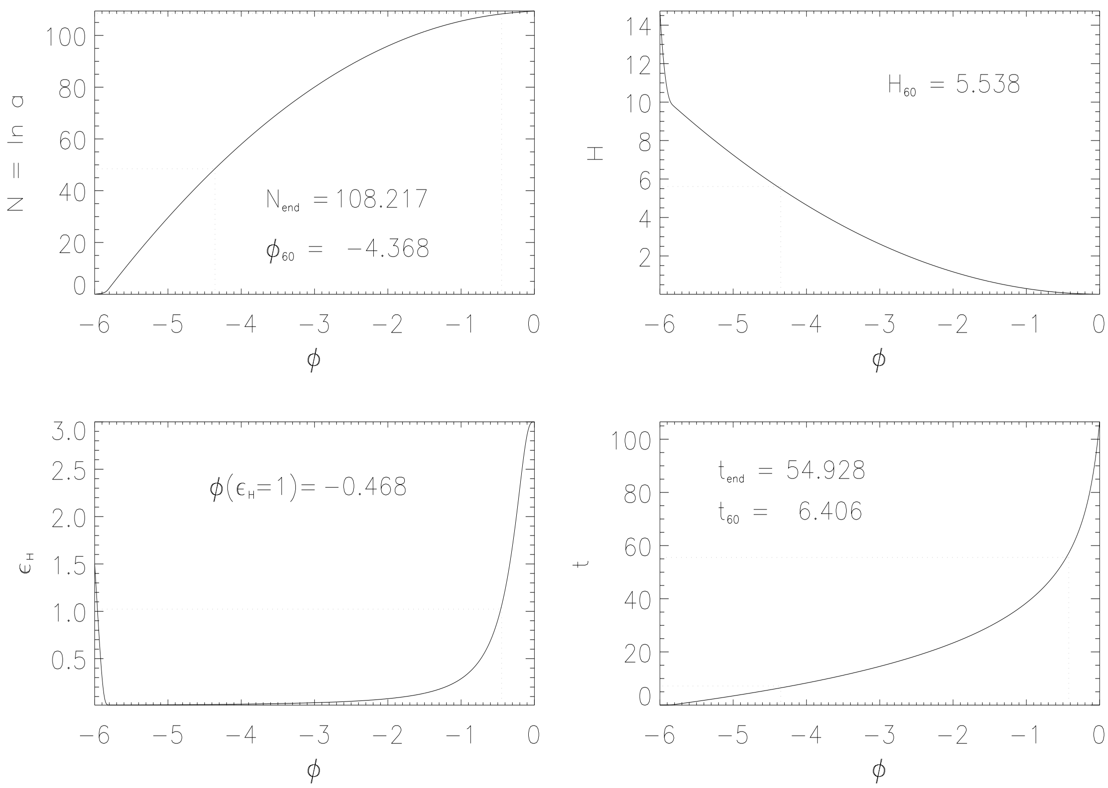


Figure 5.4: The numerical solution of the self-coupling inflation with a potential $V(\phi) = 10^{-2}\phi^4$. The simulation starts from $\phi = -6$ and stops at $\phi = 0$: (1) The lower left diagram shows inflation ends at $\phi = -0.468$; (2) From this value, using the upper left diagram to trace back 60 $e$-foldings gives $\phi_{60} = -4.368$; (3) The upper right diagram shows the Hubble parameter at this epoch is 5.538; (4) The lower right diagram gives the corresponding $t_{\rm end} = 54.928$ and $t_{60} = 6.406$.

### 5.1.5 **Self-coupling inflation**

This model was solved by PSRA in subsection 2.4.6. As an analogue to the analysis in the previous subsection, we choose $\lambda/4 = 10^{-2}$ to do the simulation. Again we assume a flat Friedmann model and normalize $m_{\rm Pl}$ to unity. The results are given in Figure 5.4. It shows

$$\phi_{60} = -4.368 \tag{5.36}$$

which is in unit of Planck mass. Employing (3.28), (3.29), (3.36), (3.37) and (3.49) yields

$$n \simeq 0.950 \quad ; \quad \left.\frac{dn(k)}{d\ln k}\right|_{60} \simeq -2.623 \times 10^{-3} \tag{5.37}$$

$$n_T \simeq -0.0334 \quad ; \quad \left.\frac{dn_T(k)}{d\ln k}\right|_{60} \simeq -5.567 \times 10^{-4} \tag{5.38}$$

$$R \simeq 0.155 \tag{5.39}$$

Using the COBE normalization (3.59) gives

$$V_{60}^{1/4} \;=\; 1.861 \times 10^{-3}\; m_{\rm Pl} \;=\; 2.275 \times 10^{16}\ \text{GeV} \tag{5.40}$$

Combining this with (5.36) yields the constraint on the coupling constant

$$\lambda = 1.319 \times 10^{-13} \tag{5.41}$$

All these results are very close to those obtained by using PSRA in subsection 3.4.4. This verifies again that the PSRA is indeed a good approximation for coping with inflationary models.

Furthermore, from the numerical result $H_{60} = 5.538\ (m_{\rm Pl})$ shown in Figure 5.4 we can obtain the expansion time scale at $t_{60}$

$$H_{60}^{-1} = 5.360 \times 10^{-39}\ \ \text{sec} \tag{5.42}$$

The time taken from the horizon exit of the cosmologically interesting scale to the end of inflation can be also obtained from Figure 5.4

$$\Delta\, t \;=\; t_{\rm end} - t_{60} \;=\; 1.440 \times 10^{-36}\ \text{sec} \;\simeq\; 200\ H_{60}^{-1} \tag{5.43}$$

This verifies again the key feature of inflation—the “slow” rollover.

## 5.2 Hybrid Inflation

As we have seen in Chapter 4, to constrain the parameters involved in the hybrid inflation model exactly, numerical simulation is required. Basically the difficulty of analytical work arises from the existence of $\phi_{\rm inst}$ and the intermediate regime between the inflaton-dominated and vacuum-dominated ones. In this section, we shell investigate two cases in which the values of the parameters constrained by the COBE normalization are obtained. Here we are still considering the hybrid inflation with a potential specified by (4.1).

### 5.2.1 The (M, m) constraint

In section 4.3, we obtained the analytical solution of $(M, m)$ constrained by COBE in the regime $\lambda \sim \lambda' \sim 1$. This solution is given by (4.51) in the inflaton-dominated regime and (4.71) in the vacuum-dominated regime. We expect them to merge with each other at

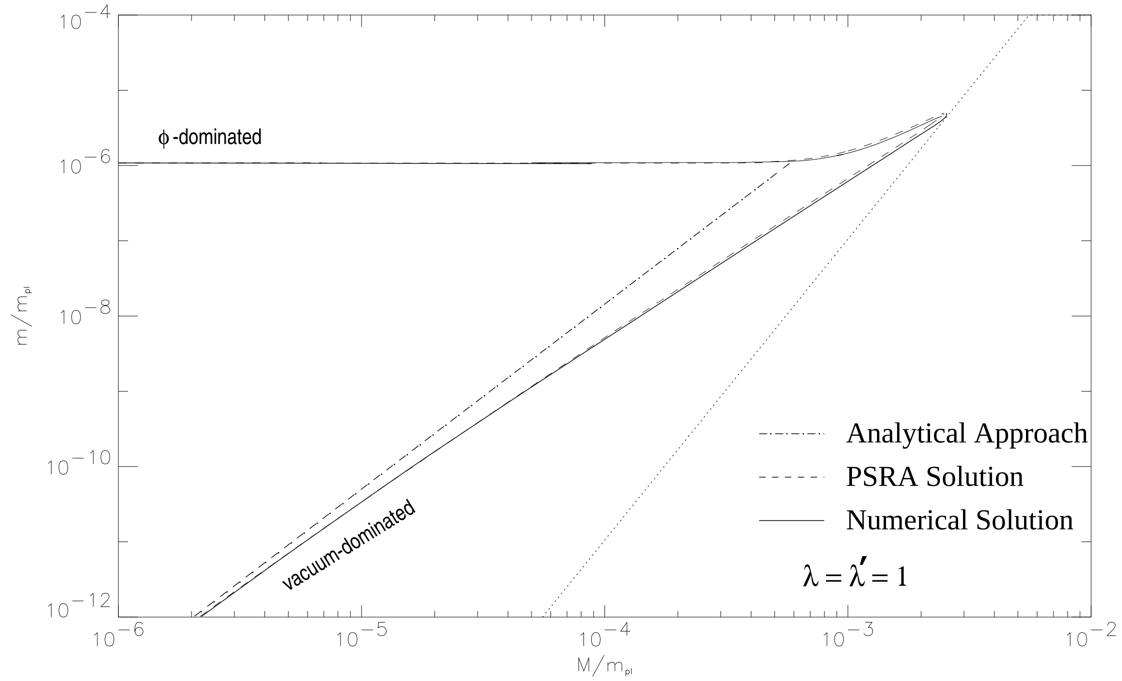


Figure 5.5: The solid line shows the numerical solution of $(M, m)$ which satisfies the COBE normalization for $\lambda = \lambda' = 1$. The dashed line is the solution employing PSRA. The analytical approximation we predicted earlier is plotted as the dot-dashed line. The dotted line is the limit to the right-hand side of which the $(M, m)$ has no solution.

around $(10^{-3}, 10^{-6})$ as given in (4.73). This solution is plotted as the dot-dashed line in Figure 5.5. However, this analytical approximation can work well only until $M \lesssim 10^{-4}$ (see (4.46) and (4.64)). Beyond this value, we require numerical simulation to get the exact solution.

The basic scheme to do the simulation is:

1. Specify $(M, m)$ one by one within the range of our interest. Here we choose the range $(10^{-6}, 10^{-12})$–$(10^{-2}, 10^{-4})$ which is interested in the context of particle physics.

2. Calculate $\phi_{\rm f} = \max\{\phi(\epsilon_H{=}1), \phi_{\rm inst}\}$ and then trace from this value back to $\phi_{60}$.

3. Use this $\phi_{60}$ and the specified $(M, m)$ to test the COBE constraint (4.29). If it is satisfied, then we plot this $(M, m)$.

There are two ways to do the second step. One is using the PSRA to calculate $\phi(\eta_V{=}1)$ instead of $\phi(\epsilon_H{=}1)$, and then using (4.26) to obtain $\phi_{60}$. This result is plotted as the dashed line in Figure 5.5. As we mentioned in subsection 4.2.1, Ref. [26] used $\phi(\epsilon_V{=}1)$

rather than $\phi(\eta_V{=}1)$ to specify the slow-roll end of inflation, so that they got the possibility of inflation restarting (see (4.14) and (4.15)). We have examined this situation and found the only possible range of this corresponds to $10^{-4} \lesssim M \lesssim 5 \times 10^{-4}$ on the horizontal line in Figure 5.5. Employing external numerical simulation, we conclude that the restart of inflation has never happened in this range.

The other way to do the second step is using numerical simulation throughout to calculate $\phi(\epsilon_H{=}1)$ and then $\phi_{60}$ without using PSRA. This result is plotted as the solid line in Figure 5.5 and the program doing this is attached as Program 4 in Appendix A. We see that most of the numerical solution coincides with the PSRA one and this verifies again that the PSRA is indeed a good approximation. Comparing this with the analytical approximation, we find the deviation is as we expected in subsection 4.3.1 and 4.3.2.

The dotted line in Figure 5.5 is the equality of (4.32), to the right-hand side of which the $(M, m)$ has no solution as we mentioned in subsection 4.2.4. It can be clearly seen that the two lines going from the inflaton-dominated and vacuum-dominated regimes merge with each other perfectly at the dotted line. This is also as we predicted in subsection 4.2.4. However, all these are the solutions for the sample parameter choice $\lambda = \lambda' = 1$. We shall now extend our investigation of the parameters.

### 5.2.2 The (M, m, $\lambda$, $\lambda'$) constraint

In the previous subsection, we specified both $\lambda$ and $\lambda'$ to be unity. Here let us keep them free. We shall treat $\lambda^{1/4}M$ and $\lambda'/\lambda^{1/2}$ as two independent parameters so that our parameter set becomes

$$(\lambda^{1/4}M, \;\; m, \;\; \lambda'/\lambda^{1/2}) \tag{5.44}$$

The basic scheme to calculate their values constrained by the COBE normalization is:

1. Specify $(\lambda^{1/4}M, m)$ one by one within the range of our interest. Here we choose the same range as that of the previous subsection $(10^{-6}, 10^{-12})$–$(10^{-2}, 10^{-4})$, apart from the factor $\lambda^{1/4}$ with $M$.

2. Use (4.29) iteratively to obtain $\phi_{60}$.

3. Start the simulation of inflation from this value until we get 60 $e$-foldings. We define the value of $\phi$ at this moment as $\phi_{\mathrm{f(COBE)}}$.

4. If $\phi_{\mathrm{f(COBE)}} > \phi(\epsilon_H{=}1)$ then we move on to the next step. If not, that means for this specific choice of $(\lambda^{1/4}M, m)$, the inflation starting off with $\phi_{60}$ given by COBE normalization is always terminated by $\phi(\epsilon_H{=}1)$ before we can get 60 $e$-foldings. In other words, this choice of $(\lambda^{1/4}M, m)$ is not allowed no matter how $\lambda$ and $\lambda'$ change.

5. $\phi_{\mathrm{f(COBE)}} > \phi(\epsilon_H{=}1)$ means that inflation must be terminated by $\phi_{\mathrm{inst}}$. Thus we have $\phi^2_{\mathrm{f(COBE)}} = \lambda M^2/\lambda'$, or equivalently

$$\frac{\lambda'}{\sqrt{\lambda}} = \frac{\sqrt{\lambda M^4}}{\phi^2_{\mathrm{f(COBE)}}} \tag{5.45}$$

which is the solution we aim finding.

This program is attached as Program 5 in Appendix A. The solution of $\phi_{60}$ in step 2 is given in Figure 5.6. As we noted in subsection 4.2.4, there should be two solutions for $\phi_{60}$ which merge with each other at the equality of (4.32). Figure 5.6 shows these two solutions. In step 4, we find a region where $\phi_{\mathrm{f(COBE)}} < \phi(\epsilon_H{=}1)$ for both solutions of $\phi_{60}$. This region is indicated as the area above the dashed line in Figure 5.7. In this region, no $(M, m, \lambda, \lambda')$ is allowed. In the same figure, the dotted line is the equality of (4.32), which is the same as the dotted line in Figure 5.5. Therefore, the region allowed to have solutions for $(M, m, \lambda, \lambda')$ is the area between the dashed and dotted lines. Finally, having subtracted the two prohibited regions (one above the dashed line and the other to the right-hand side of the dotted line in Figure 5.7), we obtain the solution (5.45) and plot it as in Figure 5.8.[1] This solution has the following features:

1. For any $(\lambda^{1/4}M, m)$ on the dashed line in Figure 5.7, $\phi_{\mathrm{f(COBE)}}$ always coincides with $\phi(\epsilon_H{=}1)$. Above the dashed line, we have seen that no solution is allowed. Beneath it, $\epsilon_H(\phi_{\mathrm{f(COBE)}})$ is always less than unity so that we need to specify a proper $\lambda'/\lambda^{1/2}$ giving $\phi_{\mathrm{inst}}$ to terminate inflation. This proper $\lambda'/\lambda^{1/2}$ is just the two sloped surfaces in Figure 5.8, and the dashed line in Figure 5.7 corresponds to the left vertical surface of each diagram in Figure 5.8. Therefore, any point on these two vertical surfaces can always reproduce the COBE normalization, because on these surfaces $\phi_{\mathrm{inst}} \propto \lambda'/\lambda^{1/2}$ is always less than the required value giving $\phi_{\mathrm{inst}}$ so that inflation can be terminated by $\phi(\epsilon_H{=}1)$. This means that the solution of $\lambda'/\lambda^{1/2}$ in Figure 5.8 includes the sloped surfaces and the left vertical surfaces.

[1] The two diagrams in this figure correspond to the two solutions of $\phi_{60}$.

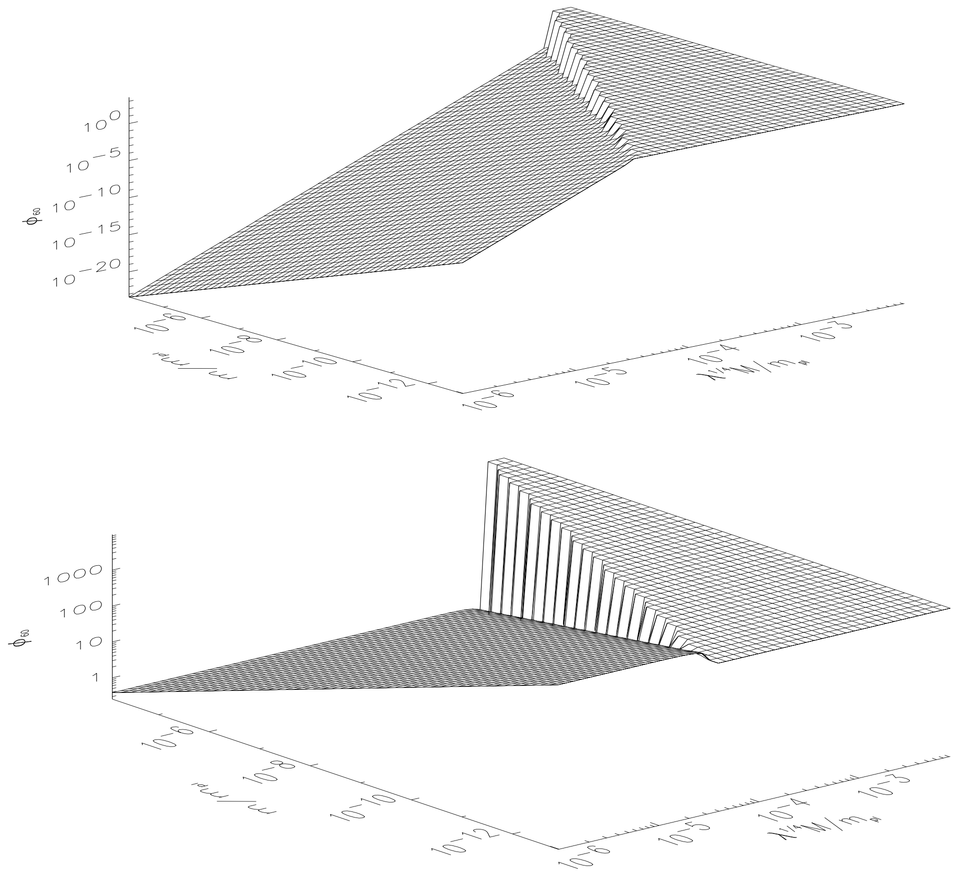


Figure 5.6: The solution of $\phi_{60}$ from the COBE constraint. The two sloped surfaces reproduce the COBE normalization. The horizontal part in each diagram is the region which has no solution for any $(\lambda^{1/4}M, m)$. It corresponds to the right-hand side of the dotted line in Figure 5.5.

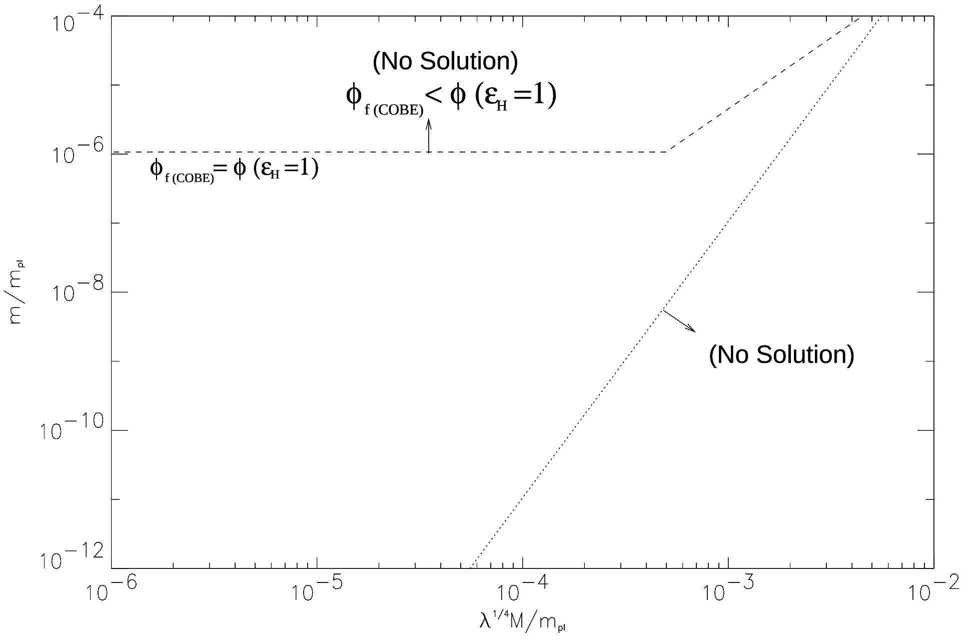


Figure 5.7: The region between the dashed and dotted lines is the only allowed region to have solution for $(M, m, \lambda, \lambda')$. The area above the dashed line has no solution because it cannot generate 60 $e$-foldings. The dotted line is the same in Figure 5.5.

2. According to the property described above, for any given $\lambda/\lambda'^{1/2}$ we can get the solution $(\lambda^{1/4}M, m)$ by slicing the two diagrams in Figure 5.8 with a horizontal surface specified by the given $\lambda/\lambda'^{1/2}$. The combination of the sliced intersections from both diagrams forms our solution.

3. Considering Figure 5.5, we know that slicing Figure 5.8 with the plane $\lambda/\lambda'^{1/2} = 1$ must give the same result. However, the result is indeed the same apart from an extra section which does not appear in Figure 5.5. This extra section corresponds exactly to the sloped part of the dashed line in Figure 5.7. It means the solid line in Figure 5.5 is not really a complete solution of $(M, m)$ in the regime $\lambda = \lambda' = 1$ and we find it is caused by the program. This also implies that the solution published in Ref. [26] is not complete. The complete solution in the regime of $\lambda = \lambda' = 1$ should include the solid line in Figure 5.5 and the dashed line in Figure 5.7.[2]

[2]The horizontal part of the dashed line in Figure 5.7 coincides with the horizontal part of the solid line in Figure 5.5.

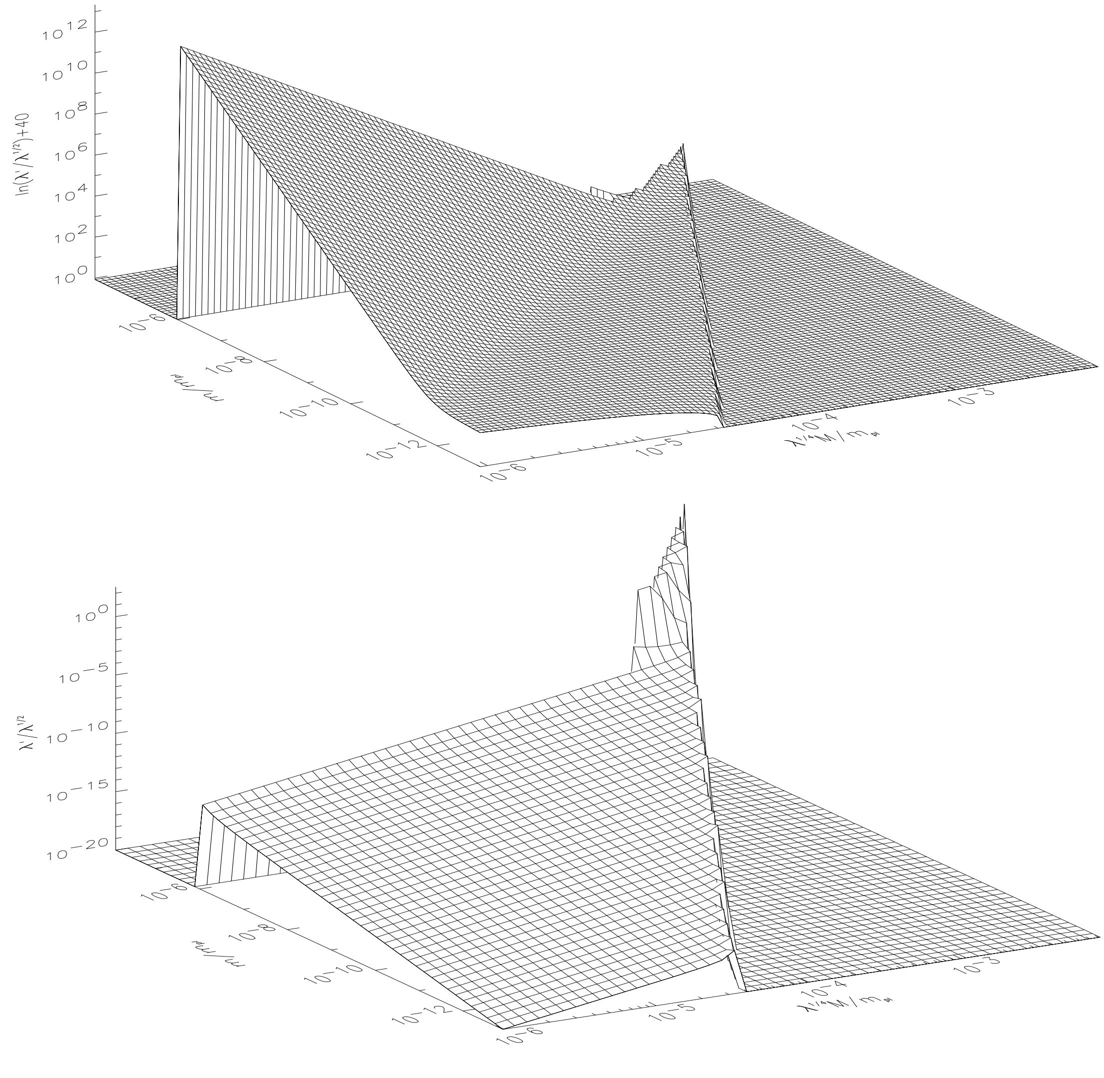

Figure 5.8: The solution of $(M, m, \lambda, \lambda')$ in the hybrid inflation model. The sloped and left vertical surfaces in each diagram reproduce the COBE normalization. The horizontal part in each diagram is the region prohibiting solutions. It corresponds to the two regions indicated in Figure 5.7.

4. The solution $(\lambda^{1/4}M, m, \lambda'/\lambda^{1/2})$ in Figure 5.8 can be extended to the general parameter space $(M, m, \lambda, \lambda')$ by rescaling the $\lambda^{1/4}M$ and $\lambda'/\lambda^{1/2}$ coordinates.

We have obtained the general solution of $(M, m, \lambda, \lambda')$ which is constrained by the COBE normalization. When we apply the hybrid inflation model with the potential form specified by (4.1) in any other context, the parameters should be constrained by the solution we obtain here.

CHAPTER 6

# CONCLUSION

In this paper, we have reviewed detailed analytical techniques which we employed to investigate various inflationary models appearing in the literature, including considerable material which is applicable in more general surroundings. Although exact solutions exist only in power-law and intermediate inflationary models, with recourse to numerical simulations we found the PSRA is indeed good enough to cope with all the models under our investigation. On the other hand, since the form of the Hubble parameter is unknown in general circumstances, the more precise analytical approach that the HSRA provides is unlikely to be widely utilized. Armed with the PSRA and numerical techniques, we have verified several vital features of inflation, including its efficient approach to flatness within the first few $e$-foldings and the slow-rollover.

With the reviewed perturbation theory, we have also provided machinery which allows one to distinguish different behaviour that various inflationary models possess, including the degree of tilt from scale-invariance and different portion of gravitational waves they predict. By the COBE normalization, we obtained further constraints on the parameters in our models. Within this regime, we have attempted a detailed investigation of the parameters involved in hybrid inflation and finally found the general solution of them shown in Figure 5.8. To end our investigation of various inflationary models, a brief summary of their features is attached as Table 6.1.

In conclusion, the phenomenology of inflation is well supported by observations and the currently valid techniques in both analytical and numerical approaches to Inflationary Cosmology are sufficient for taking advantage of present observations. If coupled with the new developments in particle physics like GUT, a truly amazing insight into the origin of the early universe is enabled. In the future, it should be the observations with higher accuracy that decide not only the viability amongst various inflationary models but also the victory and defeat of the contest between Inflationary Cosmology and other potential theories.

| FEATURES OF INFLATIONARY MODELS | | | | | |
|---|---|---|---|---|---|
| | Solution | $n$ | $n_T$ | $R$ | $V_{60}^{1/4}$ (GeV) |
| Power-law Inflation (2.48) | **Exact** (2.50) | $(0.7, 1)$ | $(-0.3, 0)$ | $(0, 1.2)$ | — |
| Intermediate Inflation (2.65) | **Exact** (2.61) | $(-3, \infty)$ | $(-4, 0)$ | $(0, 9.3)$ | — |
| Polynomial Chaotic Inflation (3.85) | **PSRA** | $(0, 0.97)$ | $(-1, -0.017)$ | $(0.077, 4.65)$ | — |
| | $\alpha = 2$ | | | | |
| | (2.72) | 0.966 | $-0.0168$ | 0.0782 | $1.95 \times 10^{16}$ |
| | $\alpha = 4$ | | | | |
| | (2.82) | 0.950 | $-0.0334$ | 0.155 | $2.27 \times 10^{16}$ |
| Hybrid Inflation (4.1) | **PSRA** (4.13) and **Numerical Simulation** | $\phi$-dominated regime | | | |
| | | $(0.96, 1)$ | $(-0.017, 0)$ | $(0, 0.078)$ | $\sim 10^{16}$ |
| | | vacuum-dominated regime | | | |
| | | $(1, 2)$ | $\lvert n_T \rvert \ll 2$ | $\ll 9.3$ | $\ll 10^{16}$ |
| | | vacuum-dominated with $\lambda = \lambda' = 1$ | | | |
| | | $(1, 1.19)$ | $\lvert n_T \rvert \ll 0.2$ | $\ll 0.9$ | $\ll 10^{15}$ |

Table 6.1: A summary of features of various inflationary models appearing in this paper. Each model is defined by the potential form specified by the equation number under its name. Its solution is indicated by the equation number in the column "Solution". In columns giving $n$, $n_T$ and $R$, the bracketed numbers specify the allowed range of values. The values of $V_{60}^{1/4}$ are those derived from the COBE normalization.

APPENDIX A

## PROGRAM 1

1

2

**PROGRAM 2**

1

2

**PROGRAM 3**

1

2

**PROGRAM 4**

1

2

**PROGRAM 4**

1

2

## PROGRAM 5

1

2

# REFERENCES


[1] Abbott, L. F., Fahri, E. & Wise, M. B. (1982) *Phys. Lett.*, **117B**, 29.

[2] Abbott, L. F. & Wise, M. B. (1984) *Nucl. Phys.*, **B244**, 541.

[3] Adams, F. C., Bond, J. R., Freese, J. A. & Olinto, A. (1993) *Phys. Rev.*, **D47**, 426.

[4] Albrecht, A., Coulson, D., Ferreira, P. & Magueijo, J. (1996) *Phys. Rev. Lett.*, **76**, 1413.

[5] Albrecht, A. & Steinhardt, P. J. (1982) *Phys. Rev. Lett.*, **48**, 1220.

[6] Albrecht, A., Steinhardt, P. J., Turner, M. S. & Wilczek, F. (1982) *Phys. Rev. Lett.*, **48**, 1437.

[7] Banks, T., Berkooz, M., Shenker, S. H., Moore, G. & Steinhardt, P. J. (1995) *Phys. Rev.*, **D52**, 3548.

[8] Bardeen, J. M. (1980) *Phys. Rev.*, **D22**, 1882.

[9] Bardeen, J. M., Steinhardt, P. S. & Turner, M. S. (1983) *Phys. Rev.*, **D28**, 679.

[10] Bardeen, J. M. (1980) *Phys. Rev.*, **D22**, 1882.

[11] Barrow, J. D. (1990) *Phys. Lett.*, **B235**, 40.

[12] Barrow, J. D. (1993) *Phys. Rev.*, **D47**, R5329.

[13] Barrow, J. D. & Liddle, A. R. (1993) *Phys. Rev.*, **D47**, R5219.

[14] Barrow, J. D. & Maeda, K. (1990) *Nucl. Phys.*, **B341**, 294.

[15] Barrow, J. D. & Saich, P. (1990) *Phys. Lett.*, **B249**, 406.

[16] Battye, R. A. & Shellard, E. P. S. (1996) *GRF essay competition*, 'Primordial Gravitational Waves', 1996.

[17] Bennett, C. L. *et al.* (1996) *Astrophys. J. Lett.*, **464**, L1.

[18] Bertschinger, E. & Dekel, A. (1989) *Astrophys. J. Lett.*, **336**, L5.

[19] Boerner, G. (1988) *The Early Universe*, Berlin: Springer.

[20] Bond, J. R. & Efstathiou, G. (1987) *Mon. Not. R. Astr. Soc.*, **226**, 665.

[21] Bunn, E. F., Liddle, A. R. & White, M. (1996) *Four-year COBE Normalization of Inflationary Cosmologies*, Sussex preprint SUSSEX-AST 96/7-2 (1996).

[22] Coleman, S. (1977) *Phys. Rev.*, **D15**, 2929.

[23] Collins, C. B. & Hawking, S. W. (1973) *Ap. J.*, **180**, 317.

[24] Copeland, E. J., Kolb, E. W., Liddle, A. R. & Lidsey, J. E. (1993) *Phys. Rev.*, **D48**, 2529.

[25] Copeland, E. J., Kolb, E. W., Liddle, A. R. & Lidsey, J. E. (1994) *Phys. Rev.*, **D49**, 1840.

[26] Copeland, E. J., Liddle, A. R., Lyth, D. H., Stewart, E. D. & Wands, D. (1994) *Phys. Rev.*, **D49**, 6410.

[27] Davis, M., Geller, M. J. & Huchra, J. (1978) *Ap. J.*, **221**, 1.

[28] Davis, M. & Peebles, P. J. E. (1983) *Ap. J.*, **267**, 465.

[29] Davis, R. L., Hodges, H. M., Smoot, G. F., Steinhardt, P. J. & Turner, M. S. (1992) *Phys. Rev. Lett.*, **69**, 1856.

[30] Dolan, L. & Jackiw R. (1974) *Phys. Rev.*, **D9**, 3320.

[31] Dolgov, A. & Linde, A. D. (1982) *Phys. Lett.*, **116B**, 329.

[32] Dolgov, A. & Silk, J. (1993) *Phys. Rev.*, **D47**, 2619.

[33] Dvali, G., Shafi, Q. & Schaefer, R. (1994) *Phys. Rev. Lett.*, **73**, 1886.

[34] Efstathiou, G. (1990) *The Physics of The Early Universe*, eds. Heavens, A., Peacock J. & Davies, A., SUSSP publications.

[35] Efstathiou, G. & Bond, J. R. (1986) *Mon. Not. R. Astr. Soc.*, **218**, 103.

[36] Efstathiou, G., Bond, J. R. & White, S. D. M. (1992) *Mon. Not. R. Astr. Soc.*, **258**, 1P.

[37] Ellis, J., Nanopoulos, D. V. & Sarkar, S. (1985) *Nucl. Phys.*, **B259**, 175.

[38] Grishchuk, L. P. (1974) *Zh. Eksp. Teor. Fiz.*, **67**, 825.

[39] Grishchuk, L. P. (1977) *Ann. N. Y. Acad. Sci.*, **302**, 439.

[40] Guth, A. H. (1981) *Phys. Rev.*, **D23**, 347.

[41] Guth, A. H. (1993) *Proc. Natl. Acad. Sci. USA*, **90**, June 1993, 4871.

[42] Guth, A. H. & Pi, S.-Y. (1982) *Phys. Rev. Lett.*, **49**, 1110.

[43] Guth, A. H. & Weinberg, E. J. (1983) *Nucl. Phys.*, **B212**, 321.

[44] Harrison, R. (1970) *Phys. Rev.*, **D1**, 2726.

[45] Hawking, S. W. (1982) *Phys. Lett.*, **115B**, 339.

[46] Hawking, S. W., Moss, I. & Stewart, J. (1982) *Phys. Rev.*, **D26**, 2681.

[47] Kawashi, M. & Sato, K. (1987) *Phys. Lett.*, **B189**, 23.

[48] Kodama, H. & Sasaki, M. (1984) *Prog. Theor. Phys. Supp.*, **78**, 1.

[49] Kodama, H. & Sasaki, M. (1987) *Int. J. Mod. Phys.*, **A2**, 491.

[50] Kofman, L. A. & Linde, A. D. (1987) *Nucl. Phys.*, **B282**, 555.

[51] Kolb, E. W. (1991) *Phys. Scr.*, **T36**, 199.

[52] Kolb, E. W. & Turner, M. S. (1994) *The Early Universe*, New York: Addison Wesley, 261.

[53] Kosowsky, A. & Turner, M. S. (1995) *Phys. Rev.*, **D52**, R1739.

[54] Krauss, L. M. & White, M. (1992) *Phys. Rev. Lett.*, **69**, 869.

[55] La, D. & Steinhardt, P. J. (1989) *Phys. Rev. Lett.*, **62**, 376.

[56] Liddle, A. R. & Lyth, D. H. (1992) *Phys. Lett.*, **B291**, 391.

[57] Liddle, A. R. & Lyth, D. H. (1993) *Phys. Rep.*, **231**, 1.

[58] Liddle, A. R., Lyth, D. H. & Sutherland, W. (1992) *Phys. Lett.*, **B279**, 244.

[59] Liddle, A. R., Parsons, P. & Barrow, J. D. (1994) *Phys. Rev.*, **D50**, 7222.

[60] Lidsey, J. E. (1991) *Phys. Lett.*, **B273**, 42.

[61] Lidsey, J. E. & Coles, P. (1992) *Mon. Not. R. Astr. Soc.*, **258**, 57P.

[62] Lidsey, J. E., Liddle, A. R., Kolb, E. W., Copeland, E. J., Barreiro, T. & Abney, M. (1995) *Reconstructing The Inflaton Potential — an Overview*, Sussex preprint SUSSEX-AST 95/8-3 (1995).

[63] Lifshitz, E. M. (1946) *J. Phys.* (Moscow), **10**, 116.

[64] Linde, A. D. (1982) *Phys. Lett.*, **108B**, 389.

[65] Linde, A. D. (1982) *Phys. Lett.*, **116B**, 335.

[66] Linde, A. D. (1983) *Phys. Lett.*, **129B**, 177.

[67] Linde, A. D. (1987) *Physics Today*, **40**, 61.

[68] Linde, A. D. (1990) *Phys. Lett.*, **B249**, 18.

[69] Linde, A. D. (1991) *Phys. Lett.*, **B259**, 38.

[70] Lucchin, F. & Matarrese, S. (1985) *Phys. Rev.*, **D32**, 1316.

[71] Lucchin, F., Matarrese, S. & Mollerach, S. (1992) *Astrophys. J. Lett.*, **401**, 49.

[72] Lyth, D. H. (1985) *Phys. Rev.*, **D31**, 1792.

[73] Lyth, D. H. (1990) *Phys. Lett.*, **B246**, 359.

[74] Lyth, D. H. & Stewart, E. D. (1990) *Astrophys. J.*, **361**, 343.

[75] Lyth, D. H. & Stewart, E. D. (1992) *Phys. Lett.*, **B274**, 168.

[76] Lyth, D. H. & Stewart, E. D. (1992) *Phys. Rev.*, **D46**, 532.

[77] Lyth, D. H. & Stewart, E. D. (1996) *More Varieties of Hybrid Inflation*, Lancaster preprint LANCS-TH/9613 (1996).

[78] Martin, J. L. (1988) *General Relativity*, Chichester: Ellis Horwood Limited, 132.

[79] Mukhanov, V. F., Feldman, H. A. & Brandenberger, R. H. (1992) *Phys. Rep.*, **215**, 203.

[80] Muslimov, A. G. (1990) *Class. Quantum Grav.*, **7**, 231.

[81] Narlikar, J. V. & Padmanabhan T. (1991) *Ann. Rev. Astron. Astrophys.*, **29**, 325.

[82] Peebles, P. J. E. (1980) *The Large Scale Structure of The Universe*, Princeton U. P.

[83] Penzias, A. A. & Wilson, R. W. (1965) *Ap. J.*, **142**, 419.

[84] Randall, L., Soljačić, M. & Guth, A. H. (1996) *Nucl. Phys.*, **B472**, 377.

[85] Roberts, D., Liddle, A. R. & Lyth, D. H. (1995) *Phys. Rev.*, **D51**, 4122.

[86] Ross, G. G. & Sarkar, S. (1996) *Nucl. Phys.*, **B461**, 597.

[87] Salopek, D. S. (1992) *Phys. Rev. Lett.*, **69**, 3602.

[88] Salopek, D. S. & Bond J. R. (1990) *Phys. Rev.*, **D42**, 3936.

[89] Salopek, D. S., Bond J. R. & Bardeen, J. M. (1989) *Phys. Rev.*, **D40**, 1753.

[90] Sasaki, M. (1986) *Prog. Theor. Phys.*, **76**, 1036.

[91] Saunders, W. *et al.* (1991) *Nature*, **349**, 32.

[92] Scaramella, R. & Vittorio, N. (1990) *Astrophys. J.*, **353**, 372.

[93] Schunck, F. E. & Mielke, E. W. (1994) *Phys. Rev.*, **D50**, 4794.

[94] Smoot, G. F. *et al.* (1992) *Astrophys. J. Lett.*, **396**, L1.

[95] Souradeep, T. & Sahni, V. (1992) *Mod. Phys. Lett.*, **A7**, 3541.

[96] Starobinsky, A. A. (1982) *Phys. Lett.*, **B117**, 175.

[97] Starobinsky, A. A. (1985) *Sov. Astron. Lett.*, **11**, 133.

[98] Steinhardt, P. J. & Turner, M. S. (1984) *Phys. Rev.*, **D29**, 2162.

[99] Stewart, E. D. (1995) *Phys. Rev.*, **D51**, 6847.

[100] Stewart, E. D. (1995) *Phys. Lett.*, **B345**, 414.

[101] Stewart, E. D. & Lyth, D. H. (1993) *Phys. Lett.*, **B302**, 171.

[102] Taylor, A. N. & Rowan-Robinson, M. (1992) *Nature*, **359**, 396.

[103] Vilenkin, A. & Ford, L. H. (1982) *Phys. Rev.*, **D25**, 1231.

[104] Weinberg, S. (1972) *Gravitation and Cosmology*, New York: Wiley.

[105] White, M., Scott, D. & Silk, J. (1994) *Ann. Rev. Astron. Astrophys.*, **32**, 319.

[106] Wright, E. *et al.* (1992) *Astrophys. J. Lett.*, **396**, L13.

[107] Zel'dovich, Ya. B. (1970) *Astron. Astrophys.*, **5**, 84.